

HAZARD MAPPING OF THE PHILIPPINES USING LIDAR (PHIL-LIDAR 1)

LiDAR Surveys and Flood Mapping of Guinarona River







© University of the Philippines Diliman and Visayas State University 2017

Published by the UP Training Center for Applied Geodesy and Photogrammetry (TCAGP)
College of Engineering
University of the Philippines – Diliman
Quezon City
1101 PHILIPPINES

This research project is supported by the Department of Science and Technology (DOST) as part of its Grants-in-Aid Program and is to be cited as:

E.C. Paringit, and F.F. Morales, (Eds.) (2017), *LiDAR Surveys and Flood Mapping of Guinarona River*. Quezon City: University of the Philippines Training Center for Applied Geodesy and Photogrammetry - 101 pp

The text of this information may be copied and distributed for research and educational purposes with proper acknowledgement. While every care is taken to ensure the accuracy of this publication, the UP TCAGP disclaims all responsibility and all liability (including without limitation, liability in negligence) and costs which might incur as a result of the materials in this publication being inaccurate or incomplete in any way and for any reason.

For questions/queries regarding this report, contact:

Engr. Florentino Morales, Jr.

Project Leader, PHIL-LiDAR 1 Program
Visayas State University
Baybay, Leyte, Philippines 6521
ffmorales_jr@yahoo.com

Enrico C. Paringit, Dr. Eng.

Program Leader, Phil-LiDAR 1 Program
University of the Philippines Diliman
Quezon City, Philippines 1101
E-mail: ecparingit@up.edu.ph

National Library of the Philippines
ISBN: 978-621-430-204-8



TABLE OF CONTENTS

TABLE OF CONTENTS.....	iii
LIST OF TABLES.....	v
LIST OF FIGURES.....	vii
LIST OF ACRONYMS AND ABBREVIATIONS.....	x
CHAPTER 1: OVERVIEW OF THE PROGRAM AND PAMPLONA RIVER.....	1
1.1 Background of the Phil-LiDAR 1 Program.....	1
1.2 Overview of the Pamplona River Basin.....	1
CHAPTER 2: LIDAR DATA ACQUISITION OF THE PAMPLONA FLOODPLAIN.....	4
2.1 Flight Plans.....	4
2.2 Ground Base Stations.....	6
2.3 Flight Missions.....	10
2.4 Survey Coverage.....	12
CHAPTER 3: LIDAR DATA PROCESSING OF THE PAMPLONA FLOODPLAIN.....	14
3.1 Overview of the LiDAR Data Pre-Processing.....	14
3.2 Transmittal of Acquired LiDAR Data.....	15
3.3 Trajectory Computation.....	15
3.4 LiDAR Point Cloud Computation.....	17
3.5 LiDAR Data Quality Checking.....	18
3.6 LiDAR Point Cloud Classification and Rasterization.....	22
3.7 LiDAR Image Processing and Orthophotograph Rectification.....	24
3.8 DEM Editing and Hydro-Correction.....	26
3.9 Mosaicking of Blocks.....	28
3.10 Calibration and Validation of Mosaicked LiDAR Digital Elevation Model (DEM).....	30
3.11 Integration of Bathymetric Data into the LiDAR Digital Terrain Model.....	33
3.12 Feature Extraction.....	35
3.12.1 Quality Checking of Digitized Features' Boundary	35
3.12.2 Height Extraction	36
3.12.3 Feature Attribution	36
3.12.4 Final Quality Checking of Extracted Features.....	37
CHAPTER 4: LIDAR VALIDATION SURVEY AND MEASUREMENTS OF THE PAMPLONA RIVER BASIN.....	38
4.1 Summary of Activities.....	38
4.2 Control Survey.....	39
4.3 Baseline Processing.....	44
4.4 Network Adjustment.....	45
4.5 Cross-section and Bridge As-Built survey and Water Level Marking.....	47
4.6 Validation Points Acquisition Survey.....	51
4.7 River Bathymetric Survey.....	53
CHAPTER 5: FLOOD MODELING AND MAPPING.....	56
5.1 Data Used for Hydrologic Modeling.....	56
5.1.1 Hydrometry and Rating Curves.....	56
5.1.2 Precipitation.....	56
5.1.3 Rating Curves and River Outflow.....	57
5.2 RIDF Station.....	58
5.3 HMS Model.....	60
5.4 Cross-section Data.....	65
5.5 Flo 2D Model.....	66
5.6 Results of HMS Calibration.....	67
5.7 Calculated outflow hydrographs and discharge values for different rainfall return periods.....	69
5.7.1 Hydrograph using the Rainfall Runoff Model	69
5.8 River Analysis (RAS) Model Simulation.....	70
5.9 Flow Depth and Flood Hazard.....	70
5.10 Inventory of Areas Exposed to Flooding.....	77
5.11 Flood Validation.....	90
REFERENCES.....	92
ANNEXES.....	93
Annex 1. Optech Technical Specification of the Pegasus Sensor.....	93
Annex 2. NAMRIA Certification of Reference Points Used in the LIDAR Survey.....	94
Annex 3. Baseline Processing Reports of Control Points used in the LIDAR Survey.....	97
Annex 4. The LIDAR Survey Team Composition.....	101

Annex 5. Data Transfer Sheet for Pamplona Floodplain	102
Annex 6. Flight Logs for the Flight Missions.....	103
Annex 7. Flight Status Reports.....	109
Annex 8. Mission Summary Reports.....	115
Annex 9. Pamplona Model Basin Parameters.....	160
Annex 10. Pamplona Model Reach Parameters.....	163
Annex 11. Pamplona Field Validation Points.....	165
Annex 12. Educational Institutions affected by flooding in Pamplona Floodplain.....	170
Annex 13. Health Institutions affected by flooding in Pamplona Floodplain.....	170

LIST OF TABLES

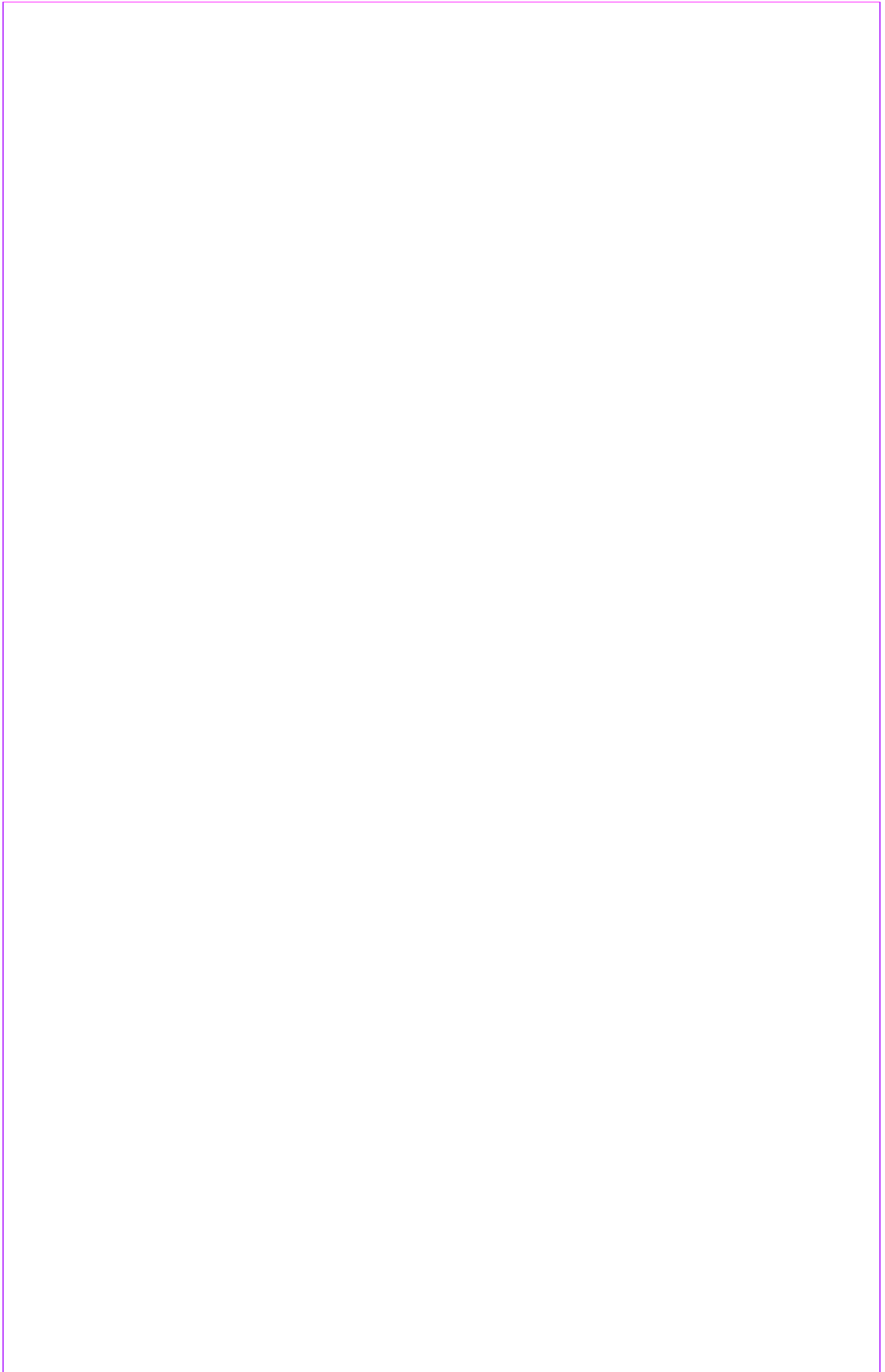
Table 1. Flight planning parameters for the Pegasus LiDAR system.....	4
Table 2. Details of the recovered NAMRIA horizontal reference point APA-13 used as base station for the LiDAR acquisition.....	7
Table 3. Details of the recovered NAMRIA horizontal reference point CGY-87 used as base station for the LiDAR acquisition.....	8
Table 4. Details of the recovered NAMRIA horizontal reference point CGY-110 used as base station for the LiDAR acquisition.....	9
Table 5. Ground control points that were used during the LiDAR data acquisition.....	10
Table 6. Flight missions for the LiDAR data acquisition of the Pamplona Floodplain.....	10
Table 7. Actual parameters used during the LiDAR data acquisition of the Pamplona Floodplain.....	11
Table 8. List of municipalities and cities surveyed of the Pamplona Floodplain LiDAR acquisition.....	12
Table 9. Self-calibration Results values for Pamplona flights.....	17
Table 10. List of LiDAR blocks for Pamplona Floodplain.....	18
Table 11. Pamplona classification results in TerraScan.....	22
Table 12. LiDAR blocks with its corresponding areas.....	26
Table 13. Shift values of each LiDAR block of Pamplona Floodplain.....	28
Table 14. Calibration Statistical Measures.....	32
Table 15. Validation Statistical Measures.....	33
Table 16. Quality Checking Ratings for Pamplona Building Features.....	35
Table 17. Building Features Extracted for Pamplona Floodplain.....	36
Table 18. Total Length of Extracted Roads for Pamplona Floodplain.....	36
Table 19. Number of Extracted Water Bodies for Pamplona Floodplain.....	37
Table 20. List of Reference and Control Points occupied for Pamplona River Survey.....	40
Table 21. Baseline Processing Summary Report for Pamplona River Survey.....	44
Table 22. Constraints applied to the adjustment of the control points.....	45
Table 23. Adjusted grid coordinates for control points used in the Pamplona River Floodplain survey.....	45
Table 24. Adjusted geodetic coordinates for control points used in the Pamplona River Floodplain validation.....	46
Table 25. The reference and control points utilized in the Pamplona River Static Survey, with their corresponding locations.....	47
Table 26. RIDF values for Aparri Rain Gauge computed by PAGASA.....	58
Table 27. Range of calibrated values for the Pamplona River Basin.....	67
Table 28. Summary of the Efficiency Test of the Pamplona HMS Model.....	68
Table 29. Peak values of the Pamplona HEC-HMS Model outflow using the Aparri RIDF 24-hour values...69	69
Table 30. Municipalities affected in Pamplona Floodplain.....	70
Table 31. Affected areas in Luna, Apayao during a 5-Year Rainfall Return Period.....	77
Table 32. Affected Areas in Pamplona, Cagayan during 5-Year Rainfall Return Period.....	78
Table 33. Affected Areas in Pamplona, Cagayan during 5-Year Rainfall Return Period.....	78
Table 34. Affected areas in Sanchez-Mira, Cagayan during a 5-Year Rainfall Return Period.....	80
Table 35. Affected Areas in Luna, Apayao during 25-Year Rainfall Return Period.....	81
Table 36. Affected Areas in Pamplona, Cagayan during 5-Year Rainfall Return Period.....	82

Table 37. Affected Areas in Pamplona, Cagayan during 5-Year Rainfall Return Period.....	82
Table 38. Affected Areas in Sanchez-Mira, Cagayan during 25-Year Rainfall Return Period.....	84
Table 39. Affected Areas in Luna, Apayao during 25-Year Rainfall Return Period.....	85
Table 40. Affected Areas in Pamplona, Cagayan during 100-Year Rainfall Return Period.....	86
Table 41. Affected Areas in Pamplona, Cagayan during 100-Year Rainfall Return Period.....	86
Table 42. Affected Areas in Sanchez-Mira, Cagayan during 100-Year Rainfall Return Period.....	88
Table 43. Areas covered by each warning level with respect to the rainfall scenarios.....	89
Table 44. Actual flood vs simulated flood depth at different levels in the Pamplona River Basin.....	91
Table 45. The summary of the Accuracy Assessment in the Pamplona River Basin Survey.....	91

LIST OF FIGURES

Figure 1. Map of the Pamplona River Basin (in brown).....	2
Figure 2. Flight Plan and base stations used for the Pamplona Floodplain survey.	5
Figure 3. GPS set-up over APA-13 located at the edge of the PCCP, 70m NE of a waiting shed near the barangay hall in Tumog, Municipaity of Luna.	7
Figure 4. GPS set-up over CGY-87 located on a solar dryer at Brgy. Cabayabasan, fronting the barangay hall, in municipality of Lal-lo.....	8
Figure 5. GPS set-up over CGY-110 located inside the compound of Pamplona Central School, Municipality of Pamplona.	9
Figure 6. Actual LiDAR survey coverage of the Pamplona Floodplain.	13
Figure 7. Schematic diagram for Data Pre-Processing Component.	14
Figure 8. Smoothed Performance Metric Parameters of Pamplona Flight 2842P.	15
Figure 9. Solution Status Parameters of Pamplona Flight 2842P.	16
Figure 10. Best Estimated Trajectory of the LiDAR missions conducted over Pamplona Floodplain.....	17
Figure 11. Boundary of the processed LiDAR data over Pamplona Floodplain	18
Figure 12. Image of data overlap for Pamplona Floodplain.	19
Figure 13. Pulse density map of merged LiDAR data for Pamplona Floodplain.....	20
Figure 14. Elevation Difference Map between flight lines for Pamplona Floodplain Survey.	21
Figure 15. Quality checking for a Pamplona flight 2842P using the Profile Tool of QT Modeler.	22
Figure 16. Tiles for Pamplona Floodplain (a) and classification results (b) in TerraScan.	23
Figure 17. Point cloud before (a) and after (b) classification	23
Figure 18. The production of last return DSM (a) and DTM (b), first return DSM (c) and secondary DTM (d) in some portion of Pamplona Floodplain.	24
Figure 19. Pamplona Floodplain with available orthophotographs.....	25
Figure 20. Sample orthophotograph tiles for Pamplona Floodplain.	25
Figure 21. Portions in the DTM of Pamplona floodplain – a road before (a) and after (b) manual editing; disconnected rivers before (c) and after (d) manual editing; interpolated bank before (e) and after (f) object retrieval; and a pit before (g) and after (h) manual editing.	27
Figure 24. Correlation plot between calibration survey points and LiDAR data.....	32
Figure 25. Correlation plot between validation survey points and LiDAR data.	33
Figure 26. Map of Pamplona Floodplain with bathymetric survey points shown in blue.	34
Figure 27. Blocks (in blue) of Silaga building features that were subjected to QC	35
Figure 28. Extracted features for Pamplona Floodplain.	37
Figure 29. Extent of the bathymetric survey (in blue line) in Pamplona River	38
and the LiDAR data validation survey (in red).	38
Figure 30. The GNSS Network established in the Panplona River Survey.....	39
Figure 31. GNSS base set up, Trimble® SPS 985, at KAY-3, situated on top of a flood gate near Pudtol Municipal Building in Brgy. Imelda, Municipality of Pudtol, Cagayan	41
Figure 32. GNSS receiver setup, Trimble® SPS 882, at CG-343, located at the approach of Likban Bridge in Brgy. Libertad, Municipality of Abulug, Cagayan.....	41
Figure 33. GNSS receiver setup, Trimble® SPS 882, at CG-373, located at the approach of Bangan Bridge in Brgy. Bangan, Municipality of Sanchez Mira, Cagayan	42
Figure 34. GNSS receiver setup, Trimble® SPS 852, at UP-CLA, located at the approach of Cabicungan Bridge in Brgy. Dibalio, Municipality of Claveria, Cagayan.....	42
Figure 35. GNSS receiver setup, Trimble® SPS 882, at UP-LIN, located at the approach of Linao Bridge in Brgy. Bangag-Zingag, Municipality of Aparri, Cagayan	43
Figure 36. GNSS receiver setup, Trimble® SPS 985, at UP-PAM, located at the approach of New Pamplona Bridge in Brgy. Masi, Municipality of Pamplona, Cagayan.....	43

Figure 37. New Pamplona Bridge facing downstream.....	47
Figure 38. New Pamplona bridge cross-section location map.....	48
Figure 39. New Pamplona Bridge cross-section diagram	49
Figure 40. Bridge as-built form of New Pamplona Bridge	50
Figure 41. Water-level markings on New Pamplona Bridge	51
Figure 42. Validation points acquisition survey set up along Pamplona River Basin	51
Figure 43. Validation point acquisition survey of Pamplona River basin	52
Figure 44. Bathymetric survey using Ohmex™ single beam echo sounder in Pamplona River	53
Figure 45. Extent of the Pamplona River Bathymetry Survey.....	54
Figure 46. The Pamplona riverbed profile.	55
Figure 47. Location map of the Pamplona HEC-HMS model used for calibration.	56
Figure 48. Cross-section plot of Pamplona Bridge.....	57
Figure 49. Rainfall and outflow data used for modeling.....	57
Figure 50. Rainfall and outflow data of Pamplona River Basin, which was used for modeling.	58
Figure 51. Location of Aparri RIDF Station relative to Pamplona River Basin.....	59
Figure 52. Synthetic storm generated for a 24-hr period rainfall for various return periods.	59
Figure 53. Soil Map of Pamplona River Basin	60
Figure 54. Land Cover Map of Pamplona River Basin.....	61
Figure 55. Slope Map of Pamplona River Basin.....	62
Figure 56. Stream Delineation Map of Pamplona River Basin.....	63
Figure 57. Pamplona River Basin model generated in HEC-HMS.....	64
Figure 58. Linao River Cross-section generated using HEC GeoRAS tool.....	65
Figure 59. A screenshot of the river sub-catchment with the computational area to be modeled in FLO-2D Grid Developer System Pro (FLO-2D GDS Pro)	66
Figure 60. Outflow hydrograph of Pamplona produced by the HEC-HMS model compared with observed outflow	67
Figure 61. The Outflow hydrograph at the Pamplona Station generated using Aparri RIDF simulated in HEC-HMS.....	69
Figure 62. Sample output map of Pamplona RAS Model	70
Figure 63. A 100-year flood hazard map for Pamplona Floodplain	71
Figure 64. A 100-year Flow Depth Map for Pamplona Floodplain.....	72
Figure 65. A 25-year Flood Hazard Map for Pamplona Floodplain	73
Figure 66. A 25-year Flow Depth Map for Pamplona Floodplain.....	74
Figure 67. A 5-year Flood Hazard Map for Pamplona Floodplain	75
Figure 68. A 5-year Flow depth map for Pamplona Floodplain.	76
Figure 69. Affected Areas in Luna, Apayao during 5-Year Rainfall Return Period	77
Figure 70. Affected Areas in Pamplona, Cagayan during 5-Year Rainfall Return Period	79
Figure 71. Affected Areas in Pamplona, Cagayan during 5-Year Rainfall Return Period	79
Figure 72. Affected Areas in Sanchez-Mira, Cagayan during 5-Year Rainfall Return Period.....	80
Figure 73. Affected Areas in Luna, Apayao during 25-Year Rainfall Return Period	81
Figure 74. Affected Areas Pamplona, Cagayan during 25-Year Rainfall Return Period	83
Figure 75. Affected Areas Pamplona, Cagayan during 25-Year Rainfall Return Period	83
Figure 76. Affected Areas Sanchez-Mira, Cagayan during 25-Year Rainfall Return Period	84
Figure 77. Affected Areas Luna, Apayao during 100-Year Rainfall Return Period	85
Figure 78. Affected Areas Pamplona, Cagayan during 100-Year Rainfall Return Period	87
Figure 79. Affected Areas Pamplona, Cagayan during 100-Year Rainfall Return Period	87
Figure 80. Affected Areas Sanchez-Mira, Cagayan during 100-Year Rainfall Return Period	88
Figure 81. Pamplona Flood Validation Points	90
Figure 82. Flood map depth vs. actual flood depth.....	91



LIST OF ACRONYMS AND ABBREVIATIONS

AAC	Asian Aerospace Corporation	IMU	Inertial Measurement Unit
Ab	abutment	kts	knots
ALTM	Airborne LiDAR Terrain Mapper	LAS	LiDAR Data Exchange File format
ARG	automatic rain gauge	LC	Low Chord
AWLS	Automated Water Level Sensor	LGU	local government unit
BA	Bridge Approach	LiDAR	Light Detection and Ranging
BM	benchmark	LMS	LiDAR Mapping Suite
CAD	Computer-Aided Design	m AGL	meters Above Ground Level
CN	Curve Number	MMS	Mobile Mapping Suite
CSRS	Chief Science Research Specialist	MSL	mean sea level
DAC	Data Acquisition Component	NSTC	Northern Subtropical Convergence
DEM	Digital Elevation Model	PAF	Philippine Air Force
DENR	Department of Environment and Natural Resources	PAGASA	Philippine Atmospheric Geophysical and Astronomical Services Administration
DOST	Department of Science and Technology	PDOP	Positional Dilution of Precision
DPPC	Data Pre-Processing Component	PPK	Post-Processed Kinematic [technique]
DREAM	Disaster Risk and Exposure Assessment for Mitigation [Program]	PRF	Pulse Repetition Frequency
DRRM	Disaster Risk Reduction and Management	PTM	Philippine Transverse Mercator
DSM	Digital Surface Model	QC	Quality Check
DTM	Digital Terrain Model	QT	Quick Terrain [Modeler]
DVBC	Data Validation and Bathymetry Component	RA	Research Associate
FMC	Flood Modeling Component	RIDF	Rainfall-Intensity-Duration-Frequency
FOV	Field of View	RMSE	Root Mean Square Error
GiA	Grants-in-Aid	SAR	Synthetic Aperture Radar
GCP	Ground Control Point	SCS	Soil Conservation Service
GNSS	Global Navigation Satellite System	SRTM	Shuttle Radar Topography Mission
GPS	Global Positioning System	SRS	Science Research Specialist
HEC-HMS	Hydrologic Engineering Center - Hydrologic Modeling System	SSG	Special Service Group
HEC-RAS	Hydrologic Engineering Center - River Analysis System	TBC	Thermal Barrier Coatings
HC	High Chord	UP-TCAGP	University of the Philippines – Training Center for Applied Geodesy and Photogrammetry
IDW	Inverse Distance Weighted [interpolation method]	UTM	Universal Transverse Mercator
ISU	Isabela State University	WGS	World Geodetic System

CHAPTER 1: OVERVIEW OF THE PROGRAM AND GUINARONA RIVER

Enrico C. Paringit, Dr. Eng., and Engr. Florentino Morales, Jr.

1.1 Background of the Phil-LIDAR 1 Program

The University of the Philippines Training Center for Applied Geodesy and Photogrammetry (UP-TCAGP) launched a research program entitled “Nationwide Hazard Mapping using LiDAR” or Phil-LiDAR 1, supported by the Department of Science and Technology (DOST) Grants-in-Aid (GiA) Program. The program was primarily aimed at acquiring a national elevation and resource dataset at sufficient resolution to produce information necessary to support the different phases of disaster management. Particularly, it targeted to operationalize the development of flood hazard models that would produce updated and detailed flood hazard maps for the major river systems in the country.

Also, the program was aimed at producing an up-to-date and detailed national elevation dataset suitable for 1:5,000 scale mapping, with 50 cm and 20 cm horizontal and vertical accuracies, respectively. These accuracies were achieved through the use of the state-of-the-art Light Detection and Ranging (LiDAR) airborne technology procured by the project through DOST.

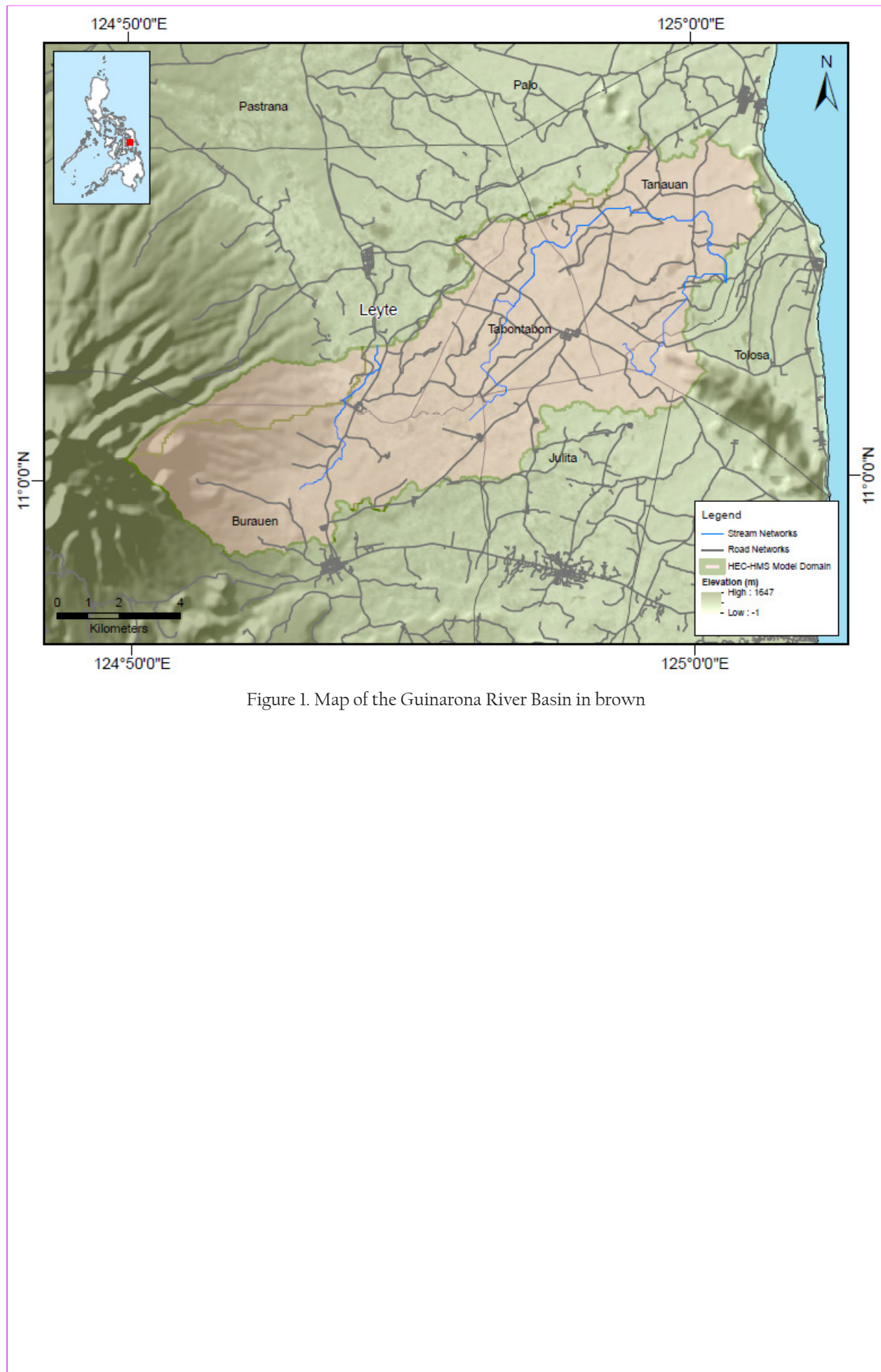
The methods applied in this report are thoroughly described in a separate publication entitled “FLOOD MAPPING OF RIVERS IN THE PHILIPPINES USING AIRBORNE LIDAR: METHODS” (Paringit, et. Al. 2017).

The implementing partner university for the Phil-LiDAR 1 Program is the Visayas State University (VSU). VSU is in charge of processing LiDAR data and conducting data validation reconnaissance, cross section, bathymetric survey, validation, river flow measurements, flood height and extent data gathering, flood modeling, and flood map generation for the 28 river basins in the Eastern Visayas Region. The university is located in Baybay in the province of Leyte.

1.2 Overview of the Guinarona River Basin

Guinarona River Basin covers the majority of the Municipalities of Tanauan, Tabontabon, and Burauen, and some of three (3) municipalities in Leyte. The DENR River Basin Control Office identified the basin to have a drainage area of 298.947 km² (RBCO, 2016).

Its main stem, Guinarona River, is part of the 28 river systems in Eastern Visayas Region. According to the 2015 national census of NSO, a total of 8,282 persons are residing within the immediate vicinity of the river which is distributed among five (5) barangays in the Municipalities of Tolosa and Tanauan (NSO, 2015). The Municipality of Tanauan is known in the province for making many home industrial products such as bamboo craft, pottery, mat weaving, bolo making, broom making, etc. (source: <http://archives.pia.gov.ph/?m=12&sec=reader&rp=3&fi=p070326.htm&no=22&date=>). Aside from these locally produced goods, their economy thrive from agriculture, livestock, fishing, and the like (source: “Feasibility Study for the Modernization of the New Tanauan Public Market”. Strategic and Comprehensive Consultants, Inc. 2008). Super typhoon Yolanda, also known internationally as Haiyan, was the strongest typhoon that hit the region on November 2013 where a million families were affected. Up to now, effects from the devastation is still evident as seen from thousands of casualties and damages in houses, infrastructure, agriculture, etc. Yolanda was identified to be a category 5 in the Saffir-Simpson Hurricane Wind Scale (source: <http://edition.cnn.com/2013/11/07/world/asia/philippines-typhoon-haiyan/>).



CHAPTER 2: LIDAR DATA ACQUISITION OF THE GUINARONA FLOODPLAIN

Engr. Ma. Rosario Concepcion O. Ang, Engr. John Louie D. Fabila, Engr. Sarah Jane D. Samalburro, Engr. Harmond F. Santos, Engr. Gladys Mae Apat, Engr. Melanie C. Hingpit, Jovy Anne S. Narisma, Engr. Vincent Louise DL. Azucena, Nereo Joshua G. Pecson, Areanne Katrice K. Umali

The methods applied in this Chapter were based on the DREAM methods manual (Sarmiento, et al., 2014) and further enhanced and updated in Paringit, et al. (2017).

2.1 Flight Plans

Plans were made to acquire LiDAR data within the delineated priority area for Guinarona floodplain in Leyte province. These missions were planned for 20 lines that run for at most four and a half (4.5) hours including take-off, landing and turning time. The flight planning parameters for the Aquarius and Gemini LiDAR systems used are found in Tables 1 and 2, respectively. Figures 2 and 3 show the flight plans for Guinarona floodplain. Annex 1 shows the technical specification of the Aquarius and Gemini LiDAR systems and the aerial camera.

Table 1. Flight planning parameters for Aquarius LiDAR system

Block Name	Flying Height (m AGL)	Overlap (%)	Field of View (θ)	Pulse Repetition Frequency (PRF) (kHz)	Scan Frequency (Hz)	Average Speed (kts)	Average Turn Time (Minutes)
BLK34A	690	30	50	70	40	120	5
BLK34B	600	30	50	70	40	120	5
BLK34K	690/650	30	36	50	50	120	5

Table 2. Flight planning parameters for Gemini LiDAR system

Block Name	Flying Height (m AGL)	Overlap (%)	Field of View (θ)	Pulse Repetition Frequency (PRF) (kHz)	Scan Frequency (Hz)	Average Speed (kts)	Average Turn Time (Minutes)
BLK34A	1200	30	34	100	50	120	5
BLK34B	950	30	40	100	50	120	5
BLK34C	950/700	30	40/50	100	50/40	120	5
BLK34D	650	30	50	100	40	120	5
BLK34E	700	30	50	100	40	120	5
BLK34G	1200/700	30	34/50	100	50/40	120	5

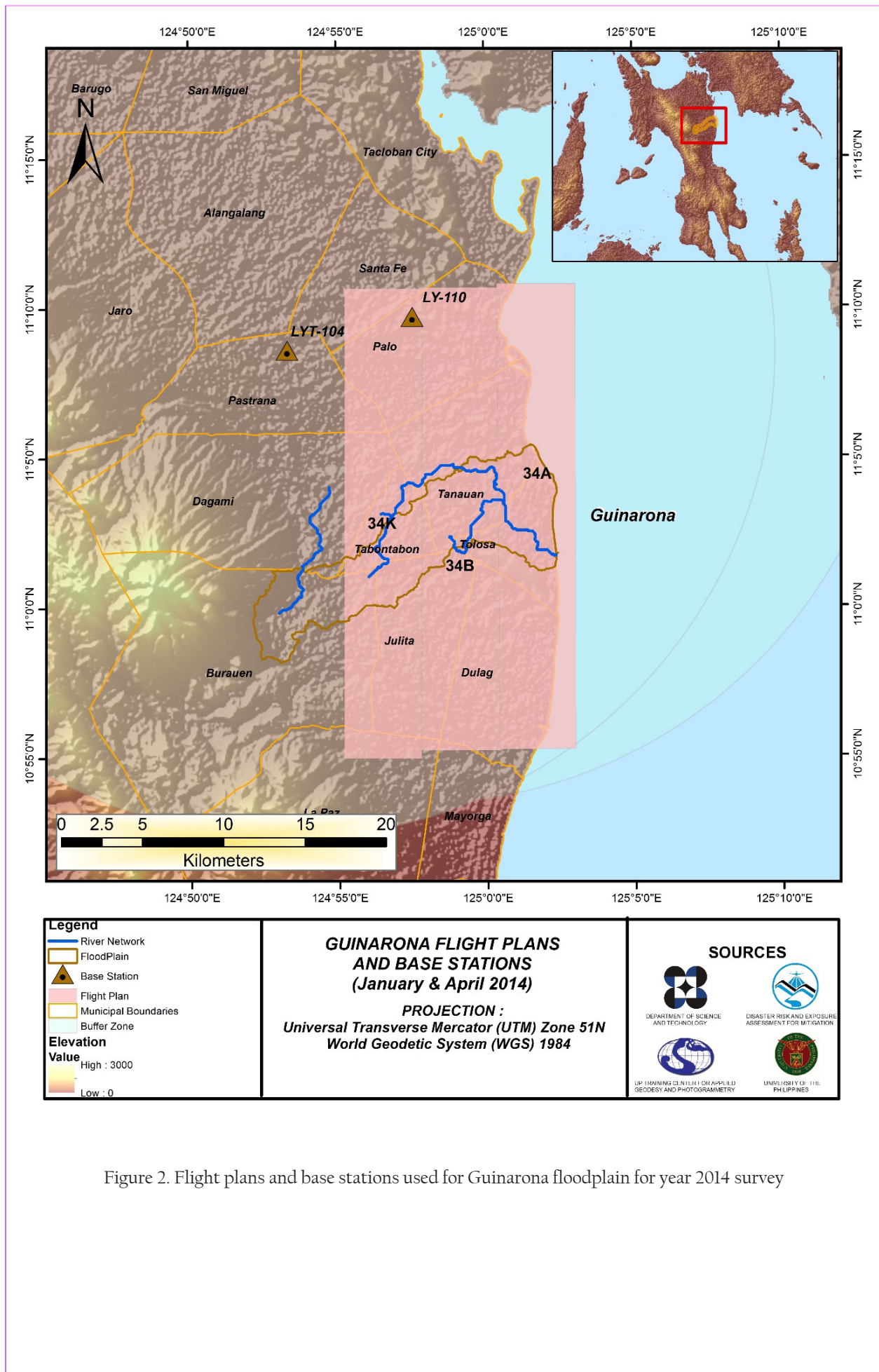


Figure 2. Flight plans and base stations used for Guinarona floodplain for year 2014 survey

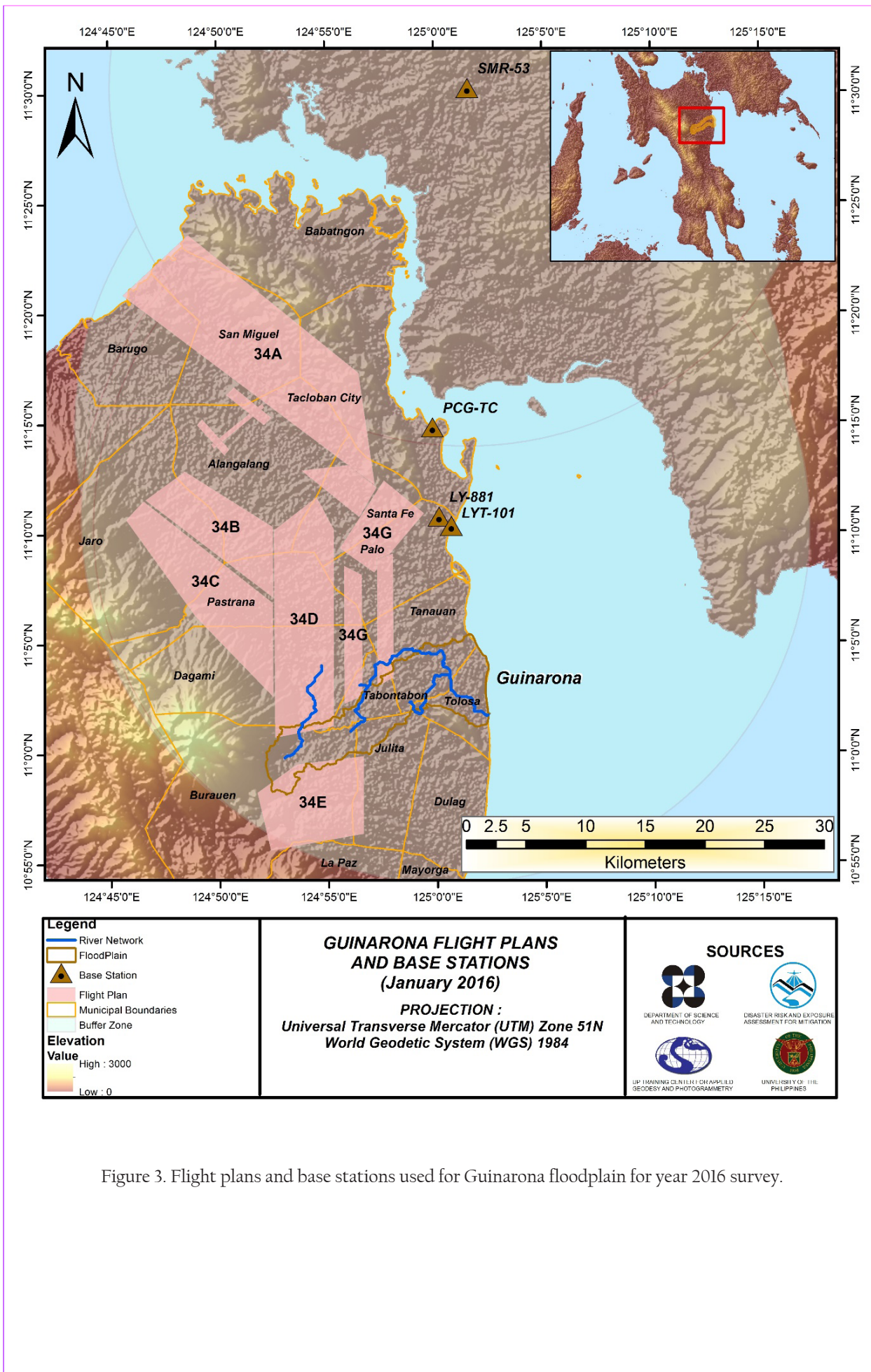


Figure 3. Flight plans and base stations used for Guinarona floodplain for year 2016 survey.

2.2 Ground Base Stations

Two (2) NAMRIA second order accuracy ground control points (GCP): LYT-101 and SMR-53 were recovered for use as base station during the survey. LYT-104 is a 3rd order NAMRIA GCP and was re-processed as 2nd order GCP to satisfy the project’s accuracy requirement. Also, LY-110 and LY-881 which are high-accuracy benchmarks were used and also re-processed as 2nd order horizontal control point for the project’s accuracy. The certifications for the NAMRIA reference points are found in Annex 2 while the baseline processing reports are found in Annex 3. These were used as base stations or reference points during flight operations for the entire duration of the survey (January 26-27 & April 20, 2014 and January 22-24, 2016). Base stations were observed using dual frequency GPS receivers, TRIMBLE SPS 852, SPS 882, and SPS 985. Flight plans and location of base stations used during the aerial LiDAR acquisition in Guinarona floodplain are shown in Figure 1 above.

Figure 4 to Figure 8 show the recovered NAMRIA reference points within the area, while Table 3 to Table 8 show the corresponding details about the following NAMRIA control stations and established points. In addition, Table 9 shows the list of all ground control points occupied in line with their respective mission names and flight numbers, together with the dates of acquisition.

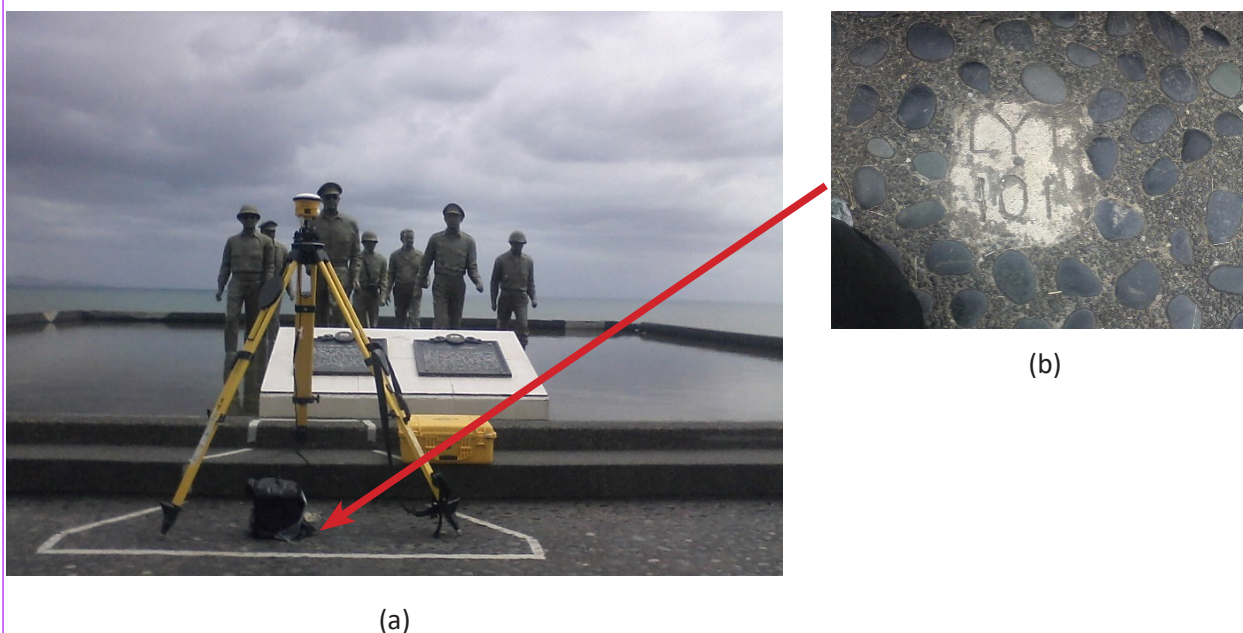


Figure 4. (a) GPS set-up over LYT-101 situated within the premises of MacArthur’s Landing Memorial Park, Palo, Leyte and (b) NAMRIA reference point LYT-101 as recovered by field team.

Table 3. Details of the recovered NAMRIA horizontal control point LYT-101 used as base station for the LiDAR data acquisition

Station Name	LYT-101	
Order of Accuracy	2nd Order	
Relative Error (horizontal positioning)	1 in 50,000	
Geographic Coordinates, Philippine Reference of 1992 Datum (PRS 92)	Latitude Longitude Ellipsoidal Height	11° 10' 23.89707" North 125° 0' 38.62071" East 6.58600 meters
Grid Coordinates, Philippine Transverse Mercator Zone 5 (PTM Zone 5 PRS 92)	Easting Northing	501,171.719 meters 1,235,497.253 meters
Geographic Coordinates, World Geodetic System 1984 Datum (WGS 84)	Latitude Longitude Ellipsoidal Height	11° 10' 19.64869" North 125° 0' 43.78230" East 69.02100 meters
Grid Coordinates, Universal Transverse Mercator Zone 51 North (UTM 51N WGS 1984)	Easting Northing	719,575.03 meters 1,235,811.61 meters

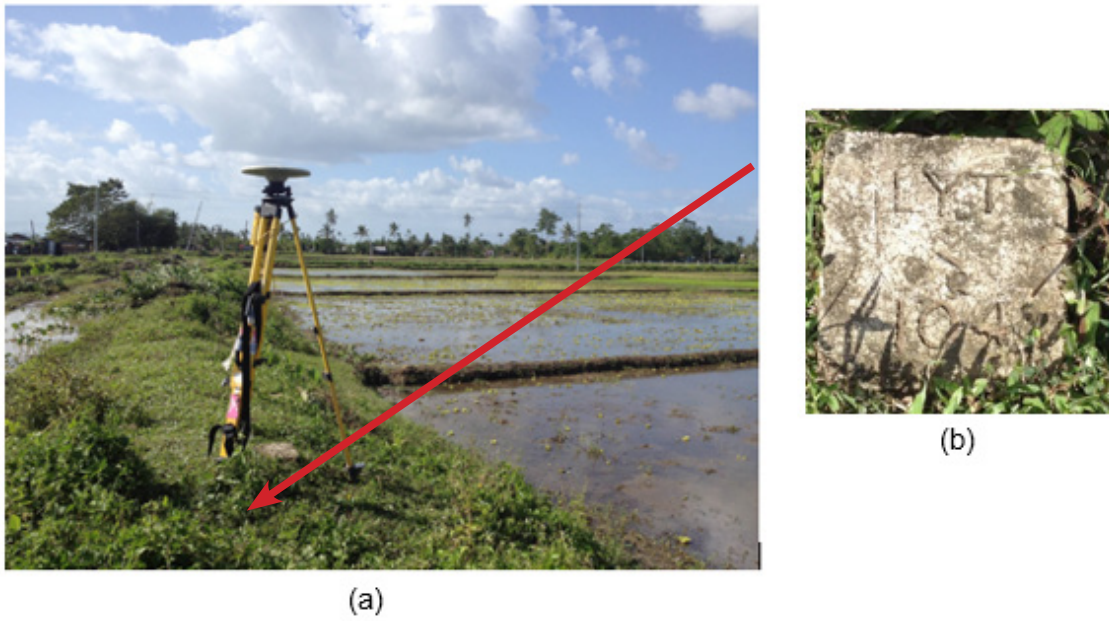


Figure 5. (a) GPS set-up over LYT-104 located and re-established along rice paddy trail, approximately 90 meters from the centerline, east side of Pastrana-Santa Fe Road, District IV, Pastrana, Leyte and (b) NAMRIA reference point LYT-104 as recovered by the field team

Table 4. Details of the recovered and re-established NAMRIA horizontal control point LYT-104 used as base station for the LiDAR data acquisition

Station Name	LYT-104	
Order of Accuracy	2nd Order	
Relative Error (horizontal positioning)	1 in 50,000	
Geographic Coordinates, Philippine Reference of 1992 Datum (PRS 92)	Latitude Longitude Ellipsoidal Height	11° 08' 38.92234" North 124° 53' 13.52786" East 33.659 meters
Geographic Coordinates, World Geodetic System 1984 Datum (WGS 84)	Easting Northing Ellipsoidal Height	11° 08' 34.67033" North 124° 53' 18.69323" East 95.861 meters
Geographic Coordinates, World Geodetic System 1984 Datum (WGS 84)	Latitude Longitude	706,089.510 meters 1,232,496.838 meters

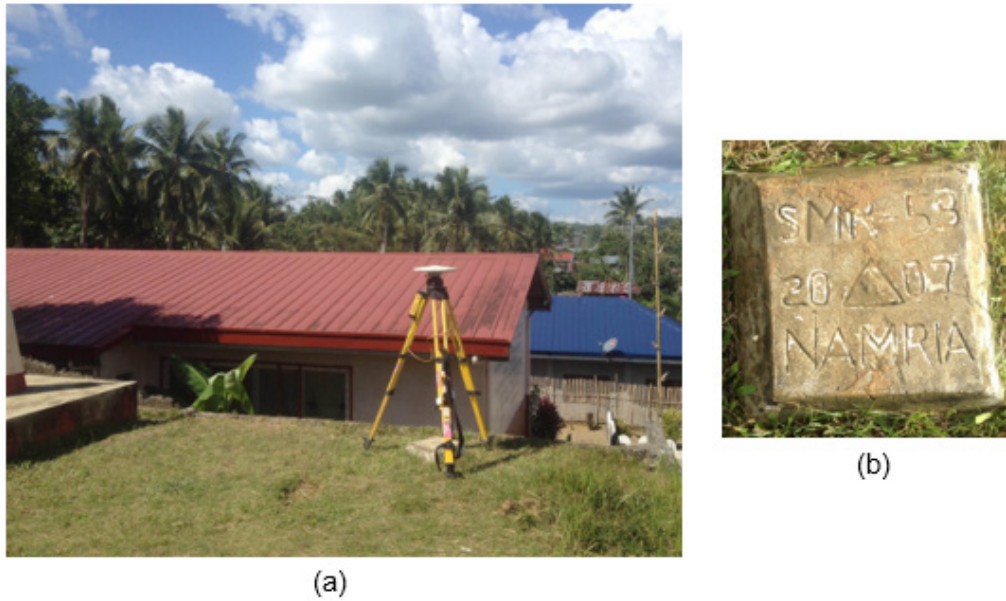


Figure 6. (a) GPS set-up over SMR-53 located near the school building flag pole of San Isidro Elementary, Brgy. San Isidro, Santa Rita and (b) NAMRIA reference point SMR-53 as recovered by the field team

Table 5. Details of the recovered NAMRIA horizontal control point SMR-53 used as base station for the LiDAR data acquisition

Station Name	SMR-53	
Order of Accuracy	2nd Order	
Relative Error (horizontal positioning)	1 in 50,000	
Geographic Coordinates, Philippine Reference of 1992 Datum (PRS 92)	Latitude Longitude Ellipsoidal Height	11° 30' 17.85657" North 125° 1' 29.837339" East 26.13400 meters
Grid Coordinates, Philippine Transverse Mercator Zone 5 (PTM Zone 5 PRS 92)	Easting Northing	502,722.403 meters 1,272,180.079 meters
Geographic Coordinates, World Geodetic System 1984 Datum (WGS 84)	Latitude Longitude Ellipsoidal Height	11° 30' 13.52495" North 125° 1' 34.96980" East 87.78700 meters
Grid Coordinates, Universal Transverse Mercator Zone 51 North (UTM 51N PRS 1992)	Easting Northing	720,874.14 meters 1,272,513.40 meters

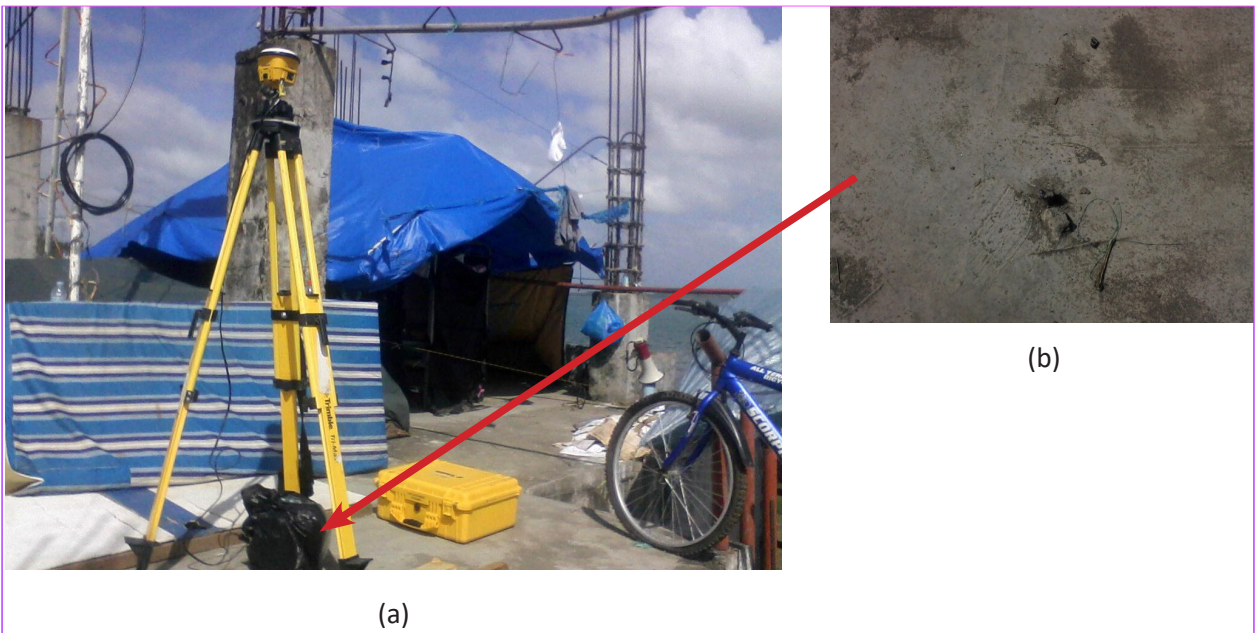


Figure 7. (a) GPS set-up over established Ground Control Point by the team on the rooftop of Philippine Coast Guard Tacloban Station, Kuta Kankabato, San Jose, Tacloban City and (b) established reference point PGC-TC as recovered by the field team

Table 6. Details of the established control point PGC-TC used as temporary base station for the LiDAR data acquisition.

Station Name	PCG-TC	
Order of Accuracy	2nd Order	
Relative Error (horizontal positioning)	1 in 50,000	
Geographic Coordinates, World Geodetic System 1984 Datum (WGS 84)	Latitude	11° 10' 19.64869" North
	Longitude	124° 59' 53.38556" East
	Ellipsoidal Height	70.882 meters
Grid Coordinates, Universal Transverse Mercator Zone 51 North (UTM 51N WGS 1984)	Easting	718,144.536 meters
	Northing	1,244,004.859 meters

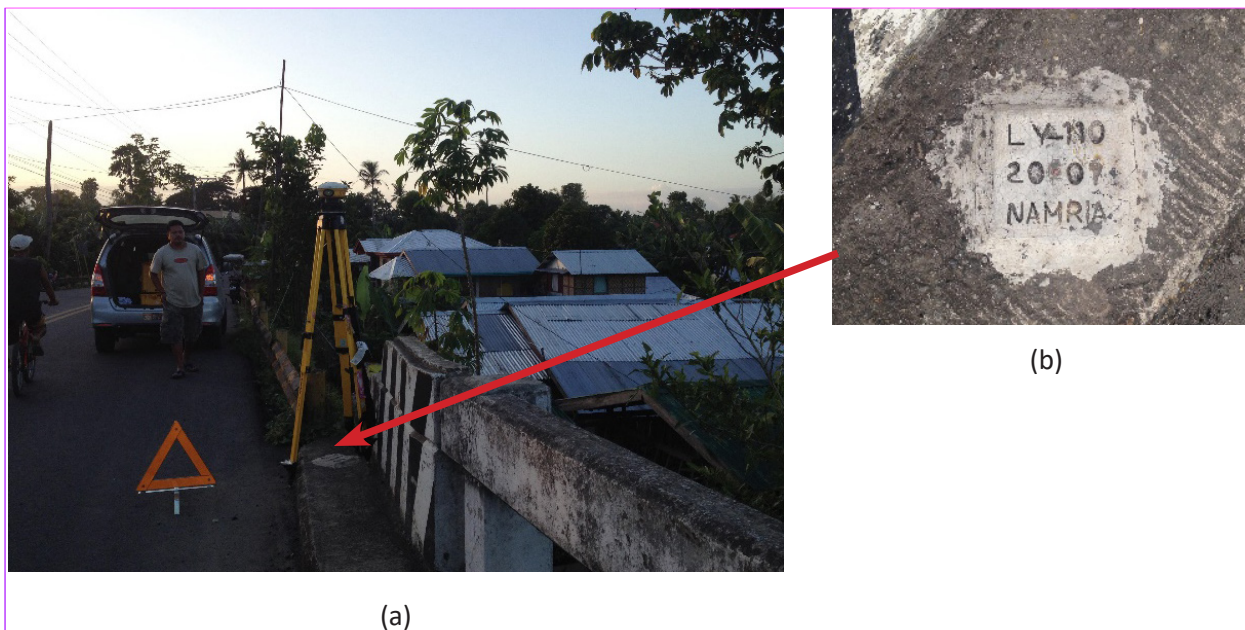


Figure 8. (a) GPS set-up over LY-110 on a bridge located about 225 meters of km. post 919, road leading to Ormoc City and (b) NAMRIA reference point LY-110 as recovered by the field team

Table 7. Details of the recovered NAMRIA Benchmark LY-110 used as base station for the LiDAR data acquisition

Station Name		LY-110
Order of Accuracy		1st Order
Relative Error (horizontal positioning)		1 in 100,000
Geographic Coordinates, Philippine Reference of 1992 Datum (PRS 92)	Latitude	11° 10' 19.48389" North
	Longitude	124° 57' 32.98736" East
	Ellipsoidal Height	14.336 meters
Geographic Coordinates, World Geodetic System 1984 Datum (WGS 84)	Latitude	11° 10' 15.23095" North
	Longitude	124° 57' 38.14961" East
	Ellipsoidal Height	76.647 meters
Grid Coordinates, Universal Transverse Mercator Zone 51 North (UTM 51N WGS 1984)	Easting	713,942.863 meters
	Northing	1,234,538.117 meters

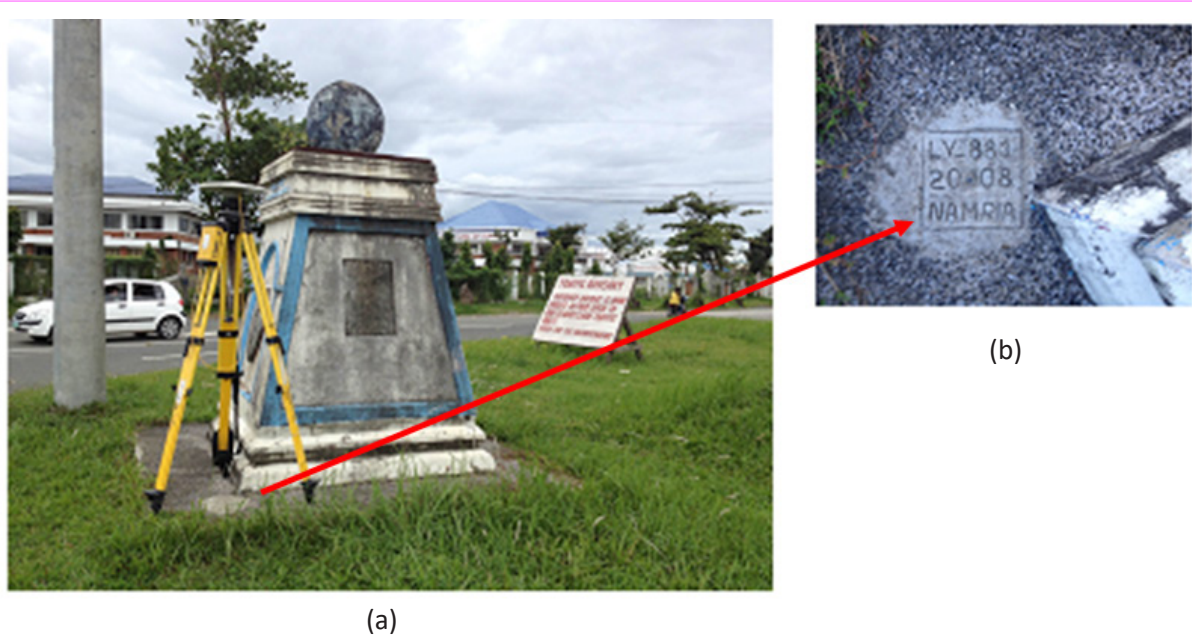


Figure 9. (a) GPS set-up over LY-881 located at the concrete foundation of Governor Center Welcome sign at the junction of the road going to Ormoc, Samar, Tacloban and MacArthur Landing Memorial Park in Brgy. Pawing, Palo, Leyte and (b) NAMRIA reference point L

Table 8. Details of the recovered NAMRIA Benchmark LY-881 used as base station for the LiDAR data acquisition

Station Name	LY-881	
Order of Accuracy	1st Order	
Relative Error (horizontal positioning)	1 in 100, 000	
Geographic Coordinates, Philippine Reference of 1992 Datum (PRS 92)	Latitude Longitude Ellipsoidal Height	11o 10' 50.05" North 125o 00' 05.58" East 5.96 meters
Geographic Coordinates, World Geodetic System 1984 Datum (WGS 84)	Latitude Longitude Ellipsoidal Height	11o 10' 45.19178" North 125o 00' 09.85226" East 68.330 meters
Grid Coordinates, Universal Transverse Mercator Zone 51 North (UTM 51N WGS 1984)	Easting Northing	718,694.89 meters 1,236,537.244 meters

Table 9. Ground control points used during LiDAR data acquisition

Date Surveyed	Flight Number	Mission Name	Ground Control Points
26-JAN-14	1026A	3BLK33AS34A026A	LYT-101 & PCG-TC
27-JAN-14	1028A	3BLK3433S027A	LYT-101 & PCG-TC
20-APR-14	1358A	3BLK34F110A	LYT-101 & LY-881
20-APR-14	1360A	3BLK34KS110B	SMR-53 & LY-881
22-JAN-16	3765G	2BLK34AD022A	LYT-104 & LY-110
23-JAN-16	3769G	2BLK34ADEG023A	LYT-104 & LY-110
23-JAN-16	3771G	2BLK34BCG023B	LYT-104 & LY-110
24-JAN-16	3773G	2BLK34CG024A	LYT-104 & LY-110

2.3 Flight Missions

Eight (8) missions were conducted to complete LiDAR data acquisition in Guinarona Floodplain, for a total of thirty hours and forty-nine minutes (30+49) of flying time for RP-C9122 and RP-C9322. All missions were acquired using Aquarius and Gemini LiDAR systems. The team line-up is shown in Annex 4. Table 10 shows the total area of actual coverage and the corresponding flying hours per mission, while Table 11 presents the actual parameters used during the LiDAR data acquisition. The data transfer sheet, flight logs and flight status reports of each mission are shown in Annexes 5, 6 and 7 respectively.

Table 10. Flight missions for LiDAR data acquisition in Guinarona floodplain

Date Surveyed	Flight Number	Flight Plan Area (km ²)	Surveyed Area (km ²)	Area Surveyed within the Floodplain (km ²)	Area Surveyed Outside the Floodplain (km ²)	Number of Images	Flying Hours	
							Hr	Min
26-Jan-14	1026A	136.116	102.515	12.967	89.548	857	2	47
27-Jan-14	1028A	140.342	205.354	38.075	167.279	1546	4	25
20-Apr-14	1358A	137.389	121.293	19.283	102.010	1194	4	11
20-Apr-14	1360A	137.389	71.461	8.040	63.421	670	3	23
22-Jan-16	3765G	248.104	180.764	4.352	176.413	0	4	11
23-Jan-16	3769G	318.850	171.755	13.731	158.024	0	4	12
23-Jan-16	3771G	132.586	150.854	1.968	148.886	0	3	29
24-Jan-16	3773G	117.396	101.527	0.000	101.527	0	4	11
TOTAL		1368.172	1105.523	98.416	1007.107	4267	30	49

Table 11. Actual parameters used during LiDAR data acquisition

Flight Number	Flying Height (m AGL)	Overlap (%)	FOV (θ)	PRF (khz)	Scan Frequency (Hz)	Average Speed (kts)	Average Turn Time (Minutes)
1026A	690	30	50	70	40	120	5
1028A	690	30	50	70	40	120	5
1358A	690	30	36	50	50	120	5
1360A	650	30	36	50	50	120	5
3765G	1200/650	30	34/50	100	50/40	120	5
3769G	1200/700	30	34/50	100	50/40	120	5
3771G	950	30	40	100	50	120	5
3773G	700	30	50	100	40	120	5

2.4 Survey Coverage

Guinarona floodplain is located in the province of Leyte situated in the municipalities of Tabontabon, Tanauan, Tolosa, Julita, and Burauen. LiDAR swath coverage for these flights also covers most parts of the municipalities of Alangalang, Dagami, Dulag, Palo, Pastrana, and Santa Fe. The list of municipalities and/or cities surveyed with at least one (1) square kilometer coverage is shown in Table 12. The actual coverage of the LiDAR acquisition for Guinarona Floodplain is presented in Figure 10.

Table 12. List of municipalities and/or cities surveyed during Guinarona floodplain LiDAR survey

Province	City/Municipality	Area of Municipality/City (km ²)	Total Area Surveyed (km ²)	Percentage of Area Surveyed
Leyte	Alangalang	145.446401	79.016167	54%
Leyte	Babatngon	136.571086	7.925334	6%
Leyte	Barugo	81.25045	19.901193	24%
Leyte	Burauen	205.307409	69.17009	34%
Leyte	Dagami	134.083191	77.842459	58%
Leyte	Dulag	63.649594	61.608494	97%
Leyte	Jaro	190.656879	58.360644	31%
Leyte	Julita	57.163995	57.163962	100%
Leyte	La Paz	136.017155	14.739685	11%
Leyte	Mayorga	39.454949	2.027544	5%
Leyte	Palo	65.337085	63.158229	97%
Leyte	Pastrana	79.170461	68.069465	86%
Leyte	San Miguel	103.859824	48.813917	47%
Leyte	Santa Fe	57.145249	54.398617	95%
Leyte	Tabontabon	20.456369	20.456369	100%
Leyte	Tacloban City	118.457964	14.103871	12%
Leyte	Tanauan	62.776965	62.56637	100%
Leyte	Tolosa	28.173553	28.06913	100%
	TOTAL	1724.98	807.39	46.81%

CHAPTER 3: LIDAR DATA PROCESSING FOR GUINARONA FLOODPLAIN

Engr. Ma. Rosario Concepcion O. Ang, Engr. John Louie D. Fabila, Engr. Sarah Jane D. Samalburo, Engr. Harmond F. Santos, Engr. Gladys Mae Apat, Engr. Melanie C. Hingpit, Jovy Anne S. Narisma, Engr. Vincent Louise DL. Azucena, Nereo Joshua G. Pecson, Areanne Katrice K. Umali

The methods applied in this Chapter were based on the DREAM methods manual (Ang, et al., 2014) and further enhanced and updated in Paringit, et al. (2017).

3.1 LiDAR Data Processing for Guinarona Floodplain

3.1.1 Overview of the LiDAR Date Pre-Processing

The data transmitted by the Data Acquisition Component are checked for completeness based on the list of raw files required to proceed with the pre-processing of the LiDAR data. Upon acceptance of the LiDAR field data, georeferencing of the flight trajectory is done in order to obtain the exact location of the LiDAR sensor when the laser was shot. Point cloud georectification is performed to incorporate correct position and orientation for each point acquired. The georectified LiDAR point clouds are subject for quality checking to ensure that the required accuracies of the program, which are the minimum point density, vertical and horizontal accuracies, are met. The point clouds are then classified into various classes before generating Digital Elevation Models such as Digital Terrain Model and Digital Surface Model.

Using the elevation of points gathered in the field, the LiDAR-derived digital models are calibrated. Portions of the river that are barely penetrated by the LiDAR system are replaced by the actual river geometry measured from the field by the Data Validation and Bathymetry Component. LiDAR acquired temporally are then mosaicked to completely cover the target river systems in the Philippines. Orthorectification of images acquired simultaneously with the LiDAR data is done through the help of the georectified point clouds and the metadata containing the time the image was captured.

These processes are summarized in the flowchart shown in Figure 11.

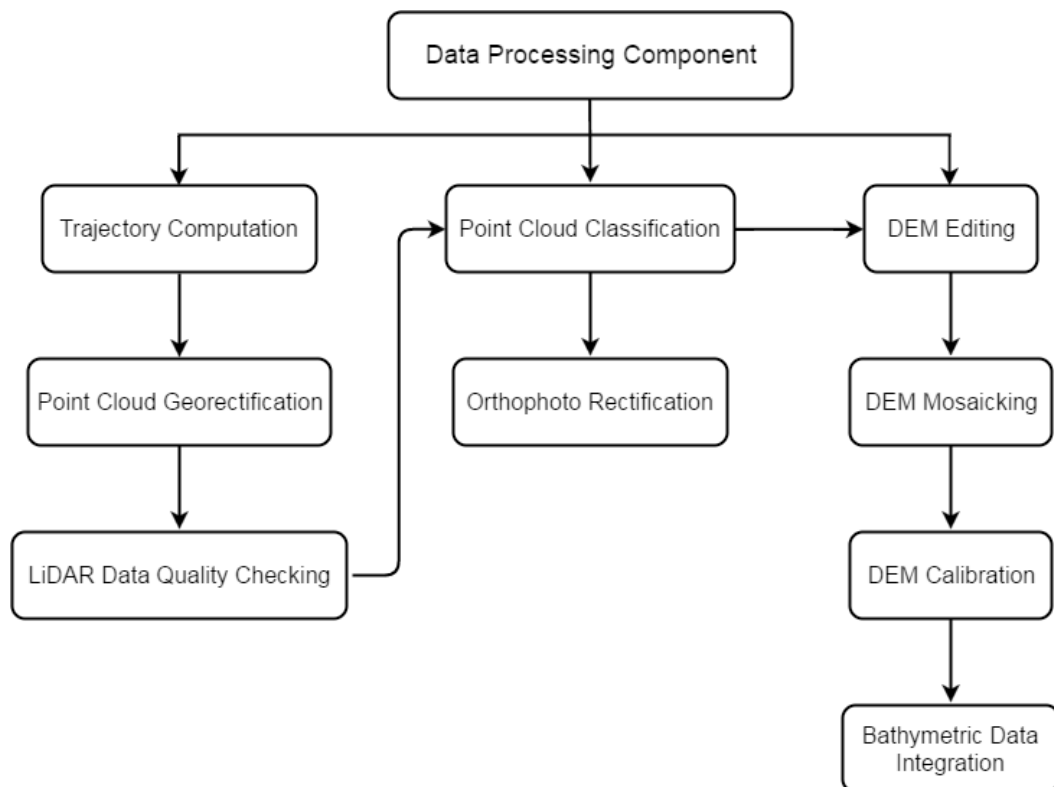


Figure 11. Schematic Diagram for Data Pre-Processing Component

3.2 Transmittal of Acquired LiDAR Data

Data transfer sheets for all the LiDAR missions for Guinarona floodplain can be found in Annex 5. Missions flown during the first survey conducted on January 2014 used the Airborne LiDAR Terrain Mapper (ALTM™ Optech Inc.) Aquarius system while missions acquired during the second survey on January 2016 were flown using the Gemini system over Province of Leyte. The Data Acquisition Component (DAC) transferred a total of 148.68 Gigabytes of Range data, 1.91 Gigabytes of POS data, 104.1 Megabytes of GPS base station data, and 298.5 Gigabytes of raw image data to the data server on April 20, 2014 for the first survey and January 23, 2016 for the second survey. The Data Pre-processing Component (DPPC) verified the completeness of the transferred data. The whole dataset for Guinarona was fully transferred on February 12, 2016, as indicated on the Data Transfer Sheets for Guinarona floodplain (Annex 5).

3.3 Trajectory Computation

The *Smoothed Performance Metric* parameters of the computed trajectory for flight 3769G, one of the Guinarona flights, which is the North, East, and Down position RMSE values are shown in Figure 12. The x-axis corresponds to the time of flight, which is measured by the number of seconds from the midnight of the start of the GPS week, which on that week fell on January 23, 2016 00:00AM. The y-axis is the RMSE value for that particular position.

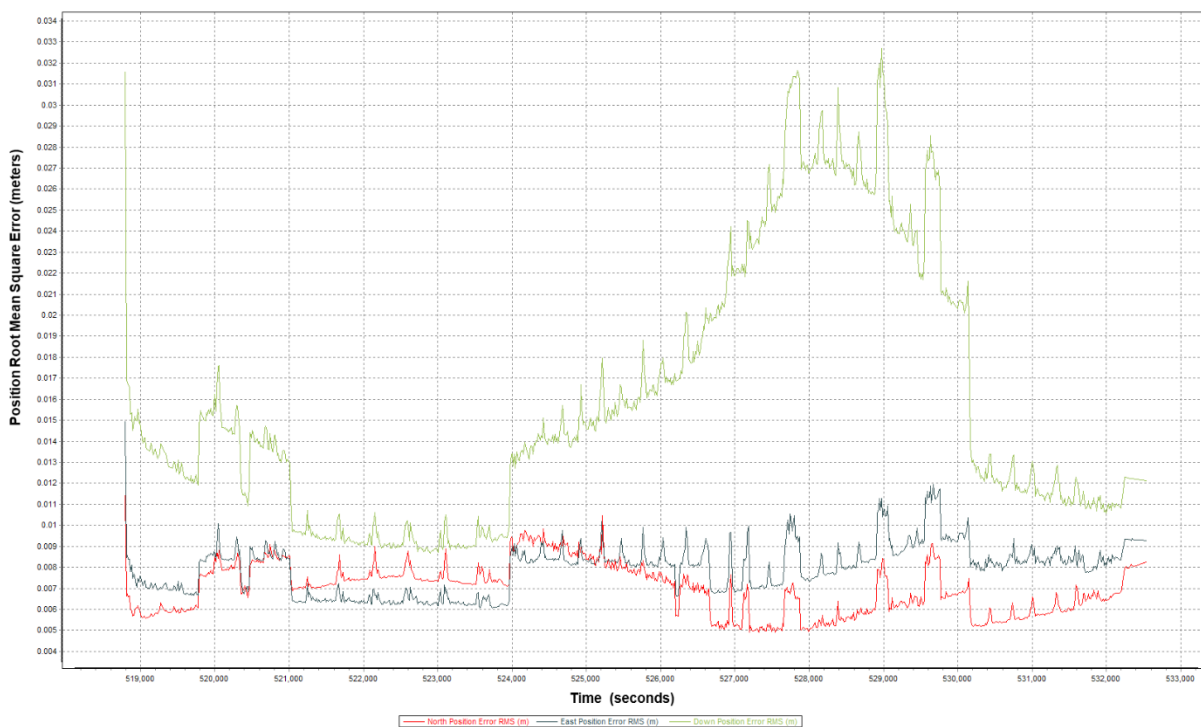


Figure 12. Smoothed Performance Metric Parameters of a Guinarona Flight 3769G

The time of flight was from 518800 seconds to 532600 seconds, which corresponds to morning of January 23, 2016. The initial spike that is seen on the data corresponds to the time that the aircraft was getting into position to start the acquisition, and the POS system starts computing for the position and orientation of the aircraft. Redundant measurements from the POS system quickly minimized the RMSE value of the positions. The periodic increase in RMSE values from an otherwise smoothly curving RMSE values correspond to the turn-around period of the aircraft, when the aircraft makes a turn to start a new flight line. Figure 12 shows that the North position RMSE peaks at 1.05 centimeters, the East position RMSE peaks at 1.20 centimeters, and the Down position RMSE peaks at 3.30 centimeters, which are within the prescribed accuracies described in the methodology.

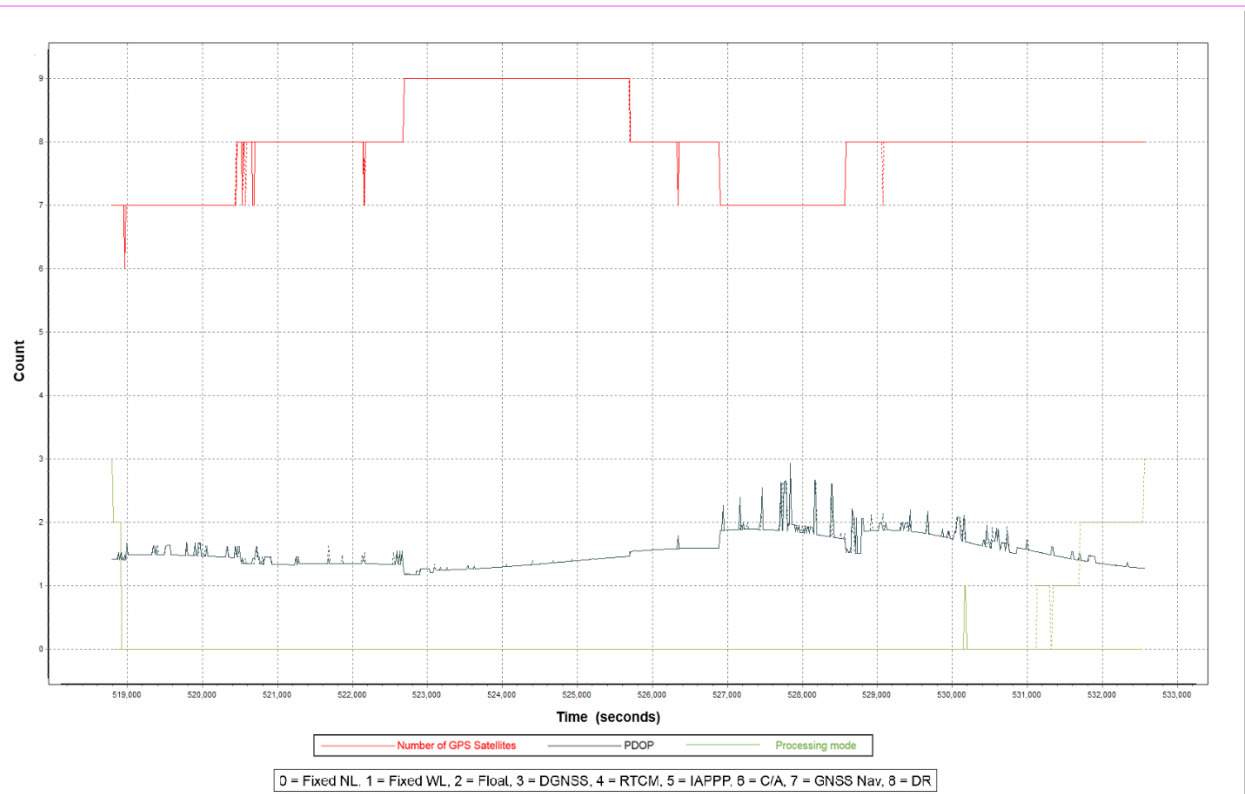


Figure 13. Solution Status Parameters of Guinarona Flight 3769G

The *Solution Status* parameters of flight 3769G, one of the Guinarona flights, which are the number of GPS satellites, Positional Dilution of Precision (PDOP), and the GPS processing mode used, are shown in Figure 13. The graphs indicate that the number of satellites during the acquisition did not go down to 6. Majority of the time, the number of satellites tracked was between 6 and 9. The PDOP value also did not go above the value of 3, which indicates optimal GPS geometry. The processing mode stayed at the value of 0 for majority of the survey with some peaks up to 1 attributed to the turns performed by the aircraft. The value of 0 corresponds to a Fixed, Narrow-Lane mode, which is the optimum carrier-cycle integer ambiguity resolution technique available for POSPAC MMS. All of the parameters adhered to the accuracy requirements for optimal trajectory solutions, as indicated in the methodology. The computed best estimated trajectory for all Guinarona flights is shown in Figure 14.

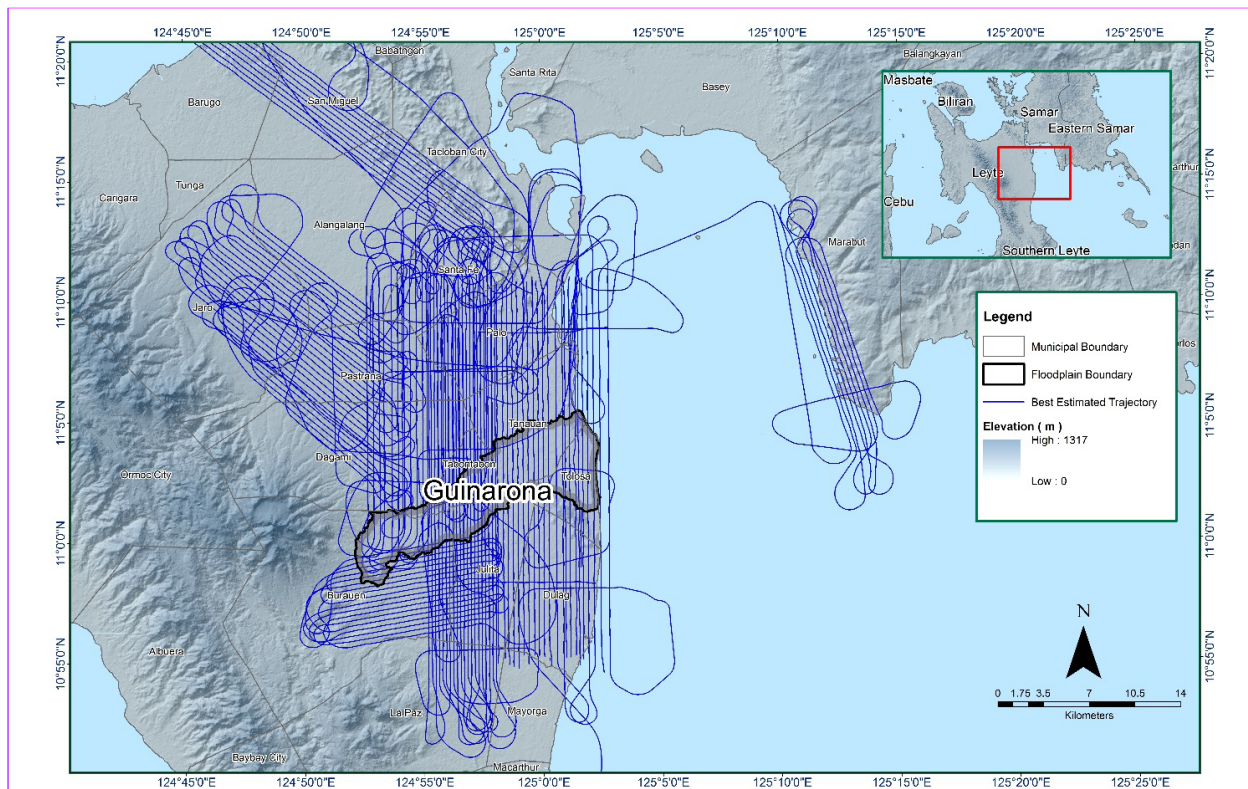


Figure 14. The best estimated trajectory of the LiDAR missions conducted over the Guinarona floodplain

3.4 LiDAR Point Cloud Computation

The produced LAS data contains 131 flight lines, with each flight line containing one channel, since the Gemini and Aquarius systems both contain one channel only. The summary of the self-calibration results obtained from LiDAR processing in LiDAR Mapping Suite (LMS) software for all flights over Guinarona floodplain are given in Table 13.

Table 13. Self-Calibration Results values for Guinarona flights

Parameter	Computed Value
Boresight Correction stdev	(<0.001degrees) 0.000767
IMU Attitude Correction Roll and Pitch Corrections stdev	(<0.001degrees) 0.000949
GPS Position Z-correction stdev	(<0.01meters) 0.0063

The optimum accuracy is obtained for all Guinarona flights based on the computed standard deviations of the corrections of the orientation parameters. Standard deviation values for individual blocks are available in the Annex 8. Mission Summary Reports.

3.5 LiDAR Data Quality Checking

The boundary of the processed LiDAR data on top of a SAR Elevation Data over Guinarona Floodplain is shown in Figure 15. The map shows gaps in the LiDAR coverage that are attributed to cloud coverage.

The total area covered by the Guinarona missions is 841.05 sq.km that is comprised of nine (9) flight acquisitions grouped and merged into nine (9) blocks as shown in Table 14.

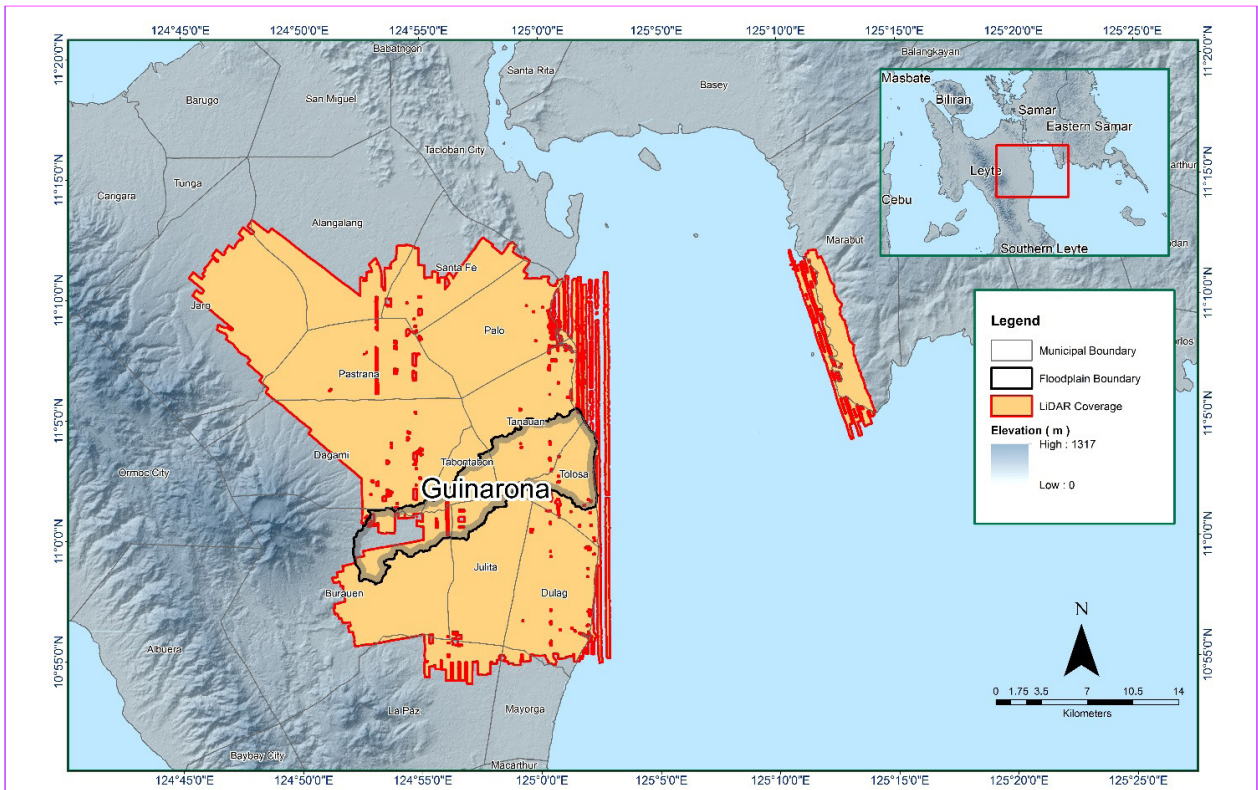


Figure 15. Boundary of the processed LiDAR data over Guinarona Floodplain

Table 13. Self-Calibration Results values for Guinarona flights

LiDAR Blocks	Flight Numbers	Area (sq. km)
Tacloban_1026A	1026A 1028A	239.72
Tacloban_1036A	1036A	25.18
SamarLeyte_Bl34F	1358A 1360A	164.18
Leyte_Bl34C	3771G 3773G	145.96
Leyte_Bl34F_additional	3769G	69.32
Leyte_Bl34F_supplement	3769G	30.86
Leyte_Bl34G_supplement	3771G 3773G	54.50
Leyte_Bl34I	3769G	49.29
Leyte_Bl34J	3765G	62.04
	TOTAL	841.05 sq.km

The overlap data for the merged LiDAR blocks, showing the number of channels that pass through a particular location is shown in Figure 16. Since the Gemini and Aquarius systems both employ one channel, we would expect an average value of 1 (blue) for areas where there is limited overlap, and a value of 2 (yellow) or more (red) for areas with three or more overlapping flight lines.

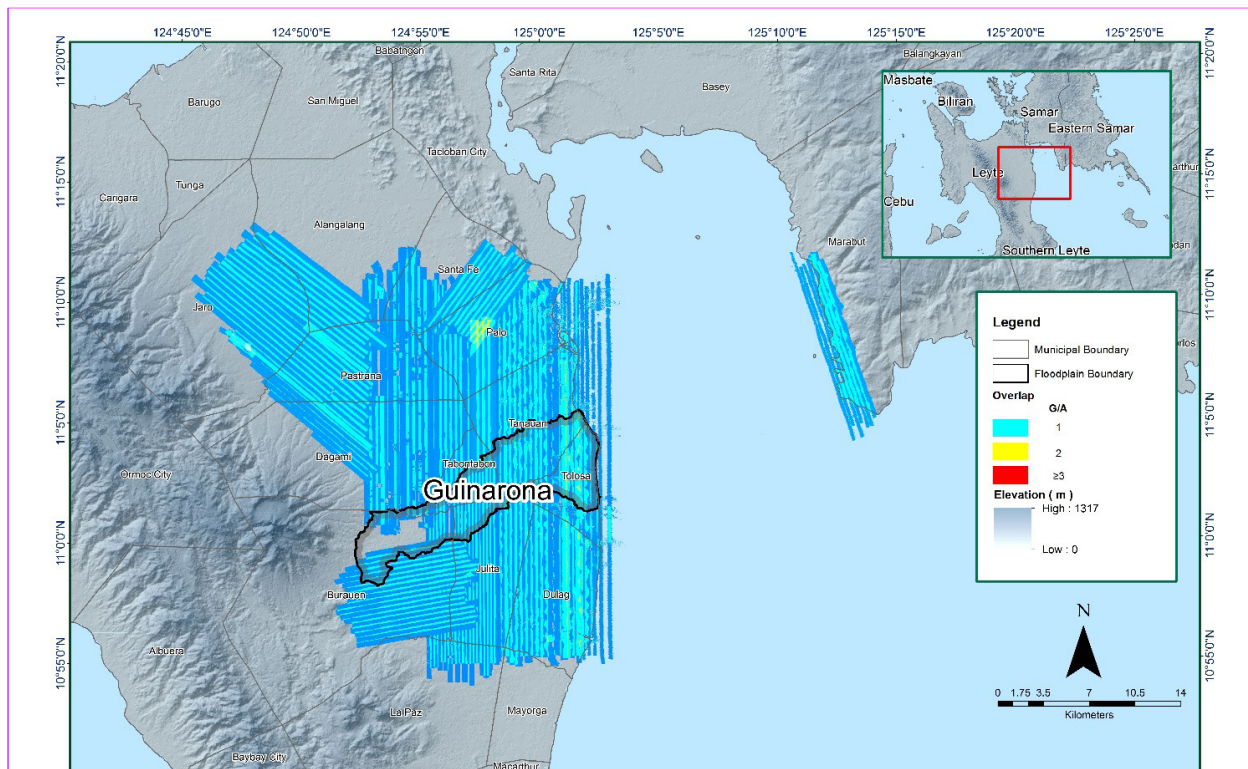


Figure 16. Image of data overlap for Guinarona floodplain

The overlap statistics per block for the Guinarona floodplain can be found in Annex 8. One pixel corresponds to 25.0 square meters on the ground. For this area, the minimum and maximum percent overlaps are 27.64% and 53.44% respectively, which passed the 25% requirement. The density map for the merged LiDAR data, with the red parts showing the portions of the data that satisfy the 2 points per square meter criterion is shown in Figure 17. It was determined that all LiDAR data for Guinarona floodplain satisfy the point density requirement, and the average density for the entire survey area is 3.60 points per square meter.

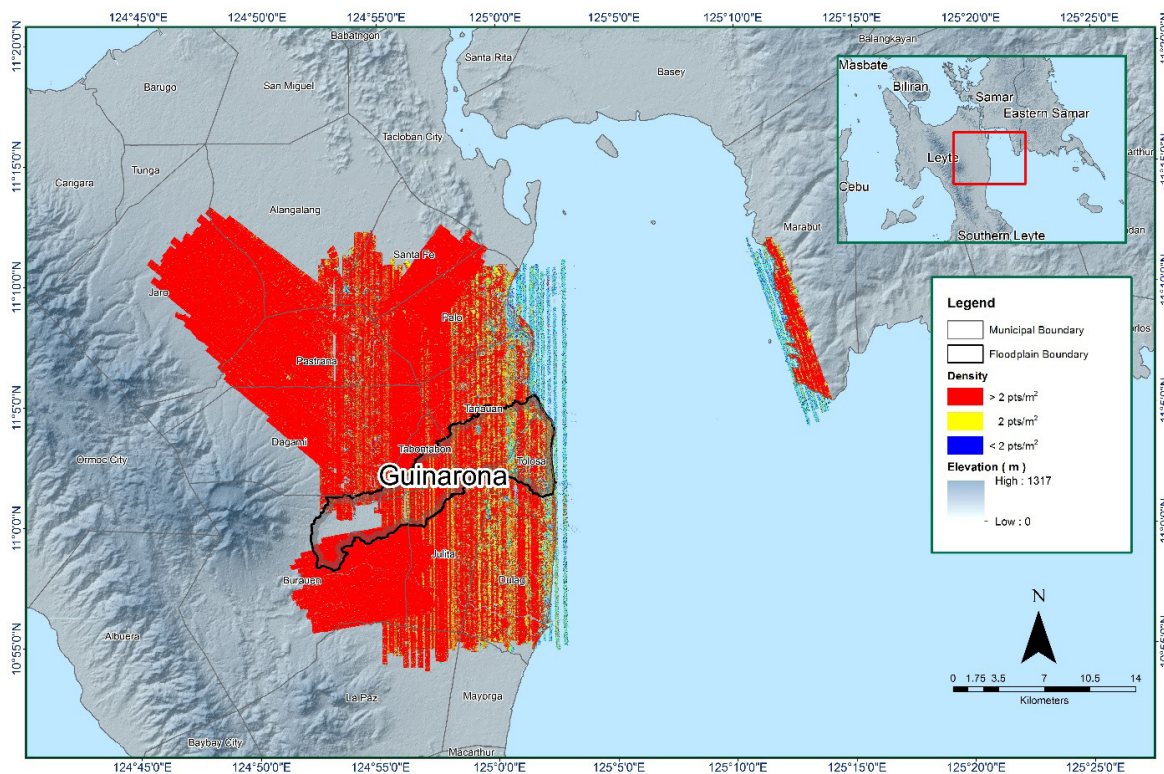


Figure 17. Density map of merged LiDAR data for Guinarona floodplain

The elevation difference between overlaps of adjacent flight lines is shown in Figure 18. The default color range is from blue to red, where bright blue areas correspond to portions where elevations of a previous flight line, identified by its acquisition time, are higher by more than 0.20m relative to elevations of its adjacent flight line. Bright red areas indicate portions where elevations of a previous flight line are lower by more than 0.20m relative to elevations of its adjacent flight line. Areas with bright red or bright blue need to be investigated further using Quick Terrain Modeler software.

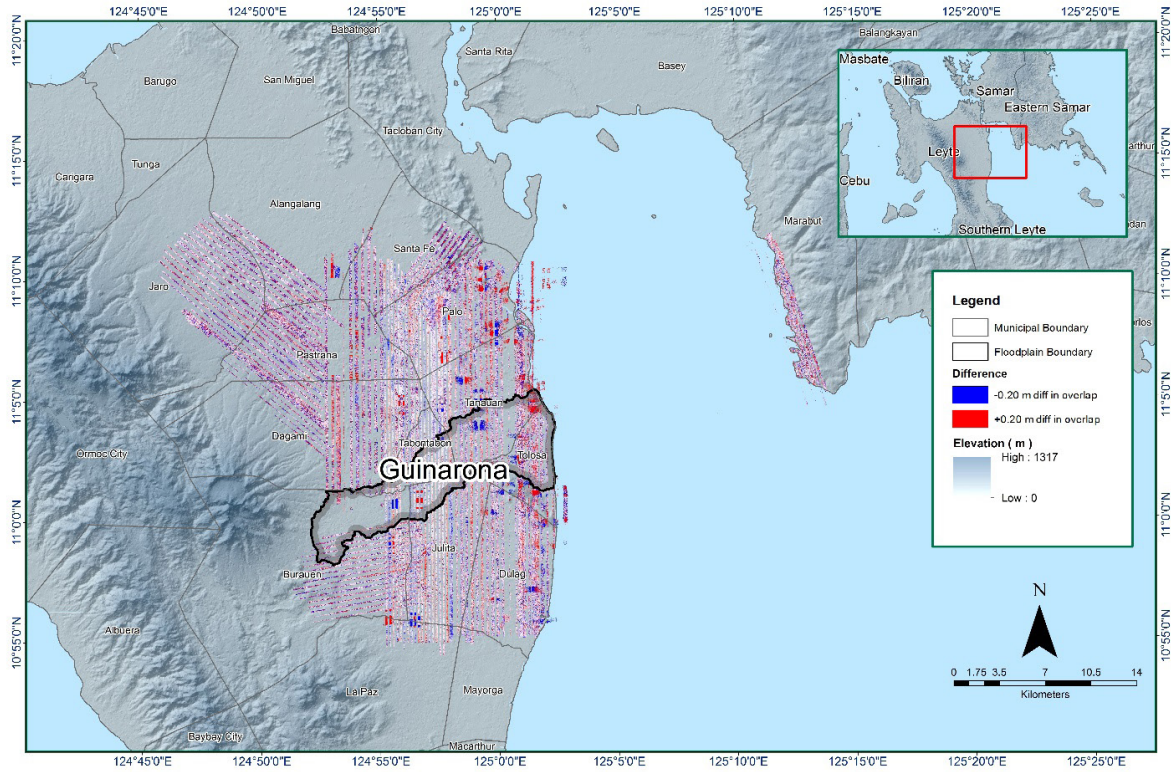


Figure 18. Elevation difference map between flight lines for Guinarona floodplain

A screen capture of the processed LAS data from a Guinarona flight 3769G loaded in QT Modeler is shown in Figure 19. The upper left image shows the elevations of the points from two overlapping flight strips traversed by the profile, illustrated by a dashed red line. The x-axis corresponds to the length of the profile. It is evident that there are differences in elevation, but the differences do not exceed the 20-centimeter mark. This profiling was repeated until the quality of the LiDAR data becomes satisfactory. No reprocessing was done for this LiDAR dataset.

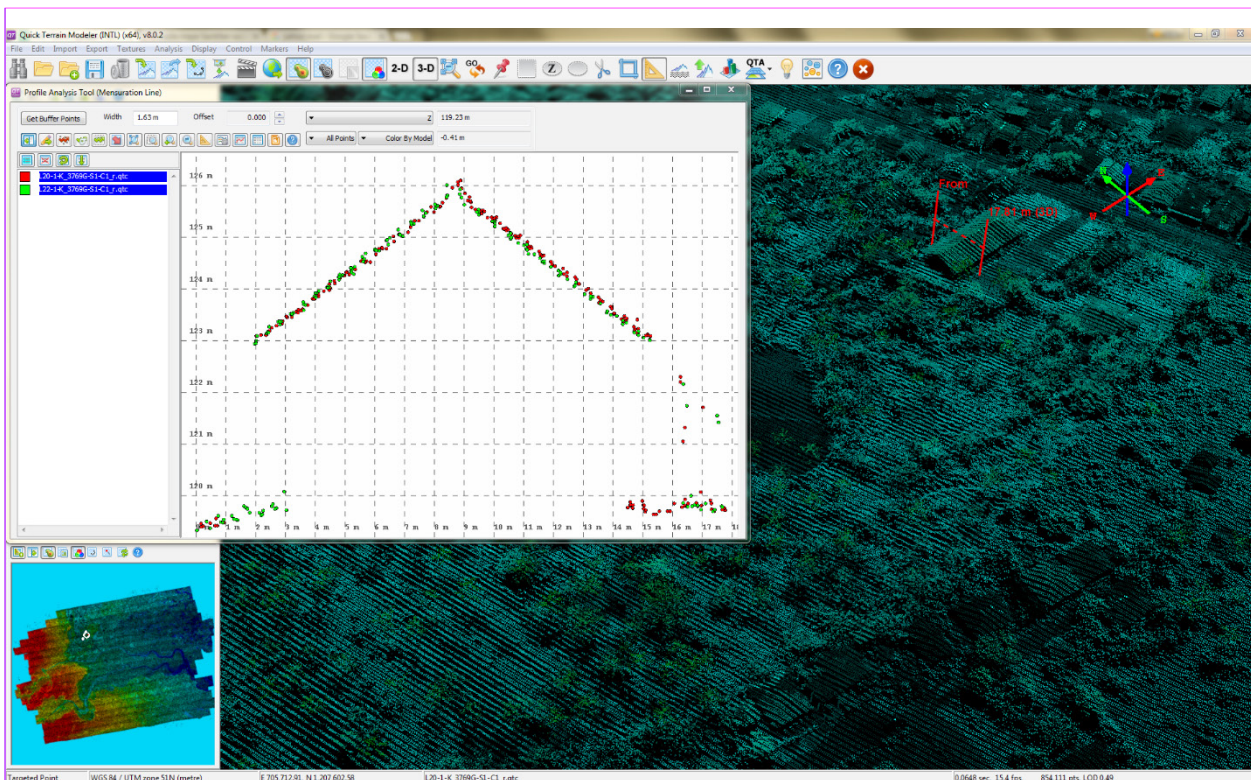


Figure 19. Quality checking for a Guinarona flight 3769G using the Profile Tool of QT Modeler

3.6 LiDAR Point Cloud Classification and Rasterization

Table 15. Guinarona classification results in TerraScan

Pertinent Class	Total Number of Points
Ground	374,947,192
Low Vegetation	433,988,124
Medium Vegetation	864,684,025
High Vegetation	390,365,256
Building	7,807,388

The tile system that TerraScan employed for the LiDAR data and the final classification image for a block in Guinarona floodplain is shown in Figure 20. A total of 1,085 1km by 1km tiles were produced. The number of points classified to the pertinent categories is illustrated in Table 15. The point cloud has a maximum and minimum height of 582.56 meters and 42.55 meters respectively.

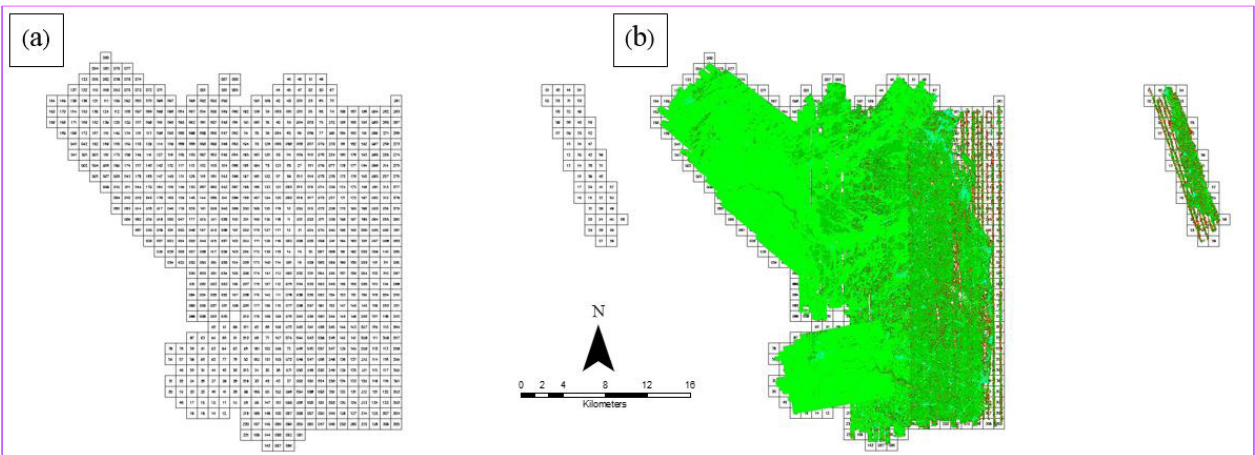


Figure 20. Tiles for Guinarona floodplain (a) and classification results (b) in TerraScan

An isometric view of an area before and after running the classification routines is shown in Figure 21. The ground points are in orange, the vegetation is in different shades of green, and the buildings are in cyan. It can be seen that residential structures adjacent or even below canopy are classified correctly, due to the density of the LiDAR data.

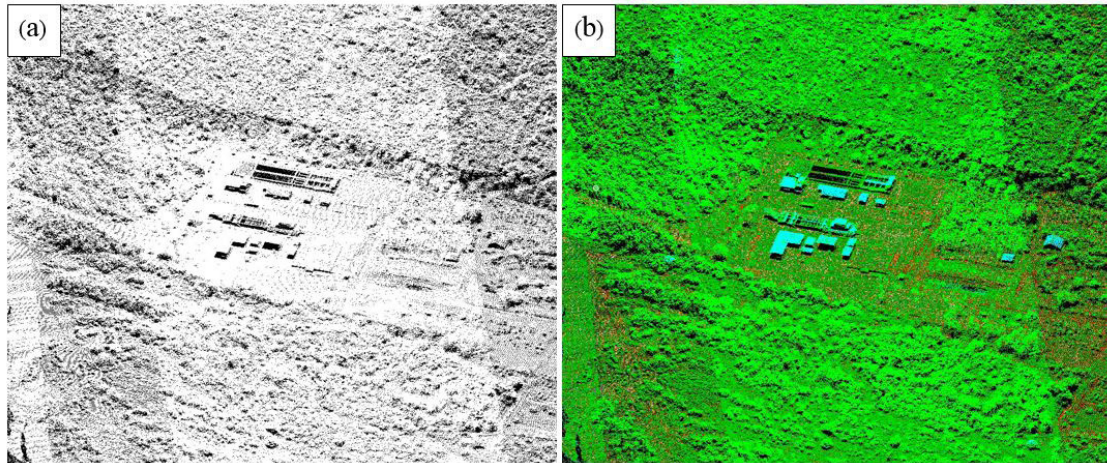


Figure 21. Point cloud before (a) and after (b) classification

The production of last return (V_ASCII) and the secondary (T_ASCII) DTM, first (S_ASCII) and last (D_ASCII) return DSM of the area in top view display are shown in Figure 22. It shows that DTMs are the representation of the bare earth while on the DSMs, all features are present such as buildings and vegetation.

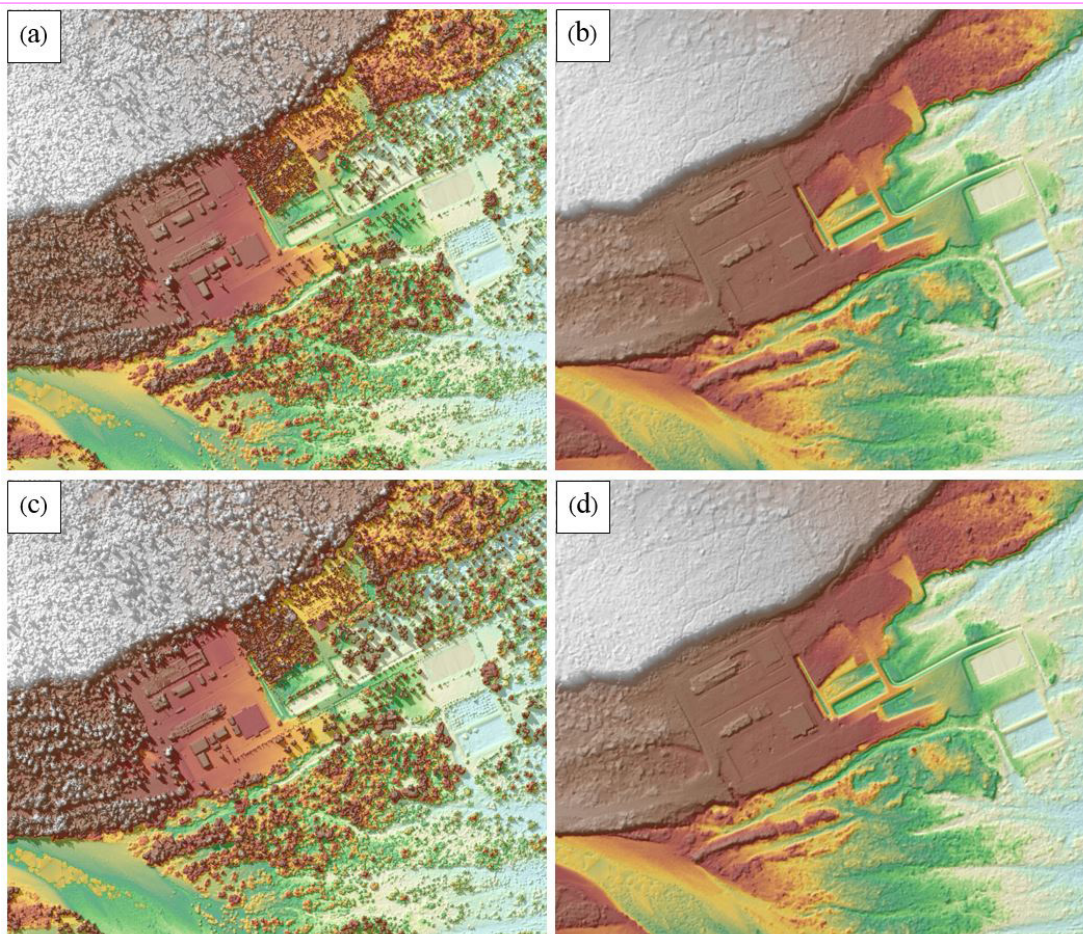


Figure 22. The production of last return DSM (a) and DTM (b), first return DSM (c) and secondary DTM (d) in some portion of Guinarona floodplain

3.7 LiDAR Image Processing and Orthophotograph Rectification

The 496 1km by 1km tiles area covered by Guinarona floodplain is shown in Figure 23. After tie point selection to fix photo misalignments, color points were added to smoothen out visual inconsistencies along the seamlines where photos overlap. The Guinarona floodplain survey attained a total of 392.99 km² in orthophotograph coverage, comprised of 3,649 images. A zoomed in version of sample orthophotographs named in reference to its tile number is shown in Figure 24.

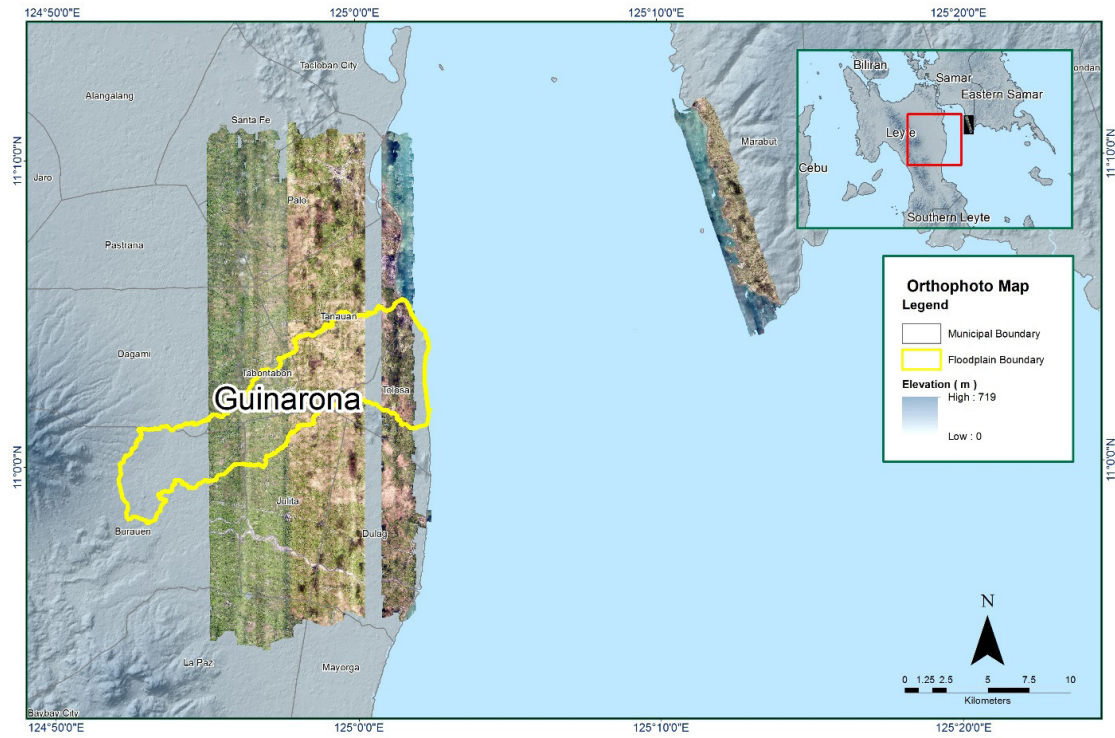


Figure 23. Guinarona floodplain with available orthophotographs



Figure 24. Sample orthophotograph tiles for Guinarona floodplain

3.8 DEM Editing and Hydro-Correction

Nine (9) mission blocks were processed for Guinarona flood plain. These blocks are composed of SamarLeyte, Leyte and Tacloban blocks with a total area of 841.05 square kilometers. Table 16 shows the name and corresponding area of each block in square kilometers.

Table 16. LiDAR blocks with its corresponding area

LiDAR Blocks	Area (sq.km)
Tacloban_1026A	239.72
Tacloban_1036A	25.18
SamarLeyte_Bl34F	164.18
Leyte_Bl34F_additional	69.32
Leyte_Bl34F_supplement	30.86
Leyte_Bl34I	49.29
Leyte_Bl34J	62.04
Leyte_Bl34G_supplement	54.50
Leyte_Bl34C	145.96
TOTAL	841.05 sq.km

Portions of DTM before and after manual editing are shown in Figure 25. Areas with no data along water bodies has to be interpolated for hydrologic correction. The bridge (Figure 25a) is also considered to be an impedance to the flow of water along the river and has to be removed (Figure 25b). The road (Figure 25c) has been misclassified and removed during classification process and has to be retrieved to complete the surface (Figure 25d) to allow the correct flow of water.

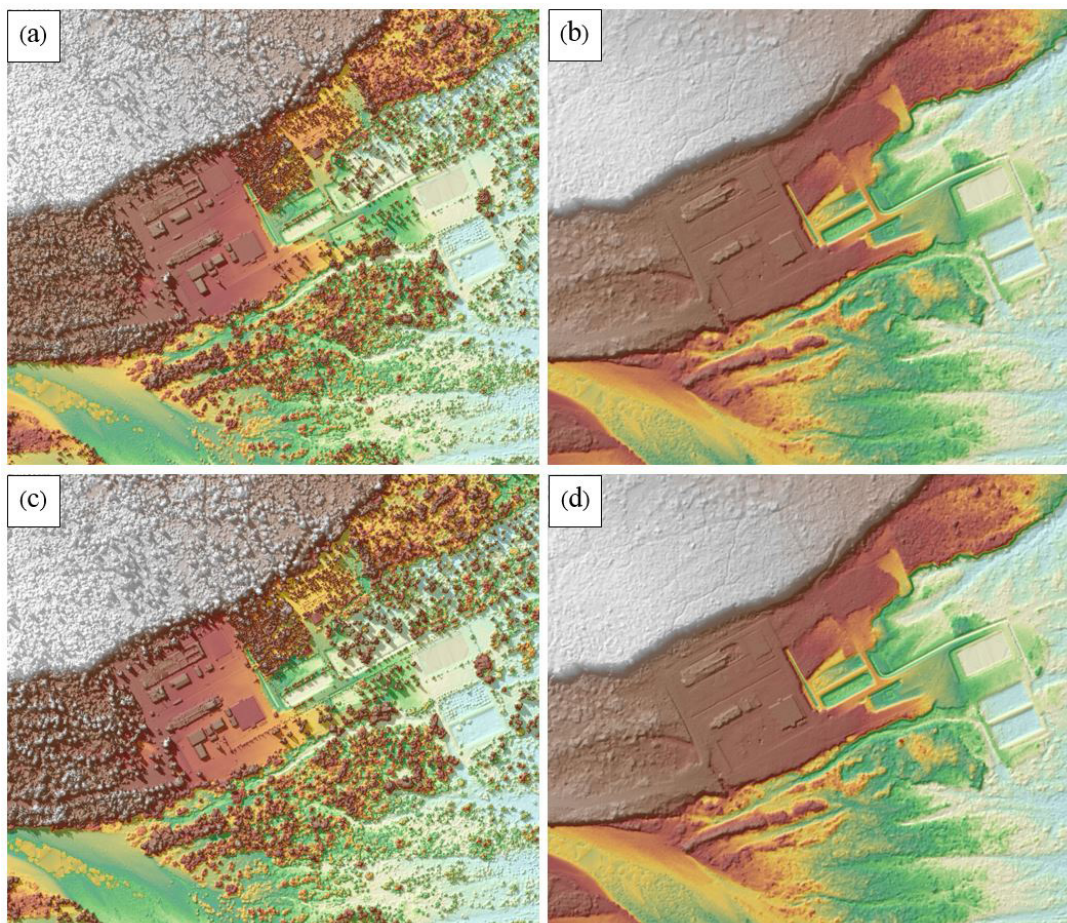


Figure 25. Portions in the DTM of Guinarona floodplain – a bridge before (a) and after (b) manual editing and a road before (c) and after (d) data retrieval

3.9 Mosaicking of Blocks

No assumed reference block was used in mosaicking because the identified reference for shifting was an existing calibrated Tacloban DEM overlapping with the blocks to be mosaicked. Table 17 shows the shift values applied to each LiDAR block during mosaicking.

Mosaicked LiDAR DTM for Guinarona floodplain is shown in Figure 26. The entire Guinarona floodplain is 88.70% covered by LiDAR data while portions with no Lidar data were patched with the available IFSAR data.

Table 17. Shift Values of each LiDAR Block of Guinarona floodplain

Mission Blocks	Area (sq.km)		
	x	y	z
Tacloban_1026A	0.00	0.00	0.00
Tacloban_1036A	0.00	0.00	0.00
SamarLeyte_Bl34F	0.00	1.00	-1.01
Leyte_Bl34F_additional	0.00	0.00	-0.89
Leyte_Bl34F_supplement	0.00	1.00	-0.83
Leyte_Bl34I	0.00	0.00	-0.79
Leyte_Bl34J	0.00	-1.00	-1.04
Leyte_Bl34G_supplement	0.00	0.00	-20.90
Leyte_Bl34C	0.00	-1.00	-1.13

3.10 Calibration and Validation of Mosaicked LiDAR DEM

The extent of the validation survey done by the Data Validation and Bathymetry Component (DVBC) in Guinarona to collect points with which the LiDAR dataset is validated is shown in Figure 27. A total of 3,602 survey points were gathered for the Binahaan and Guinarona floodplains. However, the point dataset was not used for the calibration of the LiDAR data for Guinarona because during the mosaicking process, each LiDAR block was referred to the calibrated Tacloban DEM. Therefore, the mosaicked DEM of Guinarona can already be considered as a calibrated DEM. A good correlation between the uncalibrated Tacloban LiDAR DTM and ground survey elevation values is shown in Figure 28. Statistical values were computed from extracted LiDAR values using the selected points to assess the quality of data and obtain the value for vertical adjustment. The computed height difference between the LiDAR DTM and calibration points is 0.14 meters with a standard deviation of 0.13 meters. Calibration of Tacloban LiDAR data was done by subtracting the height difference value, 0.14 meters, to Tacloban mosaicked LiDAR data. Table 18 shows the statistical values of the compared elevation values between Tacloban LiDAR data and calibration data. These values were also applicable to the Guinarona DEMs.

All survey points lie near the Guinarona flood plain and were used for the validation of the calibrated Guinarona DTM. A good correlation between the calibrated mosaicked LiDAR elevation values and the ground survey elevation, which reflects the quality of the LiDAR DTM is shown in Figure 29. The computed RMSE between the calibrated LiDAR DTM and validation elevation values is 0.20 meters with a standard deviation of 0.10 meters, as shown in Table 19.

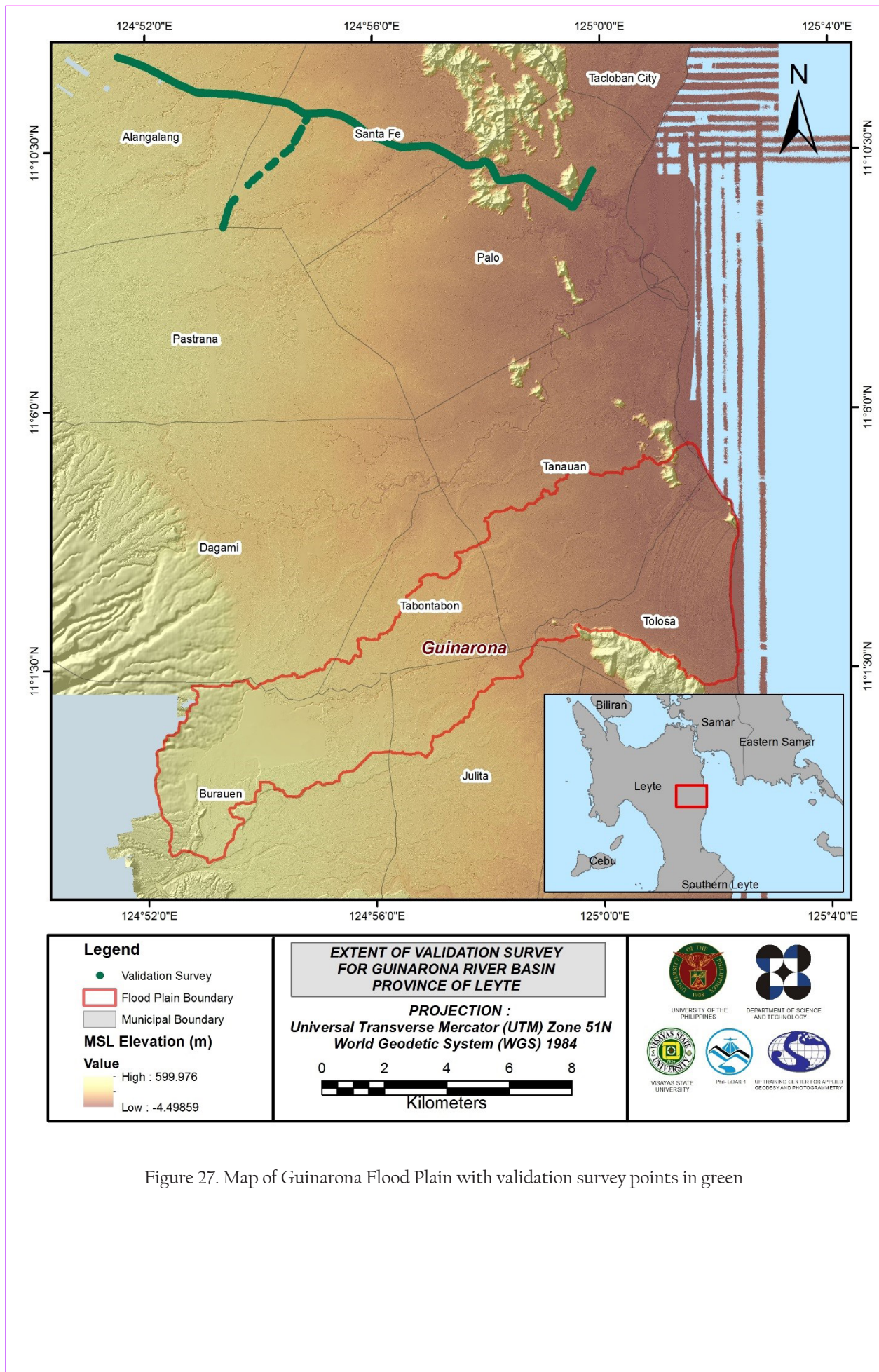


Figure 27. Map of Guinarona Flood Plain with validation survey points in green

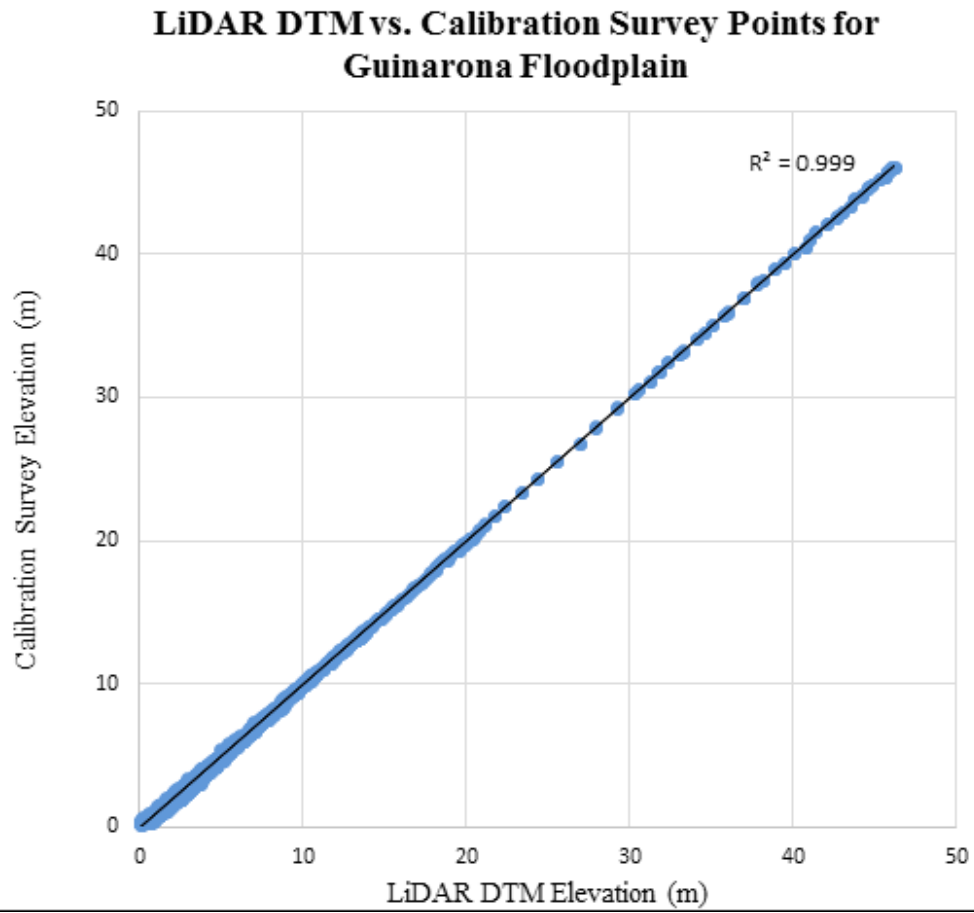


Figure 28. Correlation plot between calibration survey points and LiDAR data

Table 18. Calibration Statistical Measures

Calibration Statistical Measures	Value (meters)
Height Difference	0.14
Standard Deviation	0.13
Average	-0.05
Minimum	-0.32
Maximum	0.22

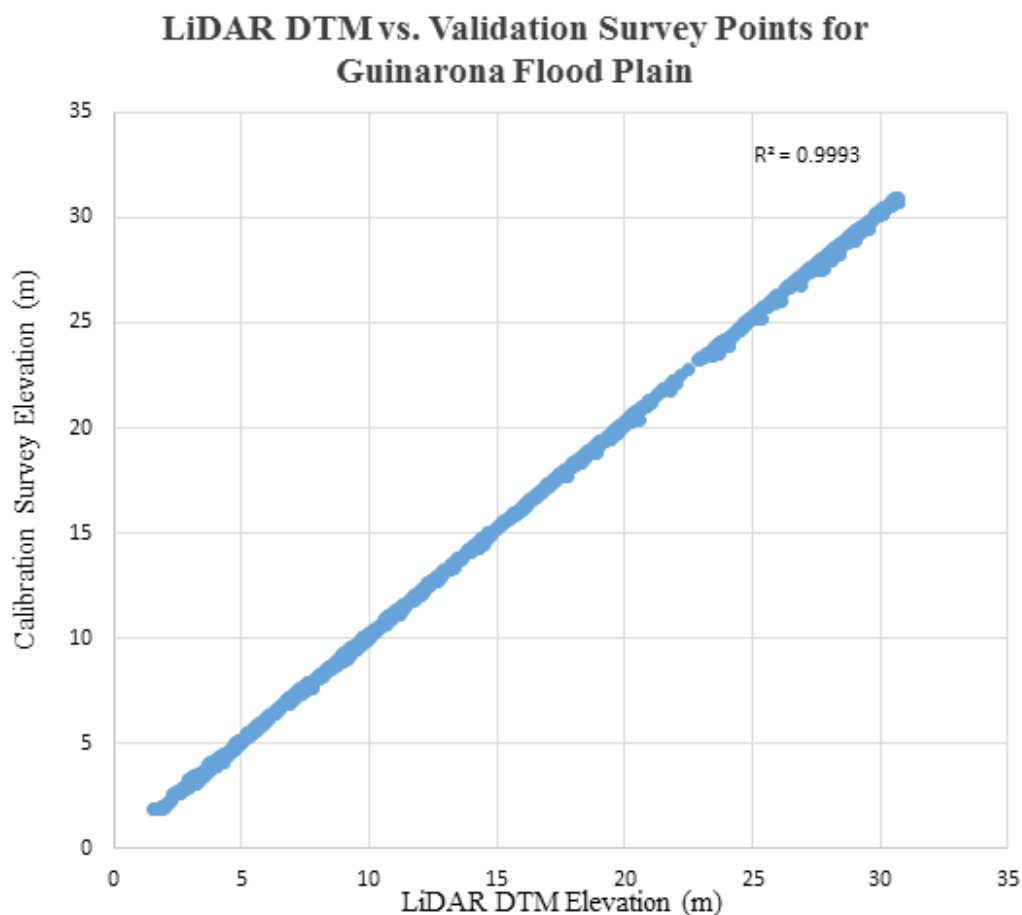


Figure 29. Correlation plot between validation survey points and LiDAR data

Table 19. Validation Statistical Measures

Validation Statistical Measures	Value (meters)
RMSE	0.20
Standard Deviation	0.10
Average	0.18
Minimum	-0.20
Maximum	0.34

3.11 Integration of Bathymetric Data into the LiDAR Digital Terrain Model

For bathy integration, centerline and zigzag data was available for Guinarona with 7,031 bathymetric survey points. The resulting raster surface produced was done by Kernel interpolation with barriers method. After burning the bathymetric data to the calibrated DTM, assessment of the interpolated surface is represented by the computed RMSE value of 0.27 meters. The extent of the bathymetric survey done by the Data Validation and Bathymetry Component (DVBC) in Guinarona integrated with the processed LiDAR DEM is shown in Figure 30.

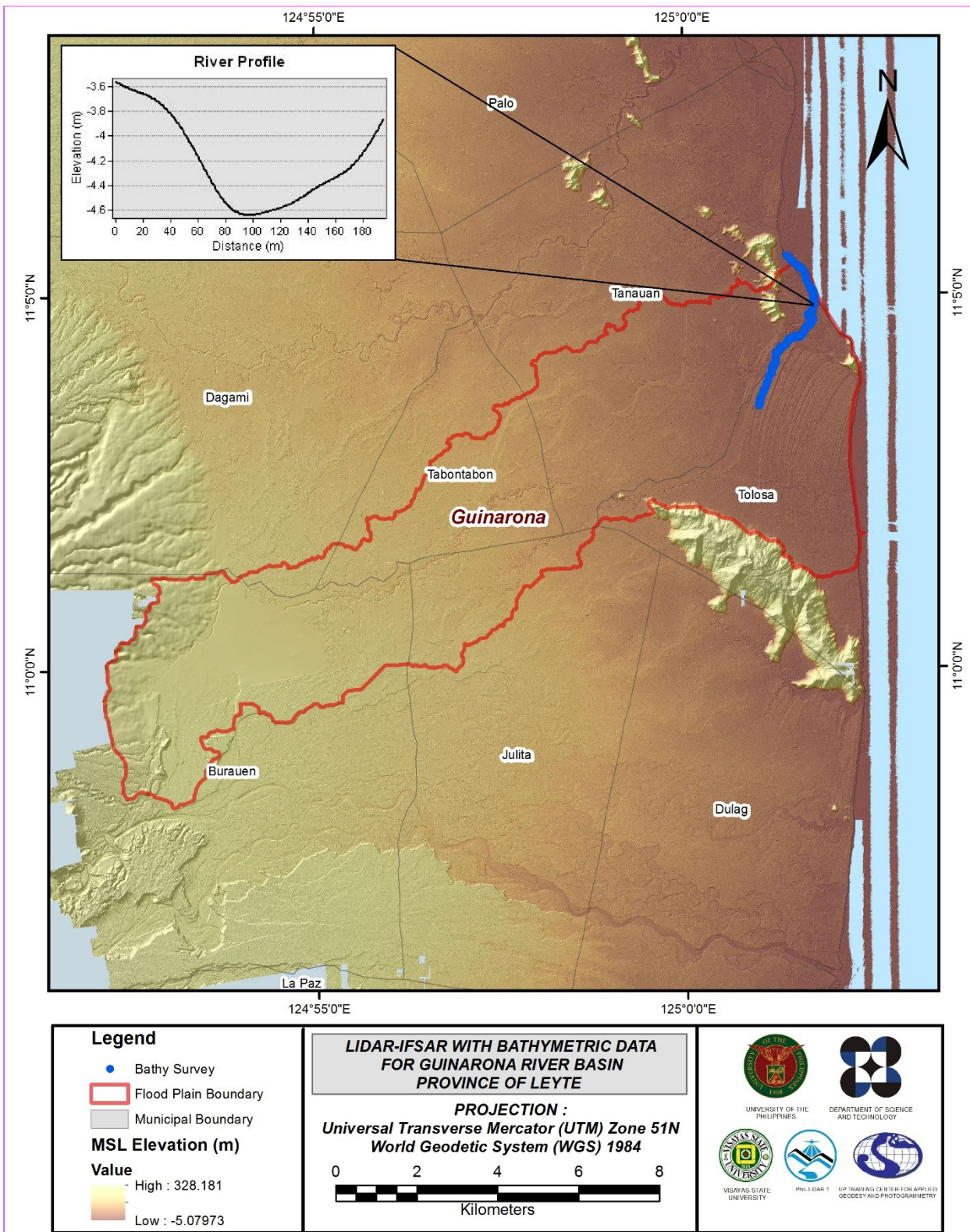


Figure 30. Map of Guinarona Flood Plain with bathymetric survey points shown in blue

3.12 Feature Extraction

The features salient in flood hazard exposure analysis include buildings, road networks, bridges and water bodies within the floodplain area with 200 m buffer zone. Mosaicked LiDAR DEM with 1 m resolution was used to delineate footprints of building features, which consist of residential buildings, government offices, medical facilities, religious institutions, and commercial establishments, among others. Road networks comprise of main thoroughfares such as highways and municipal and barangay roads essential for routing of disaster response efforts. These features are represented by a network of road centerlines.

3.12.1 Quality Checking of Digitized Features' Boundary

Guinarona floodplain, including its 200 m buffer, has a total area of 102.64 sq km. For this area, a total of 5.0 sq km, corresponding to a total of 1,082 building features, are considered for QC. Figure 31 shows the QC blocks for Guinarona floodplain.

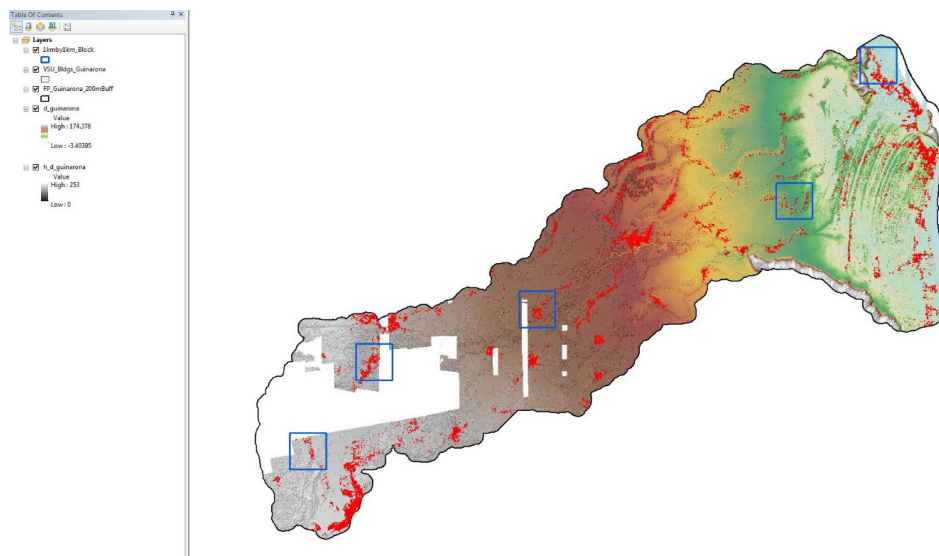


Figure 21. Point cloud before (a) and after (b) classification

Quality checking of Guinarona building features resulted in the ratings shown in Table 20.

Table 20. Quality Checking Ratings for Guinarona Building Features

FLOODPLAIN	COMPLETENESS	CORRECTNESS	QUALITY	REMARKS
Guinarona	95.18	96.67	80.31	PASSED

3.12.2 Height Extraction

Height extraction was done for 14,680 building features in Guinarona floodplain. Of these building features, 1,118 buildings were filtered out after height extraction, resulting to 13,562 buildings with height attributes. The lowest building height is at 2.00 m, while the highest building is at 8.95 m.

3.12.3 Feature Attribution

The digitized features were marked and coded in the field using handheld GPS receivers. The attributes of non-residential buildings were first identified; all other buildings were then coded as residential. An nDSM was generated using the LiDAR DEMs to extract the heights of the buildings. A minimum height of 2 meters was used to filter out the terrain features that were digitized as buildings. Buildings that were not yet constructed during the time of LiDAR acquisition were noted as new buildings in the attribute table.

Table 21 summarizes the number of building features per type. On the other hand, Table 22 shows the total length of each road type, while Table 23 shows the number of water features extracted per type.

Table 21. Building Features Extracted for Guinarona Floodplain

Facility Type	No. of Features
Residential	12,914
School	351
Market	6
Agricultural/Agro-Industrial Facilities	9
Medical Institutions	18
Barangay Hall	52
Military Institution	0
Sports Center/Gymnasium/Covered Court	10
Telecommunication Facilities	0
Transport Terminal	0
Warehouse	10
Power Plant/Substation	0
NGO/CSO Offices	23
Police Station	3
Water Supply/Sewerage	4
Religious Institutions	57
Bank	0
Factory	18
Gas Station	9
Fire Station	2
Other Government Offices	36
Other Commercial Establishments	40
Total	13,562

Table 22. Total Length of Extracted Roads for Guinarona Floodplain.

FLOODPLAIN	Road Network Length (km)					Total
	Barangay Road	City/Municipal Road	Provincial Road	National Road	Others	
Guinarona	148.15	14.59	0	17.79	0.00	180.53

Table 23. Number of Extracted Water Bodies for Guinarona Floodplain.

FLOODPLAIN	Water Body Type					Total
	Rivers/Streams	Lakes/Ponds	Sea	Dam	Fish Pen	
Guinarona	21	0	0	0	0	21

A total of 34 bridges and culverts over small channels that are part of the river network were also extracted for the floodplain.

3.12.4 Final Quality Checking of Extracted Features

All extracted ground features were completely given the required attributes. All these output features comprise the flood hazard exposure database for the flood plain. This completes the feature extraction phase of the project.

Figure 32 shows the Digital Surface Model (DSM) of Binahaan flood plain overlaid with its ground features.

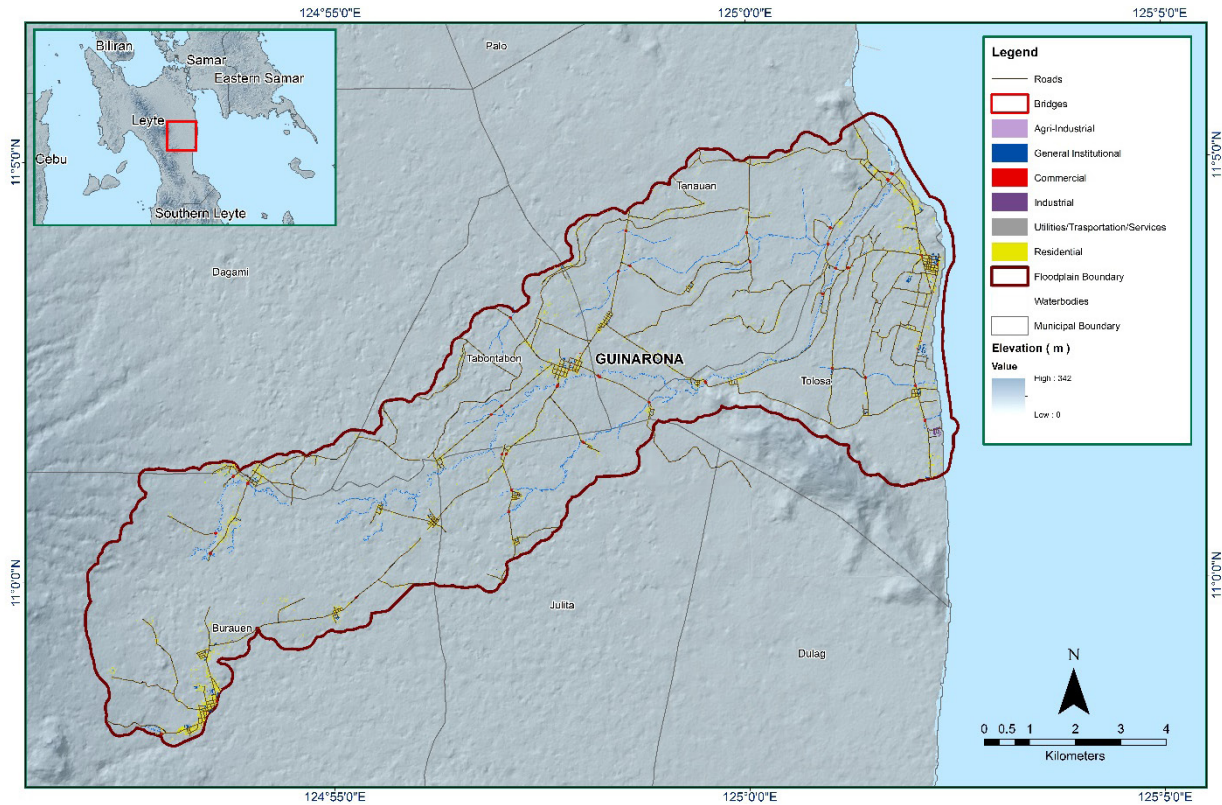


Figure 32. Extracted features for Guinarona floodplain

CHAPTER 4: LIDAR VALIDATION SURVEY AND MEASUREMENTS OF THE GUINARONA RIVER BASIN

Engr. Ma. Rosario Concepcion O. Ang, Engr. John Louie D. Fabila, Engr. Sarah Jane D. Samalburro, Engr. Harmond F. Santos, Engr. Gladys Mae Apat, Engr. Melanie C. Hingpit, Jovy Anne S. Narisma, Engr. Vincent Louise DL. Azucena, Nereo Joshua G. Pecson, Areanne Katrice K. Umali

The methods applied in this Chapter were based on the DREAM methods manual (Balicanta, et al., 2014) and further enhanced and updated in Paringit, et al. (2017).

4.1 Summary of Activities

The project team conducted field surveys in Guinarona River on April 20-22, August 26-28 and October 17 – 26, 2016 with the following scope of work: reconnaissance; control survey; cross-section and as-built survey at Guinarona Bridge in Brgy. District II Poblacion, Municipality of Tabobtabon; validation points acquisition of about 22.159 km covering Municipalities of Alangalang, Santa Fe, and Palo in Leyte; and bathymetric survey from its upstream in Brgy. Burak, Municipality of Tolosa, down to the downstream end of the river located in Brgy. Cabuynan, Municipality of Tanauan, with an approximate total length of 4.941 km using Ohmex™ single beam echo sounder and Trimble® SPS 882 GNSS PPK survey technique.

4.2 Control Survey

A GNSS baseline was established for previous fieldwork in Palo River on September 18-21, 2014 occupying the control points: LYT-101, a 2nd order GCP in Brgy. Candahug; and LY-1016, a 1st order Benchmark in Brgy. San Miguel, both in Municipality of Palo, Leyte.

The GNSS network used for Guinarona River Basin is composed of nine loops established on April 20-22, 2016 occupying the reference points: LYT-101 from the field survey on September 2014 for Palo River; and LYT-708, a 2nd order GCP in Brgy. Buntay, Municipality of Dulag, all in Leyte.

Six control points were established namely: CAM-VSU, located in front of Camire Elementary School in Brgy. Balud, Municipality of Tanauan; LIM-VSU, located on a riprap along National Road in Brgy. Olot, Municipality of Tolosa; MAG-VSU, located on top of a Mass Grave monument in Brgy. Solano, Municipality of Tanauan; NHS-VSU, located inside Tanauan National High School in Brgy. Sto Niño Poblacion, Municipality of Tanauan; PAL-VSU, located on the top of revetment along Bangon River in Brgy. Arado, Municipality of Palo; and SJQ-VSU, located near the approach of San Joaquin Bridge in Brgy. San Joaquin also in Municipality of Palo; all in Leyte. A JICA established control point namely BM-1, located at the approach of Sta. Elena Bridge in Brgy. Binongtoan, Municipality of Tanauan, was also occupied and used as marker for the survey.

The summary of reference and control points and its location is summarized in Table 24 while the GNSS network established is illustrated in Figure 34.

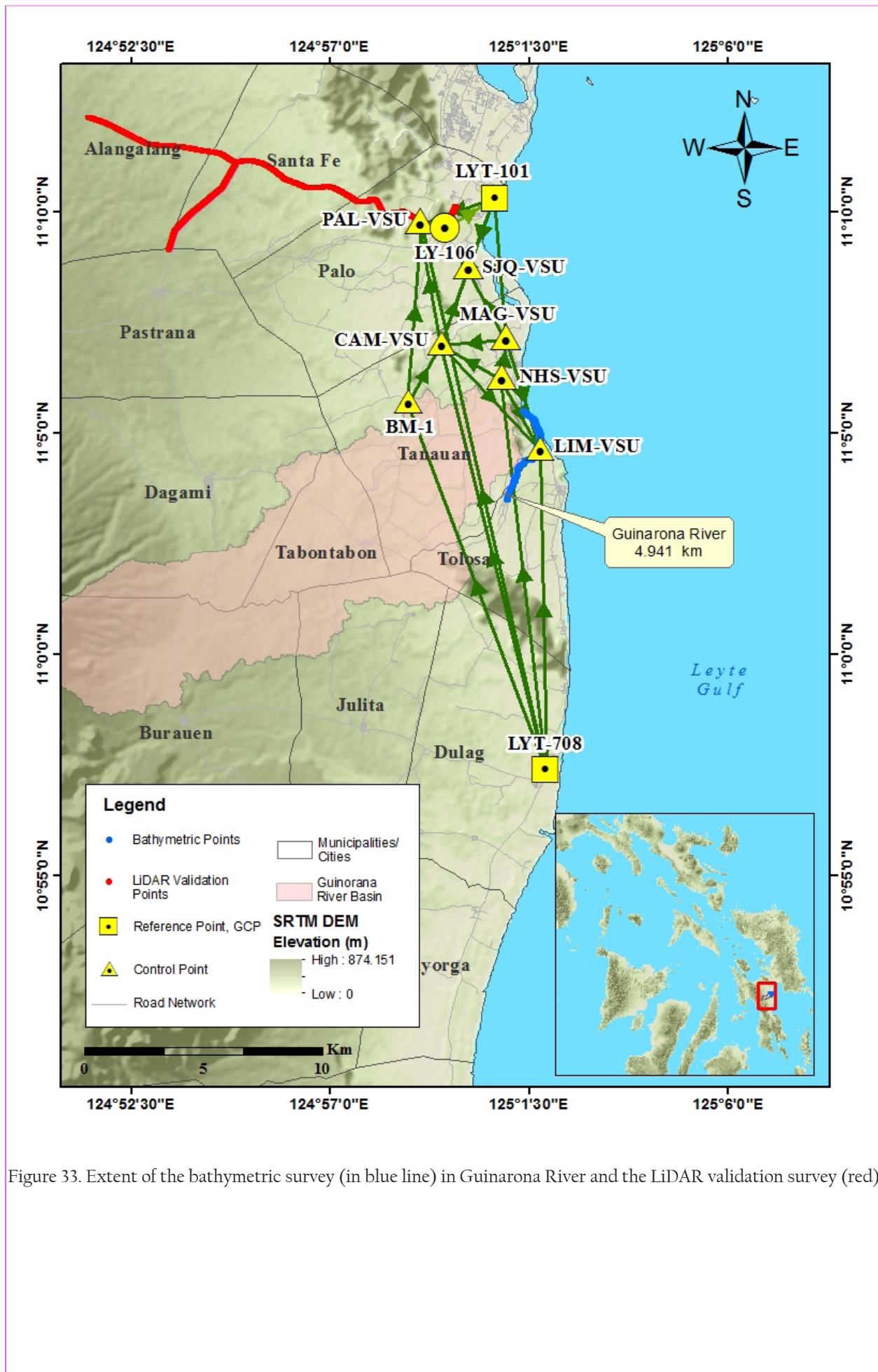


Figure 33. Extent of the bathymetric survey (in blue line) in Guinarona River and the LiDAR validation survey (red)

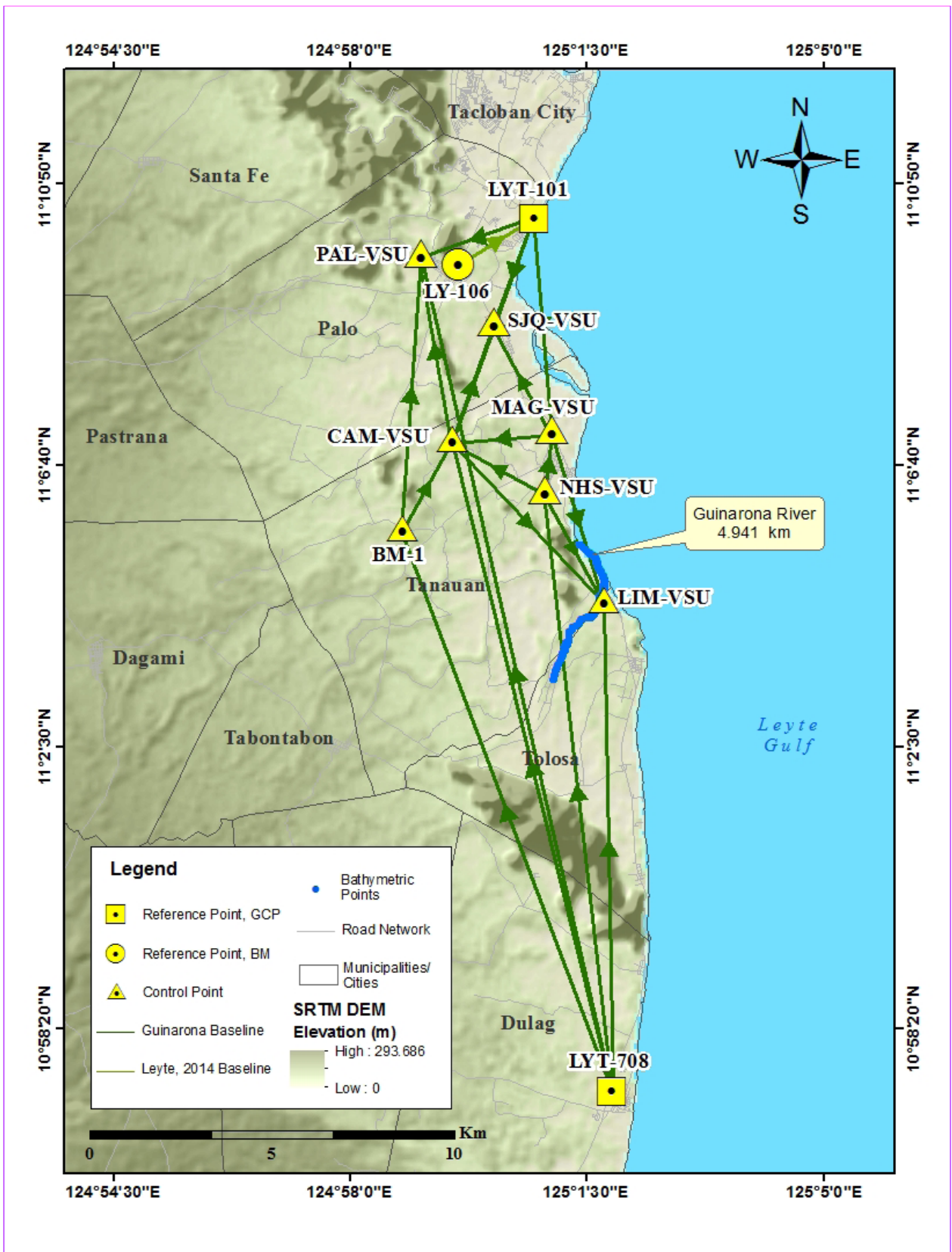


Figure 34. Extent of the bathymetric survey (in blue line) in Guinarona River and the LiDAR validation survey (red)

Table 24 . List of Reference and Control Points occupied for Guinarona River Survey

Control Point	Order of Accuracy	Geographic Coordinates (WGS 84)				
		Latitude	Longitude	Ellipsoidal Height (m)	MSL Elevation (m)	Date Established
Control Survey on September 18-21, 2014						
LYT-101	2nd Order, GCP	11°10'19.64869"	125°00'43.78230"	69.218	5.135	09-18-14
LY-106	1st Order, BM	11°09'38.36968"	124°59'35.93678"	67.850	4.028	09-18-14
Control Survey on April 20-22, 2016						
LYT-101	2nd Order, GCP	11°10'19.64869"	125°00'43.78230"	69.218	5.135	04-22-16
LYT-708	2nd Order, GCP	10°57'24.54497"	125°01'52.57808"	67.197	2.594	04-22-16
CAM-VSU	VSU established	-	-	-	-	04-22-16
LIM-VSU	VSU established	-	-	-	-	04-21-16
MAG-VSU	VSU established	-	-	-	-	04-21-16
NHS-VSU	VSU established	-	-	-	-	04-21-16
PAL-VSU	VSU established	-	-	-	-	04-22-16
SJQ-VSU	VSU established	-	-	-	-	04-20-16
BM-1	Used as Marker	-	-	-	-	04-22-16

The GNSS set-ups on recovered reference points and established control points in Guinarona River are shown in Figure 35 to Figure 44.

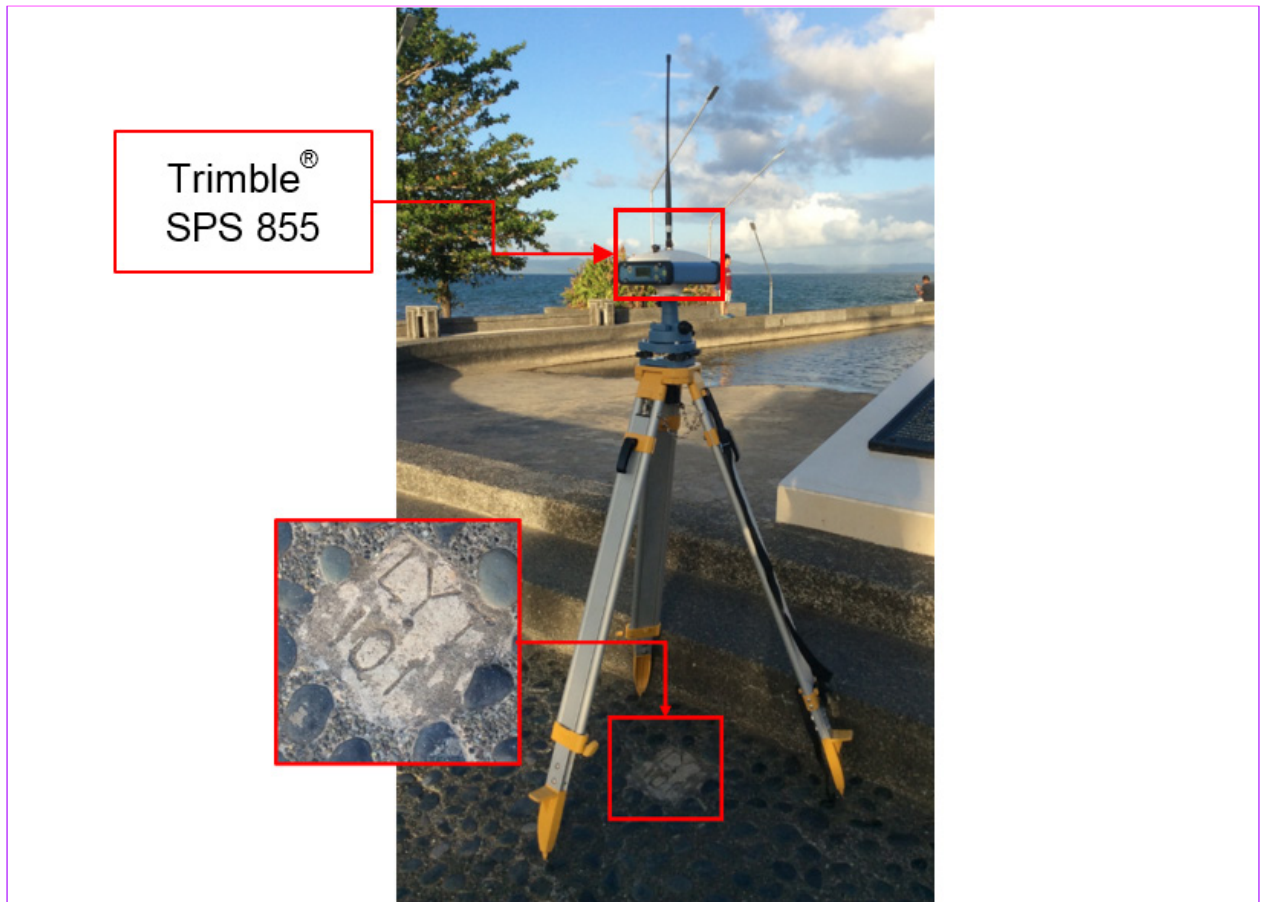


Figure 35. GNSS receiver setup, Trimble® SPS 855, at LYT-101, located in front of Gen. Douglas MacArthur Shrine, Brgy. Candahug, Mun. of Palo, Leyte

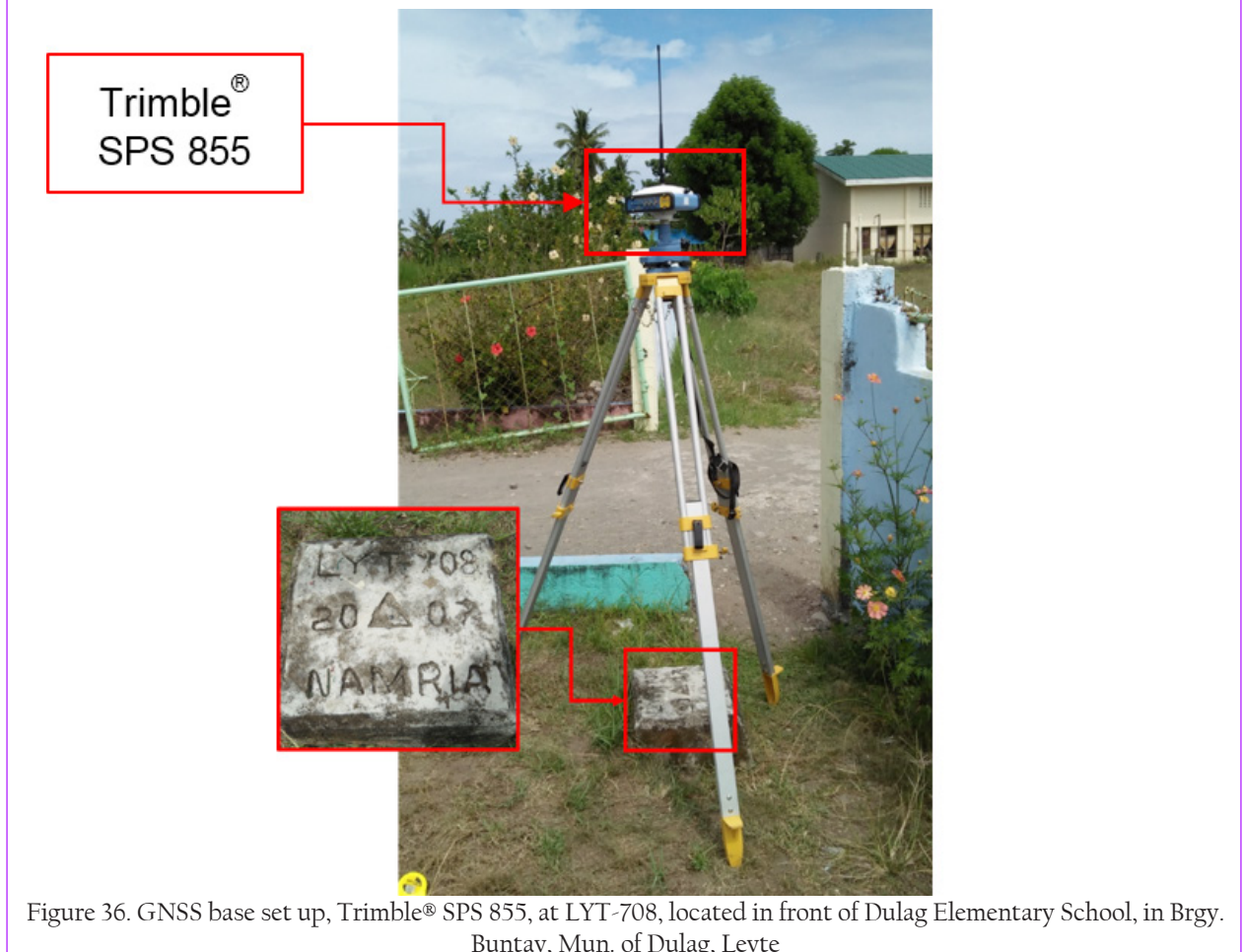


Figure 36. GNSS base set up, Trimble® SPS 855, at LYT-708, located in front of Dulag Elementary School, in Brgy. Buntay, Mun. of Dulag, Leyte

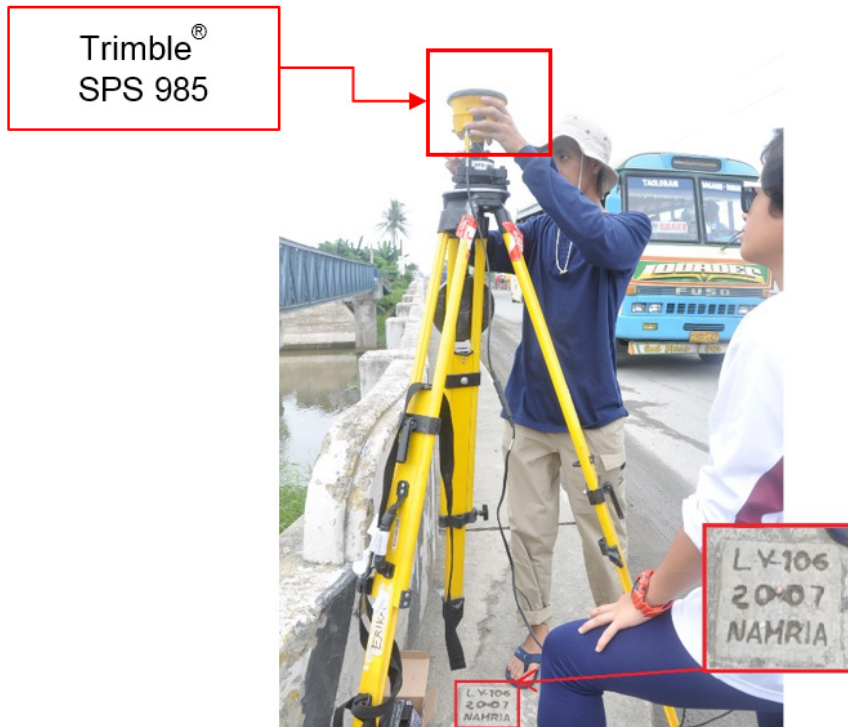


Figure 37. GNSS receiver setup, Trimble® SPS 985 at LY-106, located at the approach of Bernard Reed Bridge in Brgy. San Miguel, Municipality of Palo, Leyte

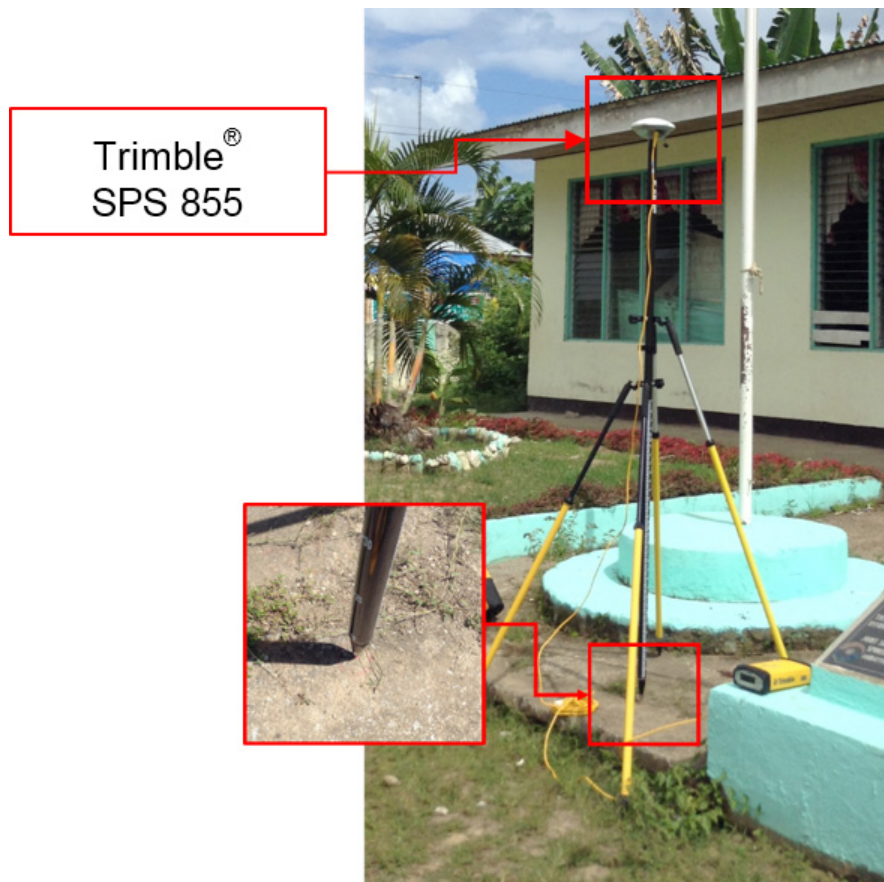


Figure 38. GNSS receiver setup, Trimble® SPS 855, at CAM-VSU, located in front of Camire Elementary School in Brgy. Balud, Municipality of Tanauan, Leyte



Figure 39. GNSS receiver setup, Trimble® SPS 855, at LIM-VSU, located on a riprap along National Road in Brgy. Olot, Municipality of Tolosa, Leyte

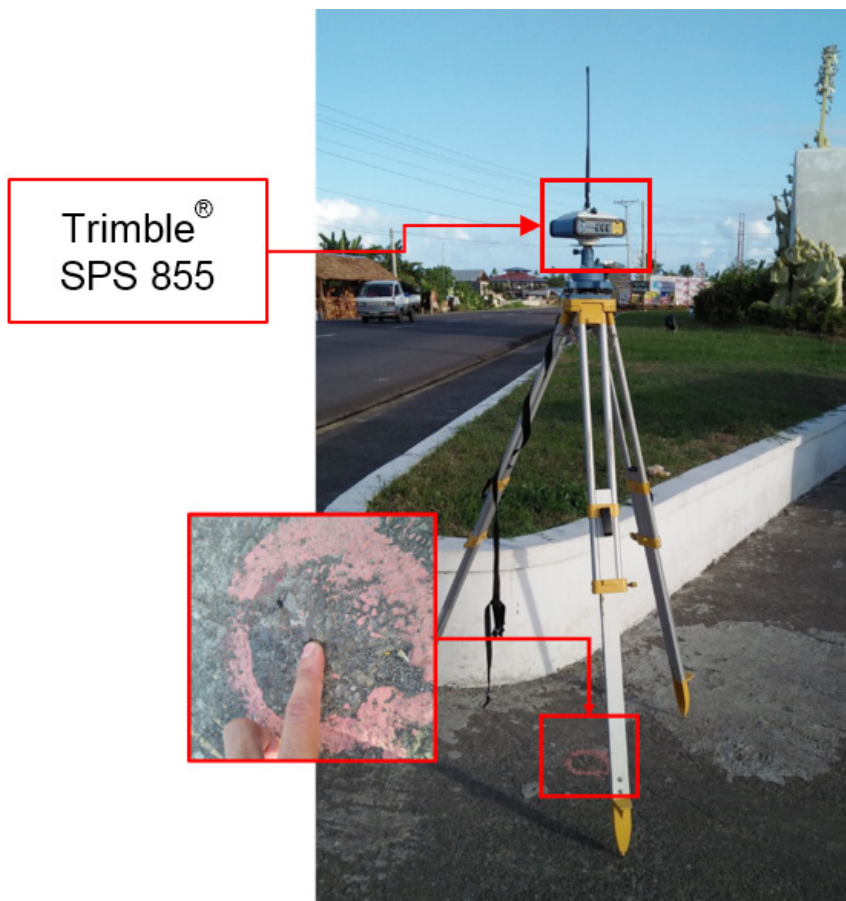


Figure 40. GNSS receiver setup, Trimble® SPS 855, at MAG-VSU, located on top of a Mass Grave monument in Brgy. Solano, Municipality of Tanauan, Leyte



Figure 41. GNSS receiver setup, Trimble® SPS 855, at NHS-VSU, located inside Tanauan National High School, in Brgy. Sto. Niño Poblacion, Municipality of Tanauan, Leyte



Figure 42. GNSS receiver setup, Trimble® SPS 855, at PAL-VSU, located on top of revetment along Bangon River in Brgy. Arado, Municipality of Palo, Leyte



Figure 43. GNSS receiver setup, Trimble® SPS 855, at SJQ-VSU, located near the approach of San Joaquin Bridge, in Brgy. San Joaquin, Municipality of Palo, Leyte



Figure 44. GNSS receiver setup, Trimble® SPS 855, at BM-1, located at the approach of Sta. Elena Bridge, in Brgy. Binongtoan, Municipality of Tanauan, Leyte

4.3 Baseline Processing

GNSS Baselines were processed simultaneously in TBC by observing that all baselines have fixed solutions with horizontal and vertical precisions within +/- 20 cm and +/- 10 cm requirement, respectively. In case where one or more baselines did not meet all of these criteria, masking is performed. Masking is done by removing/masking portions of these baseline data using the same processing software. It is repeatedly processed until all baseline requirements are met. If the reiteration yields out of the required accuracy, resurvey is initiated. Baseline processing result of control points in Guinarona River Basin is summarized in Table 25 generated by TBC software.

Table 25. Baseline Processing Summary Report for Guinarona River Survey

Observation	Date of Observation	Solution Type	H.Prec. (Meter)	V.Prec. (Meter)	Geodetic Az.	Ellipsoid Dist. (Meter)	ΔHeight (Meter)
CAMVSU --- PALVSU (B29)	04-22-16	Fixed	0.003	0.014	350°27'52"	5150.635	1.128
CAMVSU --- PALVSU (B12)	04-22-16	Fixed	0.004	0.011	350°27'52"	5150.638	1.123
BM-1 --- CAMVSU (B25)	04-22-16	Fixed	0.004	0.015	29°25'22"	2760.725	-5.501
LYT-708 --- CAMVSU (B16)	04-22-16	Fixed	0.004	0.011	346°22'27"	18299.173	1.253
MAGVSU --- CAMVSU (B18)	04-21-16 04-22-16	Fixed	0.003	0.018	264°18'10"	2682.599	1.154
CAMVSU --- LIMVSU (B13)	04-21-16 04-22-16	Fixed	0.003	0.012	137°02'08"	5986.252	-2.439
NHSVSU --- CAMVSU (B21)	04-21-16 04-22-16	Fixed	0.003	0.013	298°54'18"	2849.594	3.340
LYT101 --- CAMVSU (B4)	04-22-16	Fixed	0.004	0.019	200°13'55"	6428.995	-0.749
CAMVSU --- LYT101 (B6)	04-22-16	Fixed	0.005	0.015	200°13'55"	6429.002	-0.758
CAMVSU --- NHSVSU (B24)	04-21-16 04-22-16	Fixed	0.002	0.009	298°54'18"	2849.598	3.328
MAGVSU --- CAMVSU (B9)	04-21-16 04-22-16	Fixed	0.004	0.013	264°18'10"	2682.599	1.137
CAMVSU --- SJQVSU (B1)	04-20-16	Fixed	0.003	0.011	19°29'20"	3389.643	-2.011
SJQVSU --- CAMVSU (B2)	04-20-16	Fixed	0.004	0.013	19°29'21"	3389.649	-2.029
BM-1 --- LYT-708 (B27)	04-22-16	Fixed	0.003	0.012	339°46'15"	16390.757	6.743

BM-1 --- PALVSU (B30)	04-22-16	Fixed	0.003	0.014	3°50'35"	7500.944	-4.365
NHSVSU --- MAGVSU (B19)	04-21-16	Fixed	0.002	0.003	6°04'07"	1652.953	2.183
Observation	Date of Observation	Solution Type	H.Prec. (Meter)	V.Prec. (Meter)	Geodetic Az.	Ellipsoid Dist. (Meter)	ΔHeight (Meter)
LIMVSU --- LYT-708 (B15)	04-21-16 04-22-16	Fixed	0.004	0.015	359°00'36"	13404.986	-1.188
LIMVSU --- NHSVSU (B23)	04-21-16	Fixed	0.003	0.010	152°10'46"	3396.078	0.902
NHSVSU --- LIMVSU (B20)	04-21-16	Fixed	0.002	0.009	152°10'46"	3396.073	0.911
LYT101 --- PALVSU (B10)	04-22-16	Fixed	0.004	0.017	252°47'25"	3220.346	0.362
MAGVSU --- LIMVSU (B17)	04-21-16	Fixed	0.003	0.014	163°07'11"	4856.479	-1.289
MAGVSU --- SJQVSU (B8)	04-20-16	Fixed	0.005	0.017	332°17'36"	3308.374	-0.908
MAGVSU --- LYT101 (B7)	04-20-16	Fixed	0.005	0.021	175°34'35"	5783.217	-1.904
SJQVSU --- PALVSU (B11)	04-20-16 04-22-16	Fixed	0.003	0.012	313°31'12"	2736.111	3.135
LYT101 --- SJQVSU (B3)	04-21-16 04-20-16	Fixed	0.003	0.014	201°03'21"	3039.944	-2.771
SJQVSU --- LYT101 (B5)	04-21-16 04-20-16	Fixed	0.006	0.018	201°03'21"	3039.946	-2.793
LYT-708 --- PALVSU (B28)	04-21-16 04-22-16	Fixed	0.003	0.014	347°16'26"	23439.529	2.400
CAMVSU --- LYT-708 (B26)	04-22-16	Fixed	0.003	0.014	346°22'27"	18299.172	1.253
LIMVSU --- CAMVSU (B14)	04-21-16 04-22-16	Fixed	0.004	0.016	137°02'08"	5986.264	-2.449
LYT-708 --- NHSVSU (B22)	04-21-16	Fixed	0.004	0.013	353°40'57"	16506.862	-2.068

As shown Table 25 a total of thirty (30) baselines were processed coordinate and elevation values of reference point LYT-101; and coordinate values of LYT-708 held fixed. All of them passed the required accuracy.

4.4 Network Adjustment

After the baseline processing procedure, network adjustment is performed using TBC. Looking at the Adjusted Grid Coordinates table of the TBC generated Network Adjustment Report, it is observed that the square root of the sum of the square s of x and y must be less than 20 cm and z less than 10 cm or in equation form:

$$\sqrt{((x_e)^2 + (y_e)^2)} < 20cm \text{ and } z_e < 10 \text{ cm}$$

Where:

- X_e is the Easting Error,
- Y_e is the Northing Error, and
- Z_e is the Elevation Error

for each control point. See the Network Adjustment Report shown in Table C-3 to Table C-6 for complete details.

The nine (9) control points, LYT-101, LYT-708, CAM-VSU, LIM-VSU, MAG-VSU, NHS-VSU, PAL-VSU, SJQ-VSU and BM-1 were occupied and observed simultaneously to form a GNSS loop. Coordinates of LYT-101 and LYT-708 and elevation values LYT-101 were held fixed during the processing of the control points as presented in Table 26. Through these reference points, the coordinates and elevation of the unknown control points will be computed.

Table 26. Control Point Constraints

Point ID	Type	East σ (Meter)	North σ (Meter)	Height σ (Meter)	Elevation σ (Meter)
LYT-101	Grid				Fixed
LYT-101	Global	Fixed	Fixed		
LYT-708	Global	Fixed	Fixed		
Fixed = 0.000001 (Meter)					

The list of adjusted grid coordinates, i.e. Northing, Easting, Elevation and computed standard errors of the control points in the network is indicated in Table 27. All fixed control points have no values for grid and elevation errors.

Table 27. Adjusted Grid Coordinates

Point ID	Easting (Meter)	Easting Error (Meter)	Northing (Meter)	Nothing Error (Meter)	Elevation (Meter)	Constraint
LYT101						
719729.823	?	1235759.250	?	5.135	?	LLe
LYT-708						
721979.595	?	1211952.918	?	2.594	0.042	LL
CAM-VSU						
717547.159	0.005	1229710.821	0.004	4.347	0.034	
LIM-VSU						
721657.091	0.006	1225356.793	0.005	1.646	0.043	
MAG-VSU						
720215.141	0.006	1229995.294	0.005	3.080	0.040	
NHS-VSU						
720051.512	0.006	1228350.131	0.005	0.872	0.040	
PAL-VSU						
716659.636	0.007	1234785.356	0.006	5.614	0.039	

SJQ-VSU						
718656.753	0.006	1232914.373	0.005	2.335	0.036	
BM-1						
716206.765	0.007	1227296.771	0.006	9.860	0.050	

With the mentioned equation, $\sqrt{(x_e)^2+(y_e)^2} < 20 \text{ cm}$ for horizontal and $z_e < 10 \text{ cm}$ for the vertical; the computation for the accuracy are as follows:

- a. LYT-101
 - horizontal accuracy = Fixed
 - vertical accuracy = Fixed
- b. LYT-708
 - horizontal accuracy = Fixed
 - vertical accuracy = $4.2 < 10 \text{ cm}$
- c. CAM-VSU
 - horizontal accuracy = $\sqrt{(0.8)^2 + (0.6)^2}$
 $= \sqrt{0.64 + 0.36}$
 $= 1.00 < 20 \text{ cm}$
 - vertical accuracy = Fixed
- d. LIM-VSU
 - horizontal accuracy = $\sqrt{(0.9)^2 + (0.6)^2}$
 $= \sqrt{0.81 + 0.36}$
 $= 1.08 < 20 \text{ cm}$
 - vertical accuracy = Fixed
- e. MAG-VSU
 - horizontal accuracy = $\sqrt{(1.1)^2 + (0.8)^2}$
 $= \sqrt{1.21 + 0.64}$
 $= 1.36 \text{ cm} < 20 \text{ cm}$
 - vertical accuracy = Fixed
- f. NHS-VSU
 - horizontal accuracy = $\sqrt{(0.9)^2 + (0.6)^2}$
 $= \sqrt{0.81 + 0.36}$
 $= 1.08 \text{ cm} < 20 \text{ cm}$
 - vertical accuracy = $6.7 \text{ cm} < 10 \text{ cm}$
- g. PAL-VSU
 - horizontal accuracy = $\sqrt{(0.9)^2 + (0.6)^2}$
 $= \sqrt{0.81 + 0.36}$
 $= 1.08 \text{ cm} < 20 \text{ cm}$
 - vertical accuracy = $6.7 \text{ cm} < 10 \text{ cm}$
- h. SJQ-VSU
 - horizontal accuracy = $\sqrt{(0.9)^2 + (0.6)^2}$
 $= \sqrt{0.81 + 0.36}$
 $= 1.08 \text{ cm} < 20 \text{ cm}$
 - vertical accuracy = $6.7 \text{ cm} < 10 \text{ cm}$

i. BM-1

$$\begin{aligned} \text{horizontal accuracy} &= \sqrt{(0.9)^2 + (0.6)^2} \\ &= \sqrt{0.81 + 0.36} \\ &= 1.08 \text{ cm} < 20 \text{ cm} \\ \text{vertical accuracy} &= 6.7 \text{ cm} < 10 \text{ cm} \end{aligned}$$

Following the given formula, the horizontal and vertical accuracy result of the two occupied control points are within the required precision.

The corresponding geodetic coordinates of the observed points are within the required accuracy as shown in Table 28. Based on the result of the computation, the accuracy condition is satisfied; hence, the required accuracy for the program was met.

Table 28. Adjusted Geodetic Coordinates

Point ID	Latitude	Longitude	Ellipsoid Height (Meter)	Height Error (Meter)	Constraint
LYT-101	N11°10'19.64869"	E125°00'43.78230"	69.218	?	LLe
LYT-708	N10°57'24.54497"	E125°01'52.57808"	67.197	0.042	LL
CAM-VSU	N11°07'03.32408"	E124°59'30.51751"	68.460	0.034	
LIM-VSU	N11°04'40.74891"	E125°01'44.94709"	66.026	0.043	
MAG-VSU	N11°07'11.99451"	E125°00'58.48218"	67.314	0.040	
NHS-VSU	N11°06'18.50045"	E125°00'52.72365"	65.127	0.040	
PAL-VSU	N11°09'48.63503"	E124°59'02.39537"	69.581	0.039	
SJQ-VSU	N11°08'47.31897"	E125°00'07.78743"	66.437	0.036	
BM-1	N11°05'45.06575"	E124°58'45.82598"	73.947	0.050	

The summary of reference and control points used is indicated in Table 29.

Table 29. Reference and control points used and its location. (Source: NAMRIA, UP-TCAGP)

Control Point	Geographic Coordinates (WGS 84)			UTM ZONE 51		
	Latitude	Longitude	Ellipsoid Height (m)	Nothing (m)	Easting (m)	BM Ortho (m)
Control Survey on September 18-21, 2016						
LYT-101	2nd Order, GCP	11°10'19.64869"	125°00'43.78230"	69.218	1235759.250	719729.823
LY-106	1st Order, BM	12°23'08.14503"	124°37'40.19430"	70.990	1369731.985	676970.194
Control Survey on April 20-22, 2016						
LYT-101	2nd Order, GCP	11°10'19.64869"	125°00'43.78230"	69.218	1235759.250	719729.823
LYT-708	2nd Order, GCP	10°57'24.54497"	125°01'52.57808"	67.197	1211952.918	721979.595
CAM-VSU	VSU established	11°07'03.32408"	124°59'30.51751"	68.460	1229710.821	717547.159
LIM-VSU	VSU established	11°04'40.74891"	125°01'44.94709"	66.026	1225356.793	721657.091
MAG-VSU	VSU established	11°07'11.99451"	125°00'58.48218"	67.314	1229995.294	720215.141
NHS-VSU	VSU established	11°06'18.50045"	125°00'52.72365"	65.127	1228350.131	720051.512
PAL-VSU	VSU established	11°09'48.63503"	124°59'02.39537"	69.581	1234785.356	716659.636
SJQ-VSU	VSU established	11°08'47.31897"	125°00'07.78743"	66.437	1232914.373	718656.753
BM-1	Used as Marker	11°05'45.06575"	124°58'45.82598"	73.947	1227296.771	716206.765

4.5 Cross-section and Bridge As-Built survey and Water Level Marking

Cross-section and as-built survey were conducted on October 22 and 24, 2016 at the downstream side of Guinarona bridge in Brgy. District II Poblacion, Municipality of Tabontabon, Leyte as shown in Figure 45. A survey grade GNSS receiver Trimble® SPS 855 in PPK survey technique was utilized for this survey as shown in Figure 46.



Figure 45. Guinarona Bridge facing upstream



Figure 46. As-Built Survey of Guinarona Bridge

The cross-sectional line of Guinarona Bridge is about 100 m with forty-two (42) cross-sectional points using the control point BM-1 as the GNSS base station. The location map, cross-section diagram, and the bridge data form are shown in Figure 47 to Figure 49.

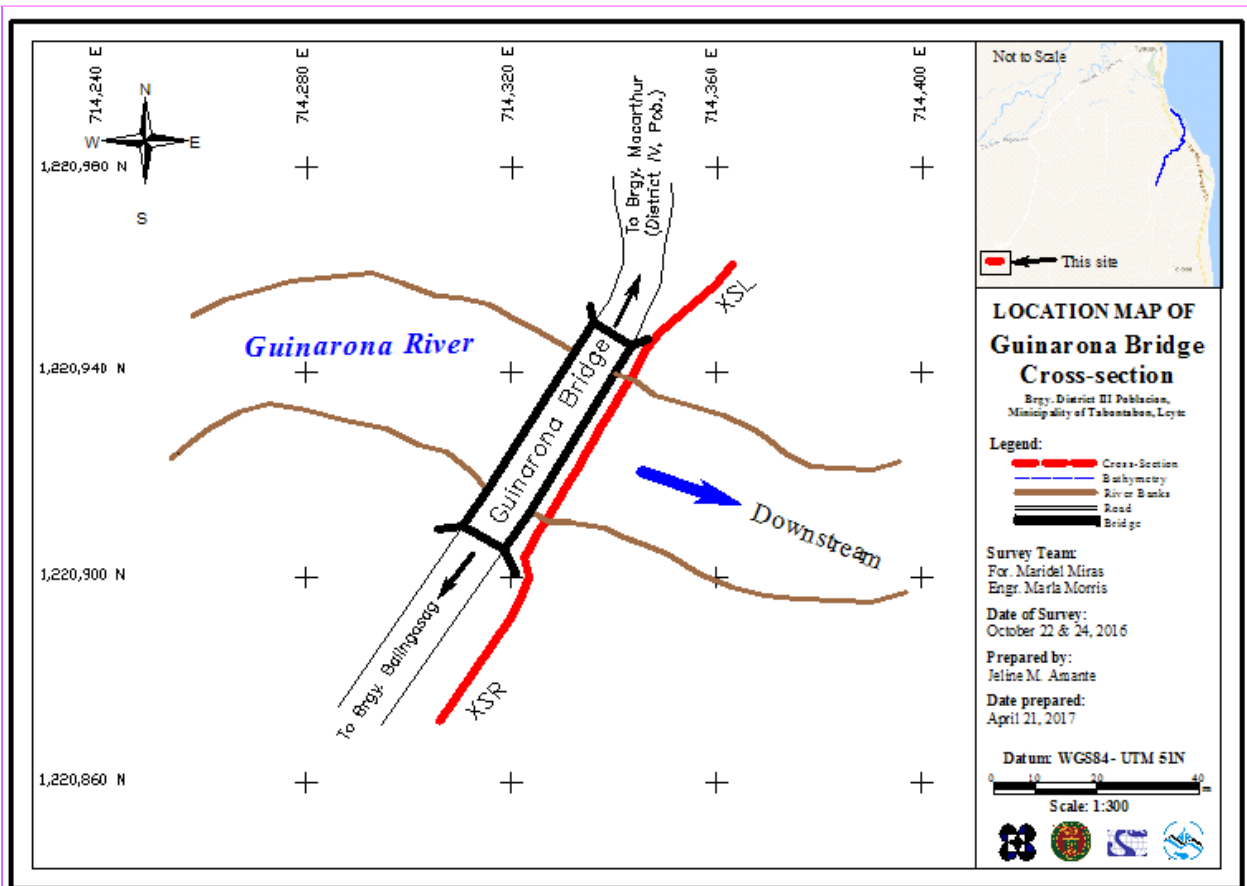


Figure 47. Guinarona bridge cross-section location map

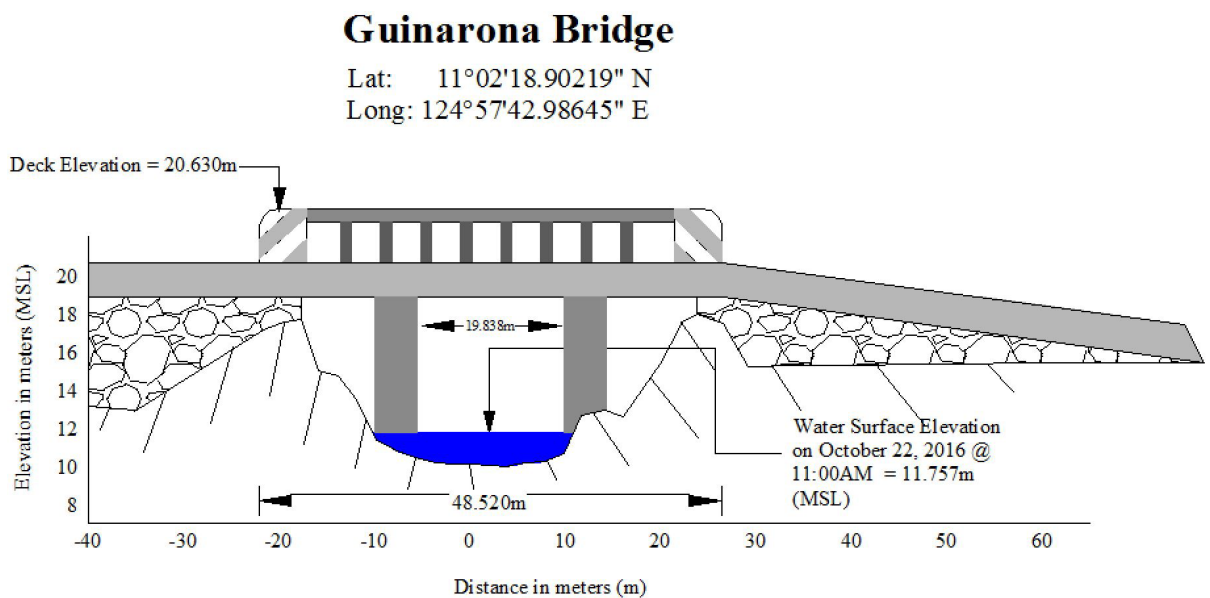


Figure 48. Guinarona Bridge cross-section diagram

Bridge Data Form

Bridge Name: <u>Guinarona Bridge</u>		Date: <u>October 22 and 24, 2016</u>	
River Name: <u>Guinarona River</u>		Time: <u>11:47 AM</u>	
Location (Brgy, City,Region): <u>Brgy. District III Poblacion, Municipality of Tabontabon, Leyte</u>			
Survey Team: <u>Maridel Miras, Marla Morris</u>			
Flow condition: average		Weather Condition: fair	
Latitude: <u>11°02'18.90219" N</u>		Longitude: <u>124°57'42.98645" E</u>	

Deck (Please start your measurement from the left side of the bank facing upstream)
Elevation: 20.630 m **Width:** 8.86 m **Span (BA3-BA2):** 48.520 m

Station	High Chord Elevation	Low Chord Elevation
1	Not available	Not available

Bridge Approach (Please start your measurement from the left side of the bank facing upstream)

	Station(Distance from BA1)	Elevation		Station(Distance from BA1)	Elevation
BA1	Not available	Not available	BA3	66.433 m	20.638 m
BA2	17.913 m	20.630 m	BA4	114.868 m	17.403 m

Abutment: Is the abutment sloping? Yes; If yes, fill in the following information:

	Station (Distance from BA1)	Elevation
Ab1	Not available	Not available
Ab2	Not available	Not available

Pier (Please start your measurement from the left side of the bank facing upstream)

Shape: circular Number of Piers: 2 Height of column footing: Not available

	Station (Distance from BA1)	Elevation	Pier Diameter
Pier 1	32.275 m	20.632 m	1.5 m
Pier 2	52.113 m	20.652 m	1.5 m

NOTE: Use the center of the pier as reference to its station

Figure 49. Bridge as-built form of Guinarona Bridge

Water surface elevation of Guinarona River was determined by a survey grade GNSS receiver Trimble® SPS 882 in PPK survey technique on October 22, 2016 at 11:00 AM with a value of 11.757 m in MSL as shown in Figure 48. This was translated into marking on the bridge’s deck using the same technique as shown in Figure 50. The marking will serve as reference for flow data gathering and depth gauge deployment of the partner HEI responsible for Guinarona River, the Visayas State University.



Figure 50. Water-level markings on Guinarona Bridge

4.6 Validation Points Acquisition Survey

Validation points acquisition survey was conducted on September 8 and October 23, 2016 using a survey-grade GNSS Rover receiver, Trimble® SPS 882, mounted at the side of a vehicle as shown in Figure 51. It was secured with a nylon rope to ensure that it was horizontally and vertically balanced. The antenna height was 2.055 m and measured from the ground up to the bottom of notch of the GNSS Rover receiver. The PPK technique utilized for the conduct of the survey was set to continuous topo mode with BM-1 occupied as the GNSS base station in the conduct of the survey.

The survey started in Brgy. Guindapunan, Municipality of Palo going west covering nine (9) barangays in Palo, seven (7) barangays in Municipality of Sta. Fe, and another seven (7) barangays in Municipality of Alangalang, and ended in Brgy. Mudboron, Alangalang. The survey gathered a total of 4,717 points with approximate length of 22 km using BM-1 as GNSS base station for the entire extent validation points acquisition survey as illustrated in the map in Figure 52.

4.7 River Bathymetric Survey

Bathymetric survey was executed on August 25, 2016 using Trimble® SPS 855 in GNSS RTK survey technique and October 23, 2016 using a Trimble® SPS 855 in GNSS PPK survey technique in continuous topo mode as illustrated in Figure 53. The survey started in Brgy. Burak, Municipality of Tolosa with coordinates 11°03'30.11457"N, 125°01'00.73679"E, and ended at the mouth of the river in Brgy. Cabuynan, Municipality of Tanauan, with coordinates 11°05'30.33016"N, 125°01'23.99098"E. The control points BM-1 and LIM-VSU were used as GNSS base stations all throughout the entire survey.

The bathymetric survey for Guinarona River gathered a total of 7,674 points covering 4.941 km of the river traversing Barangays Bislig, Cabuynan, Limbuan Guti, and Limbuan Daku in Municipality of Tanauan; and Barangays Burak and Olot in Municipality of Tolosa. A CAD drawing was also produced to illustrate the riverbed profile of Guinarona River. As shown in Figure 55, the highest and lowest elevation has an 5-m difference. The highest elevation observed was 0.232 m above MSL located in Brgy. Burak, Municipality of Tolosa; while the lowest was -5.447 m below MSL located in Brgy. Bislig, Municipality of Tanauan.



Figure 51. Validation points acquisition survey set up along Guinarona River Basin

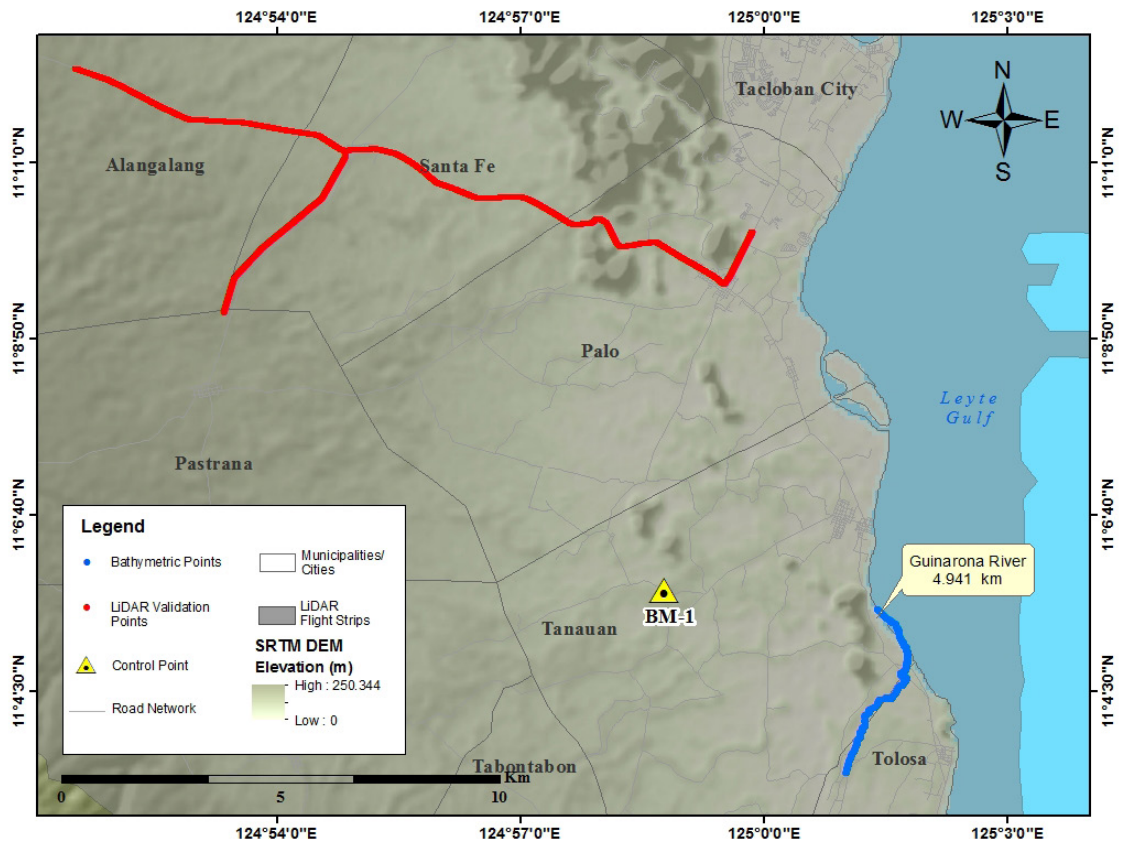


Figure 52. Validation point acquisition survey of Guinarona River basin

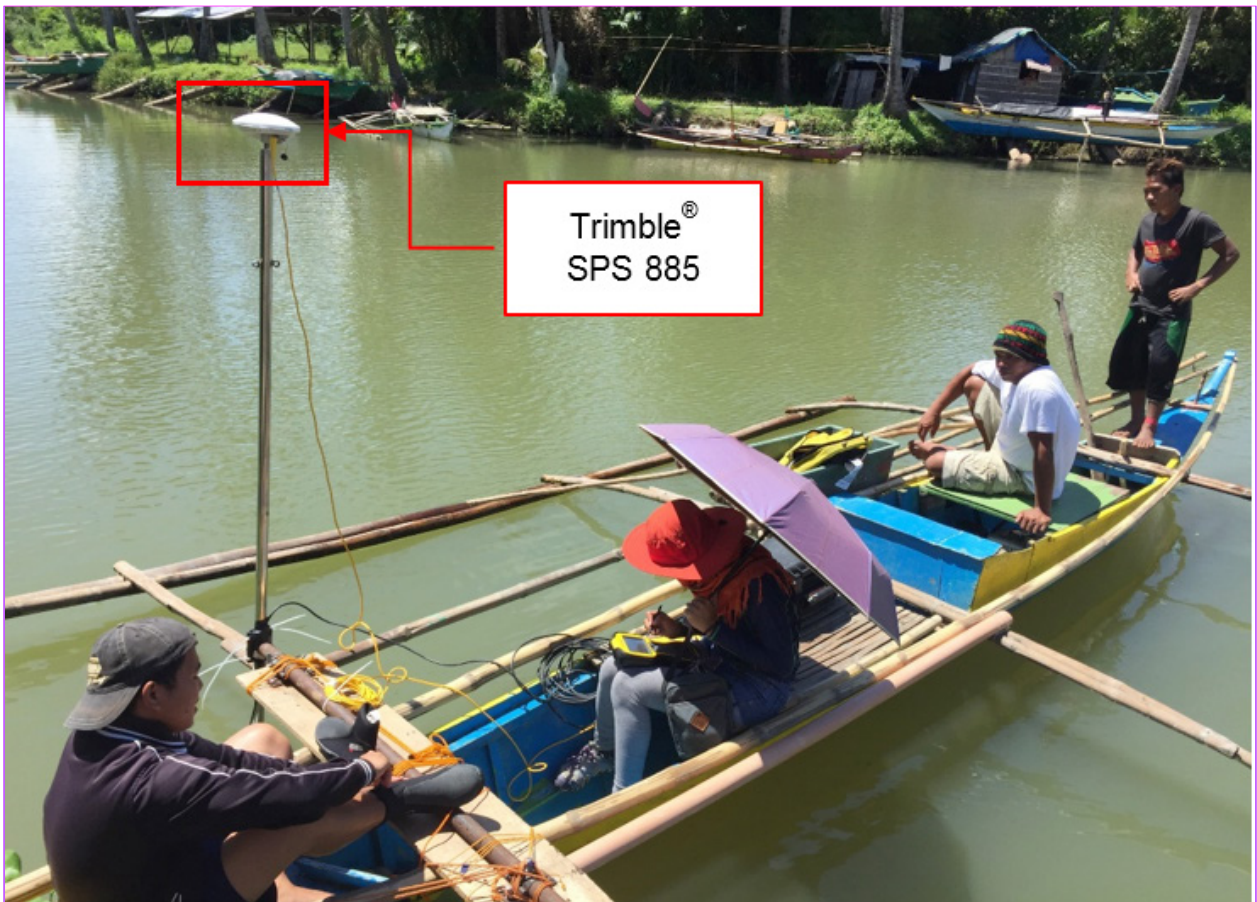


Figure 53. Bathymetric survey using a Trimble® SPS 885 in GNSS RTK survey technique in Guinarona River

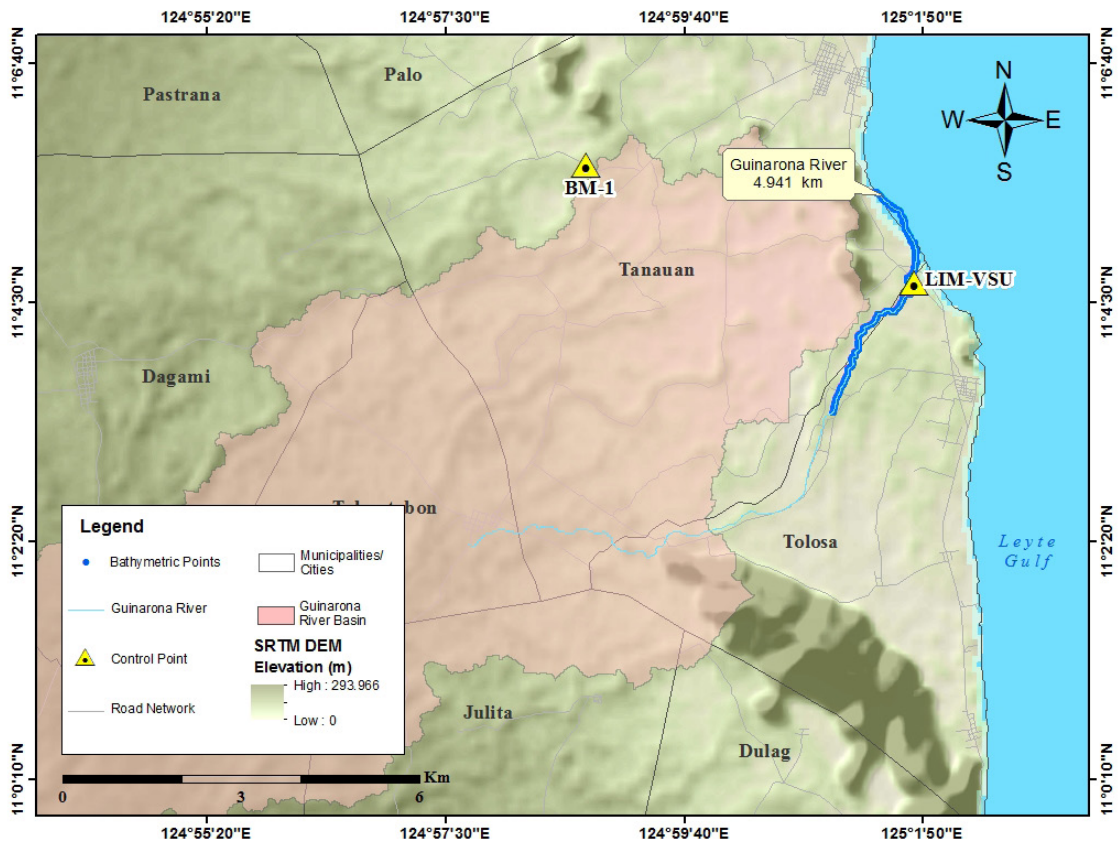


Figure 54. Bathymetric survey of Guinarona River

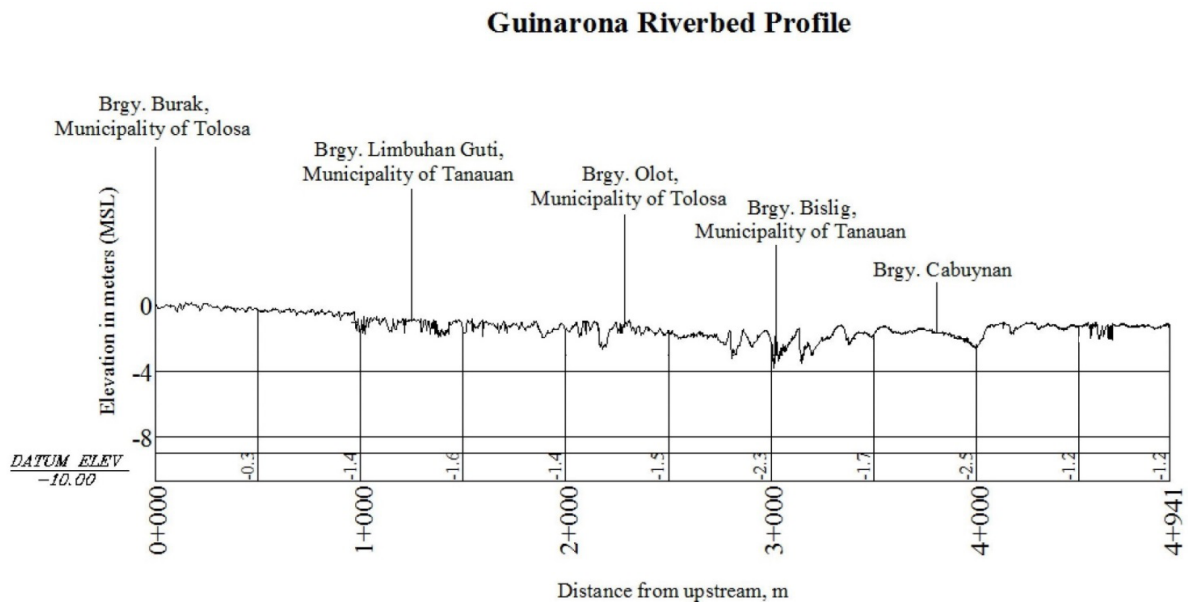


Figure 55. Guinarona Riverbed Profile

CHAPTER 5: FLOOD MODELING AND MAPPING

Engr. Ma. Rosario Concepcion O. Ang, Engr. John Louie D. Fabila, Engr. Sarah Jane D. Samalbuero , Engr. Harmond F. Santos , Engr. Gladys Mae Apat , Engr. Melanie C. Hingpit, Jovy Anne S. Narisma, Engr. Vincent Louise DL. Azucena , Nereo Joshua G. Pecson, Areeanne Katrice K. Umali

The methods applied in this Chapter were based on the DREAM methods manual (Lagmay, et al., 2014) and further enhanced and updated in Paringit, et al. (2017).

5.1 Data Used for Hydrologic Modeling

5.1.1 Hydrometry and Rating Curves

All data that affect the hydrologic cycle of the river basin were monitored, collected, and analyzed. Rainfall, water level, and flow in a certain period of time, which may affect the hydrologic cycle of the Guinarona River Basin were monitored, collected, and analyzed.

5.1.2 Precipitation

Precipitation data was taken from three automatic rain gauges (ARGs) installed by the Department of Science and Technology – Advanced Science and Technology Institute (DOST-ASTI). The location of the rain gauge is seen in Figure 56.

Total rain from Guinarona rain gauge is 77.6 mm. It peaked to 59.02 mm on 11 January 2017, 14:50. A summary of the data is seen in Table 30. The lag time between the peak rainfall and discharge is 14 hours and 50 minutes.

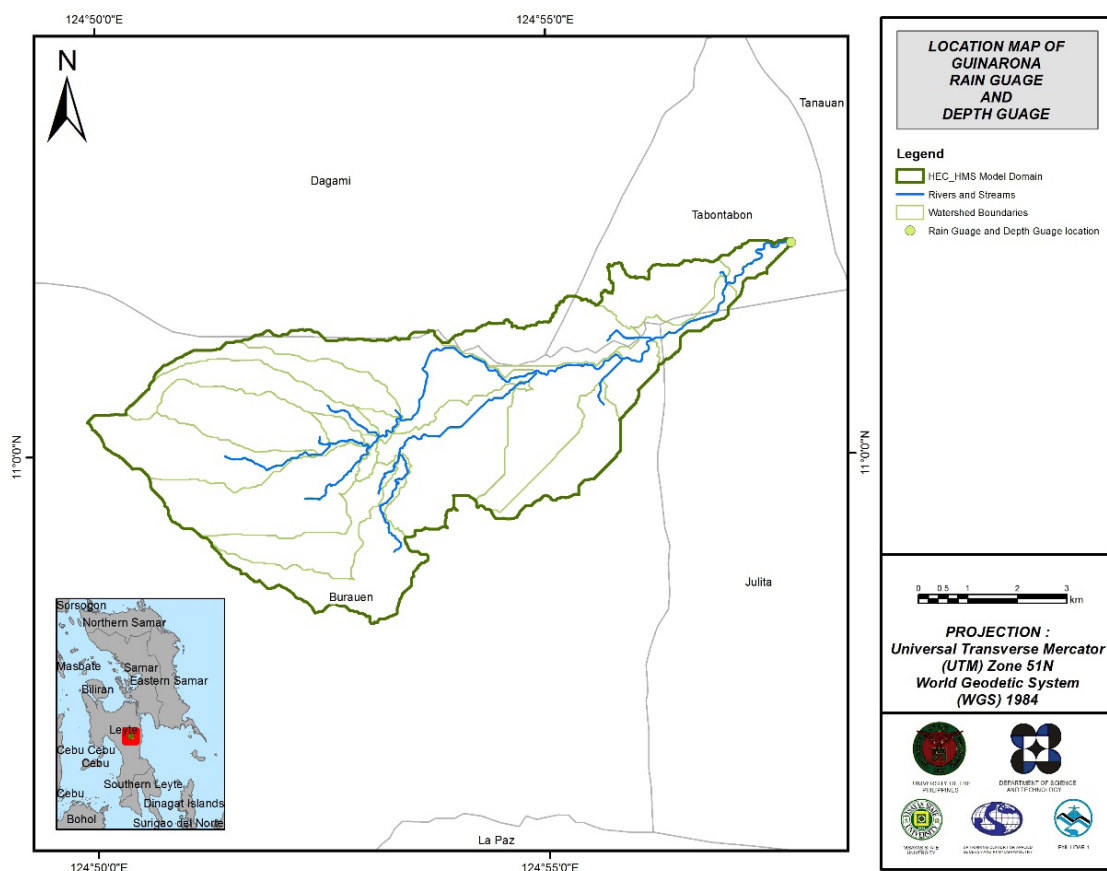


Figure 56. The location map of Guinarona HEC-HMS model used for calibration

5.1.3 Rating Curves and River Outflow

A rating curve was developed at Sohoton Bridge, Guinarona, Samar (11°20'32.48"N, 125° 9'29.09"E). It gives the relationship between the observed water levels at Sohoton Bridge and outflow of the watershed at this location.

For Sohoton Bridge, the rating curve is expressed as $Q = 9E-17e^{2.4352h}$ as shown in Figure 58.

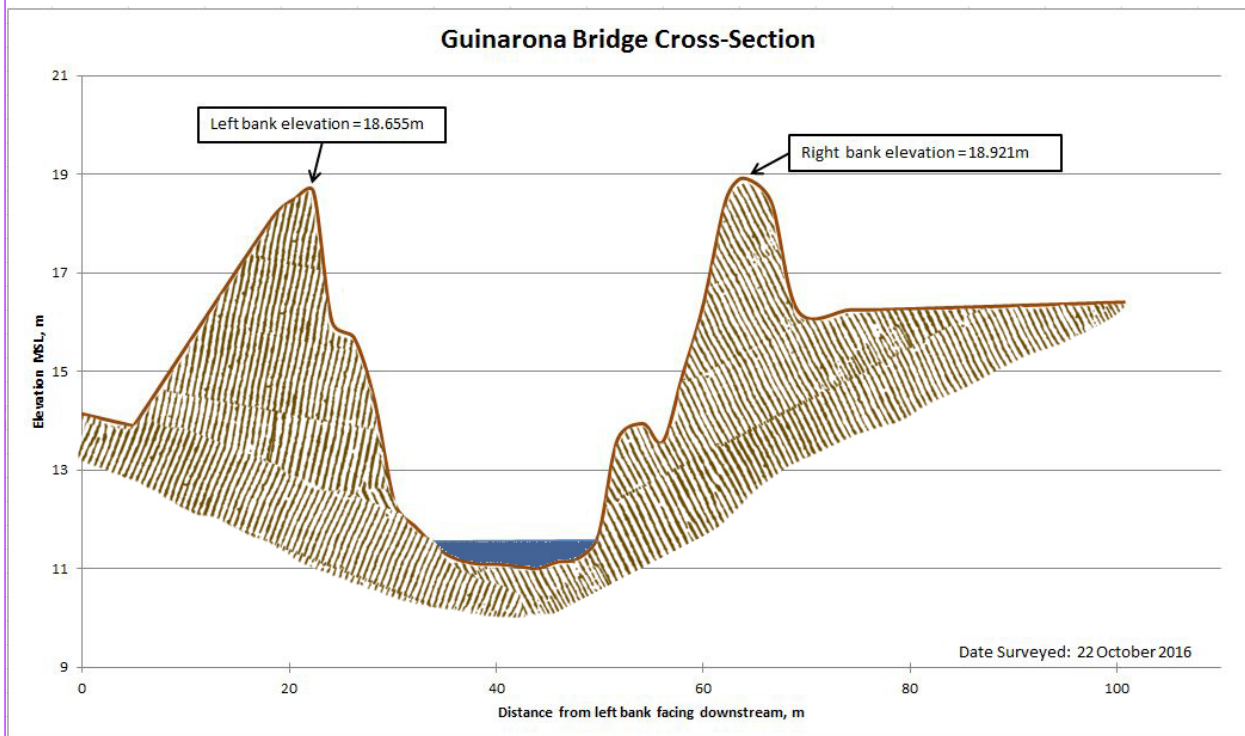


Figure 57. Cross-Section Plot of Guinarona Bridge

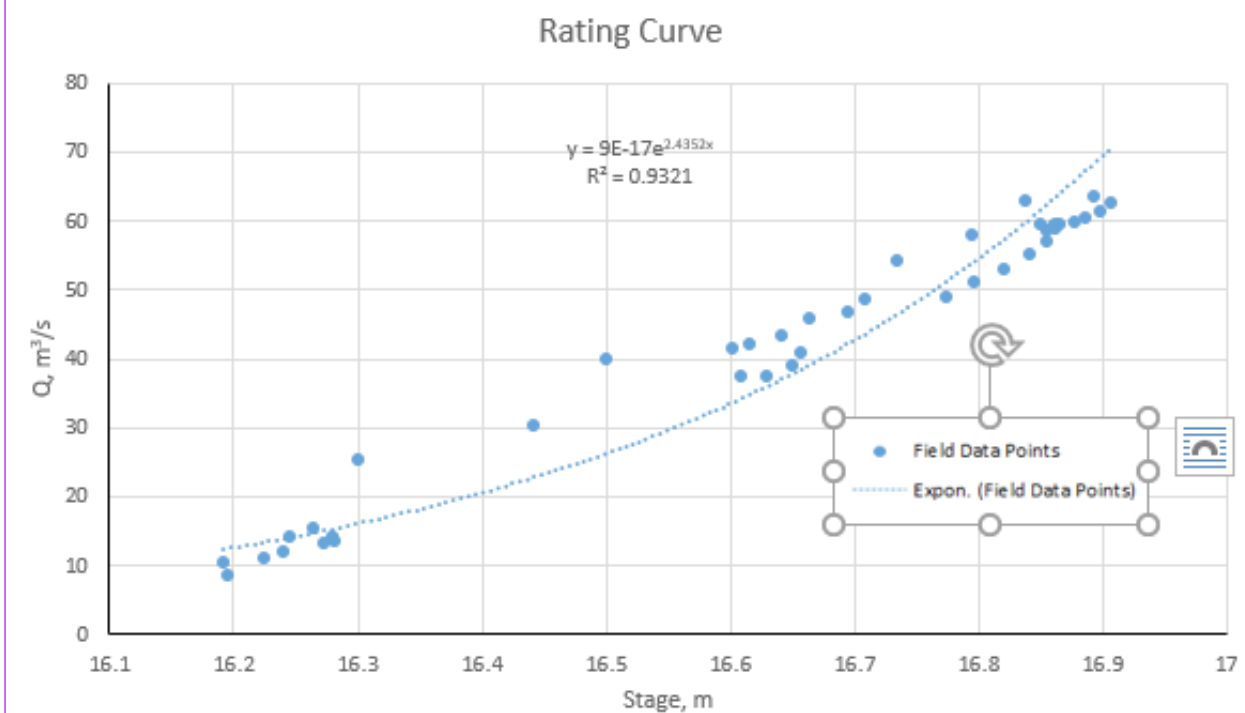


Figure 58. Rating Curve at Guinarona Bridge Sta. Rita, Samar

This rating curve equation was used to compute the river outflow at Guinarona Bridge for the calibration of the HEC-HMS model shown in Figure 59.

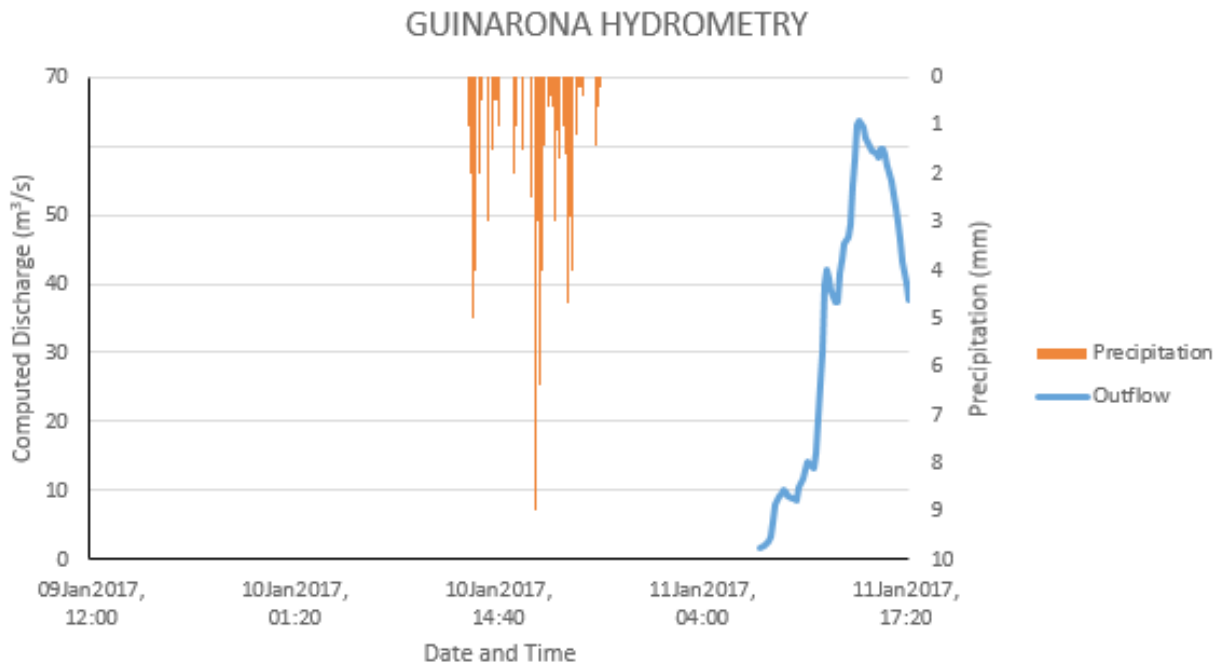


Figure 59. Rainfall and outflow data at Guinarona used for modeling

5.2 RIDF Station

The Philippines Atmospheric Geophysical and Astronomical Services Administration (PAGASA) computed Rainfall Intensity Duration Frequency (RIDF) values for the Tacloban Rain Gauge. The RIDF rainfall amount for 24 hours was converted to a synthetic storm by interpolating and re-arranging the value in such a way certain peak value will be attained at a certain time. This station chosen based on its proximity to the Guinarona watershed. The extreme values for this watershed were computed based on a 59-year record.

Table 30. RIDF values for Tacloban Rain Gauge computed by PAGASA

COMPUTED EXTREME VALUES (in mm) OF PRECIPITATION									
T (yrs)	10 mins	20 mins	30 mins	1 hr	2 hrs	3 hrs	6 hrs	12 hrs	24 hrs
2	17.8	26.9	33.6	42.8	59.7	70.5	87.2	104	120.6
5	24.3	36.7	45.7	57.4	80.7	95.2	117.9	140.6	161.4
10	28.5	43.2	53.7	67.1	94.6	111.5	138.2	164.9	188.4
15	30.9	46.8	58.3	72.5	102.5	120.7	149.6	178.6	203.7
20	32.6	49.4	61.4	76.3	108	127.1	157.7	188.1	214.3
25	33.9	51.4	63.9	79.3	112.2	132.1	163.8	195.5	222.6
50	37.9	57.5	71.4	88.3	125.2	147.4	182.9	218.2	247.9
100	41.8	63.5	78.9	97.3	138.2	162.5	201.8	240.8	273

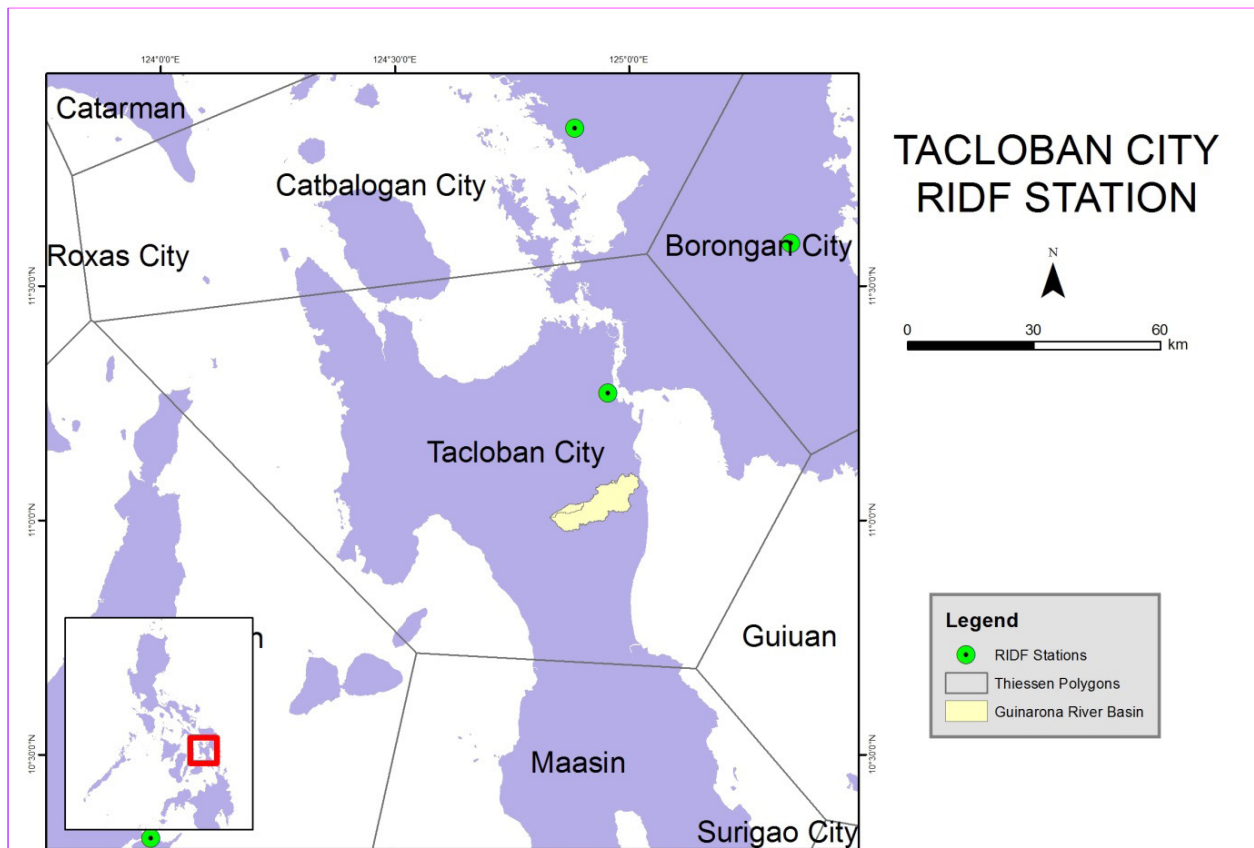


Figure 60. Location of Tacloban RIDF station relative to Guinarona River Basin

Tacloban Rainfall Intensity Duration Frequency

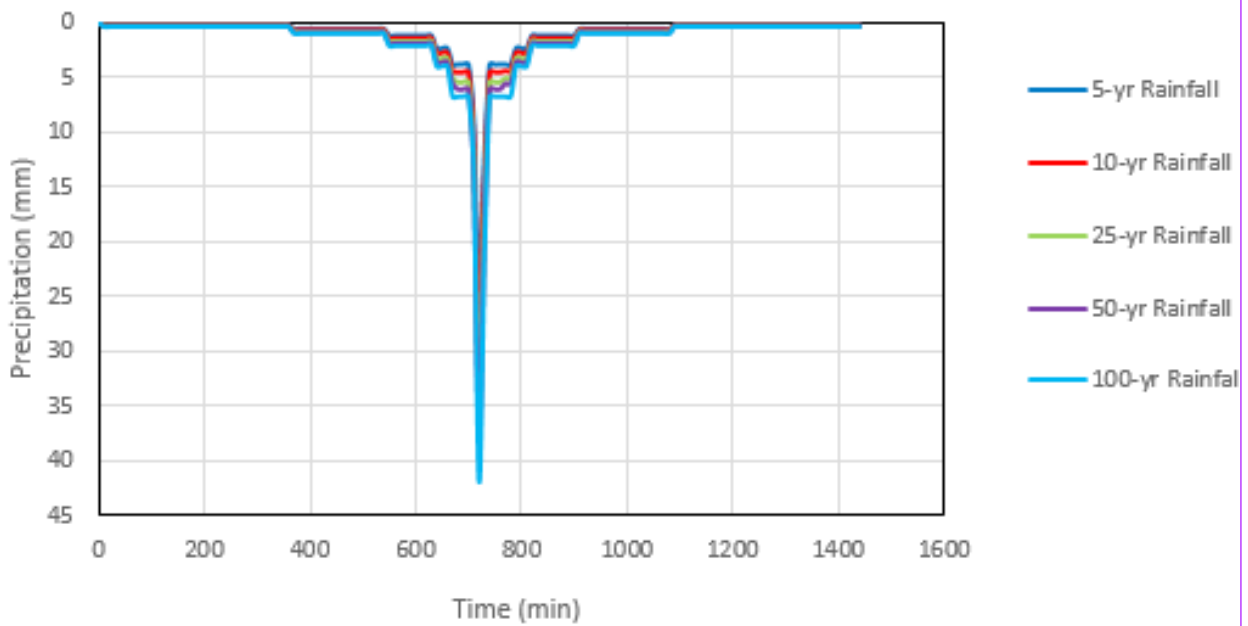


Figure 61. Synthetic storm generated for a 24-hr period rainfall for various return periods

5.3 HMS Model

The soil shapefile (dated pre-2004) was taken from the Bureau of Soils and Water Management under the Department of Agriculture. The land cover dataset is from the National Mapping and Resource information Authority (NAMRIA). The soil and land cover of the Guinarona River Basin are shown in Figures 62 and 63, respectively.

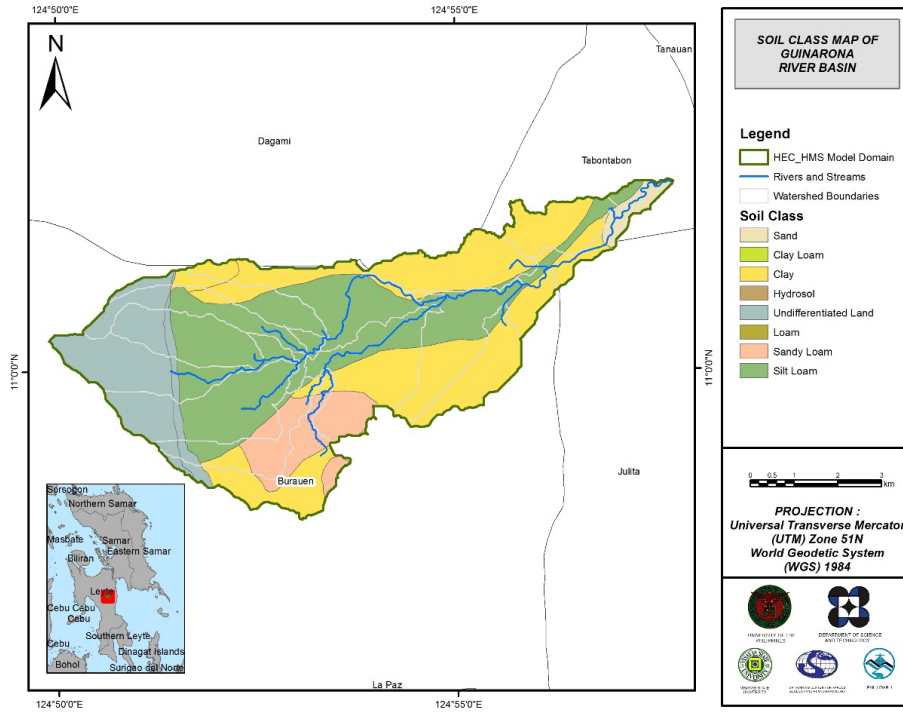


Figure 62. Soil Map of Guinarona River Basin (Source: Bureau of Soils and Water Management)

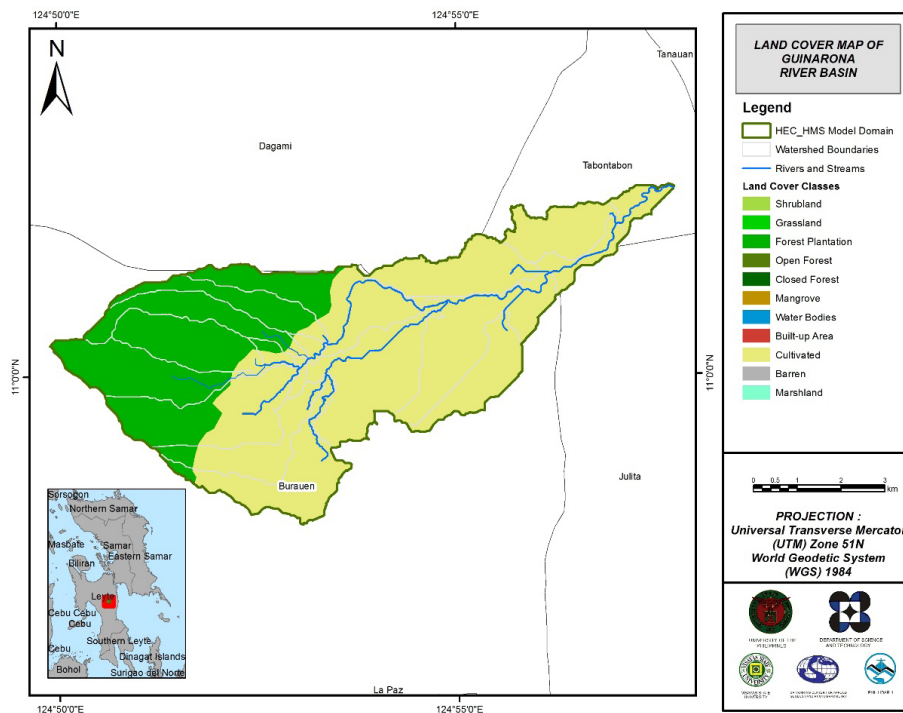


Figure 63. Land Cover Map of Guinarona River Basin (Source: NAMRIA)

For Guinarona, the soil classes identified were clay, silt loam, sandy loam, sand, and undifferentiated. The land cover types identified were forest plantation, and cultivated.

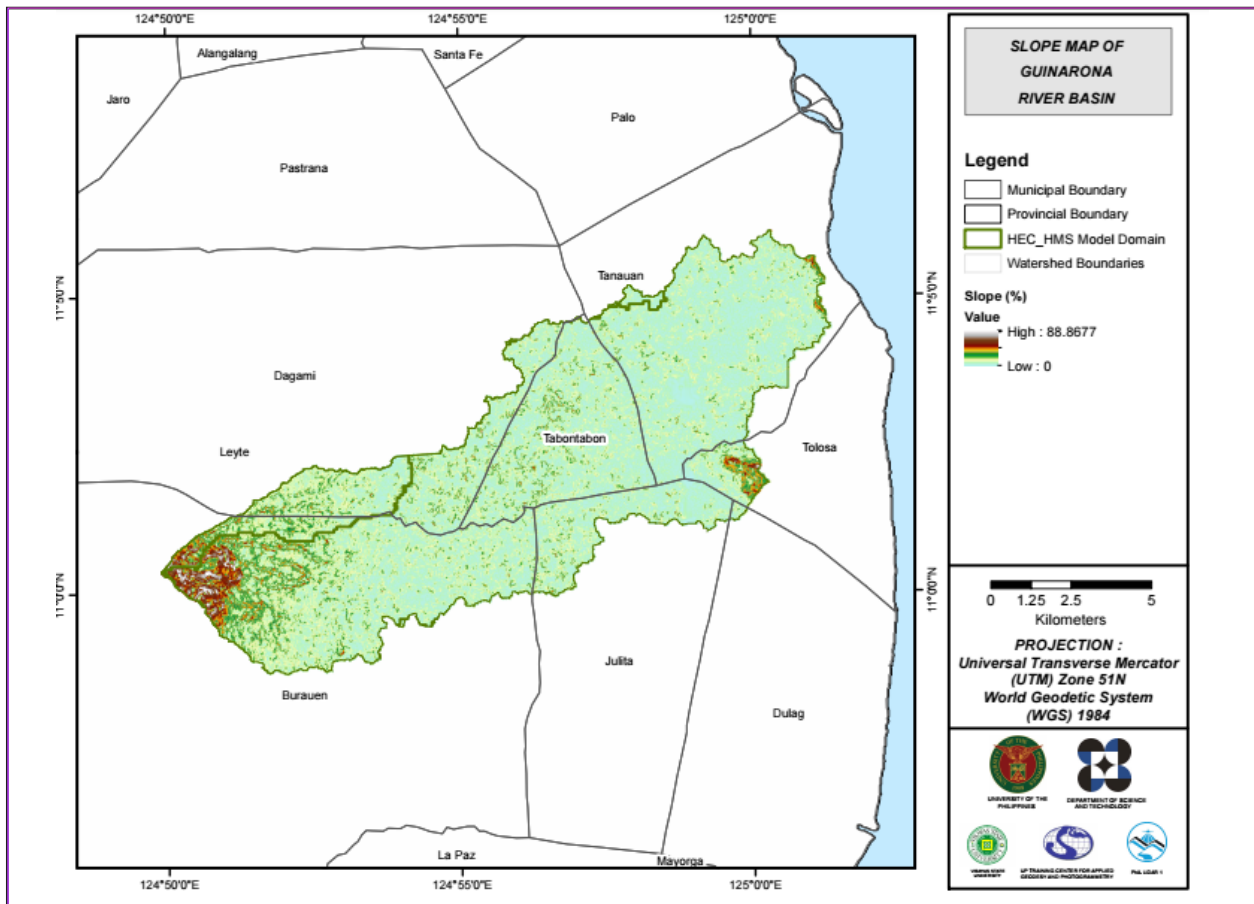


Figure 64. Slope Map of Guinarona River Basin

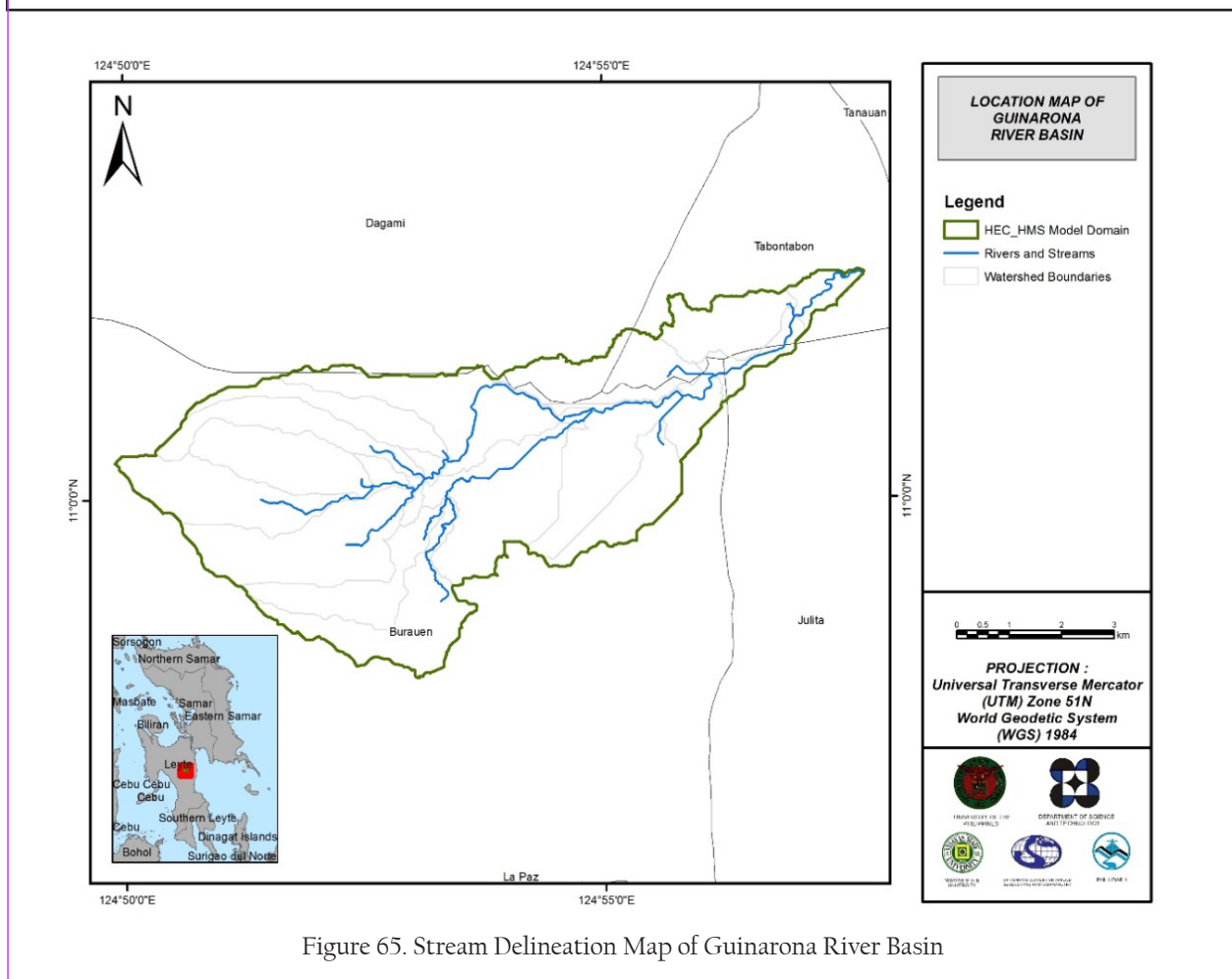


Figure 65. Stream Delineation Map of Guinarona River Basin

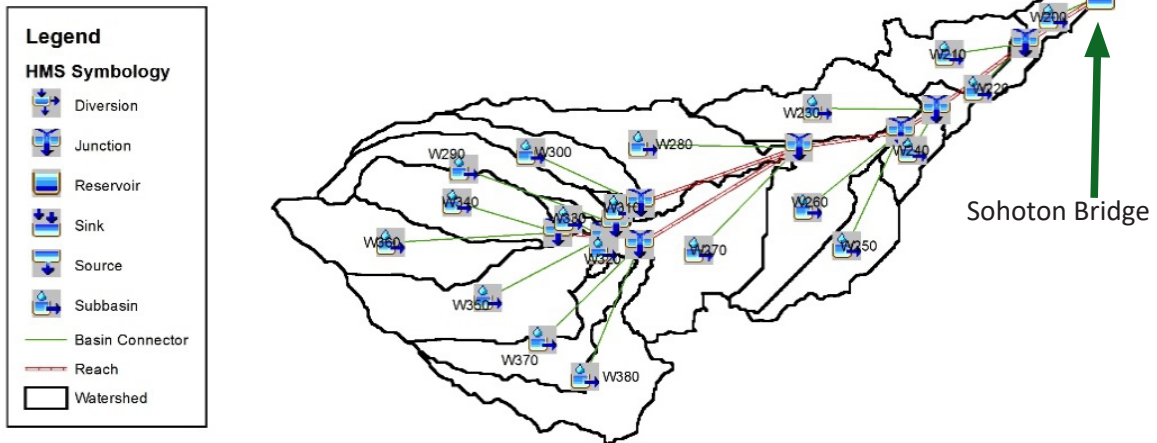


Figure 66. The Guinarona river basin model generated using HEC-HMS

Using the SAR-based DEM, the Guinarona basin was delineated and further subdivided into subbasins. The model consists of 19 sub basins, 9 reaches, and 9 junctions as shown in Figure 66. The main outlet is at Sohoton Bridge.

5.4 Cross-section Data

Riverbed cross-sections of the watershed were necessary in the HEC-RAS model setup. The cross-section data for the HEC-RAS model was derived from the LiDAR DEM data. It was defined using the Arc GeoRAS tool and was post-processed in ArcGIS.

5.5 Flo 2D Model

The automated modelling process allows for the creation of a model with boundaries that are almost exactly coincidental with that of the catchment area. As such, they have approximately the same land area and location. The entire area is divided into square grid elements, 10 meter by 10 meter in size. Each element is assigned a unique grid element number which serves as its identifier, then attributed with the parameters required for modelling such as x-and y-coordinate of centroid, names of adjacent grid elements, Manning coefficient of roughness, infiltration, and elevation value. The elements are arranged spatially to form the model, allowing the software to simulate the flow of water across the grid elements and in eight directions (north, south, east, west, northeast, northwest, southeast, southwest).

Based on the elevation and flow direction, it is seen that the water will generally flow from the west of the model to the east, following the main channel. As such, boundary elements in those particular regions of the model are assigned as inflow and outflow elements respectively.

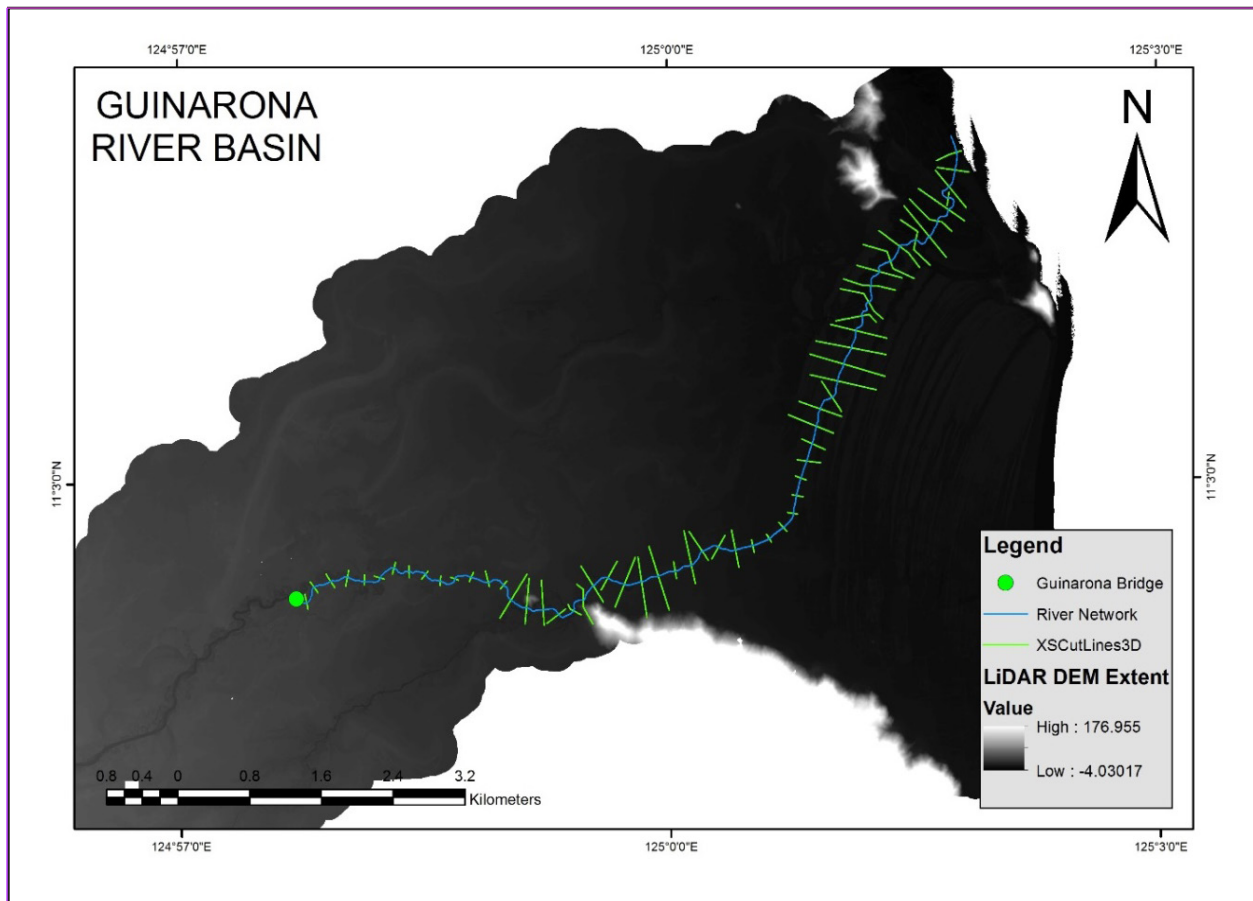


Figure 67. River cross-section of Guinarona River generated through Arcmap HEC GeoRAS tool

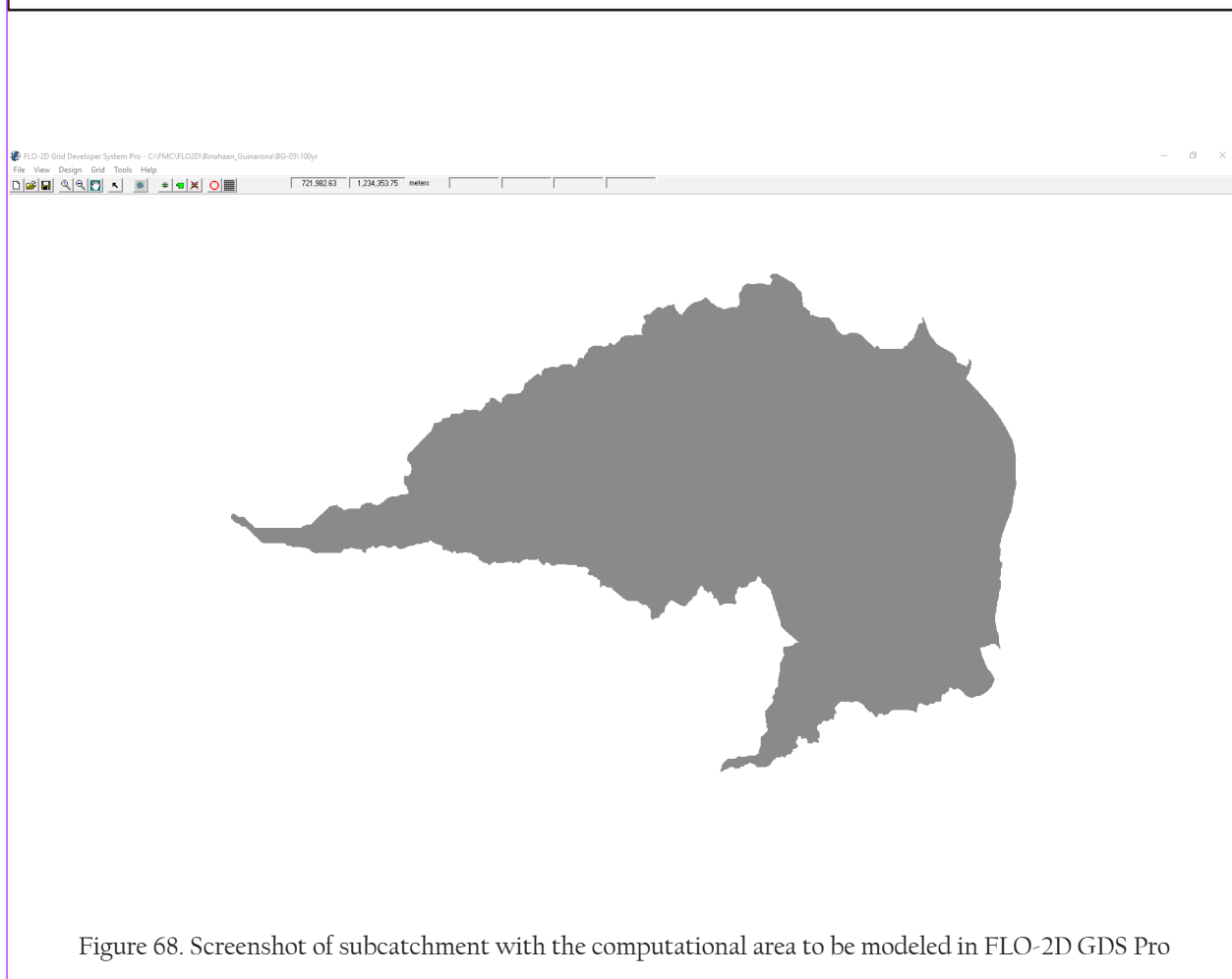


Figure 68. Screenshot of subcatchment with the computational area to be modeled in FLO-2D GDS Pro

The simulation is then run through FLO-2D GDS Pro. This particular model had a computer run time of 54.51257 hours. After the simulation, FLO-2D Mapper Pro is used to transform the simulation results into spatial data that shows flood hazard levels, as well as the extent and inundation of the flood. Assigning the appropriate flood depth and velocity values for Low, Medium, and High creates the following food hazard map. Most of the default values given by FLO-2D Mapper Pro are used, except for those in the Low hazard level. For this particular level, the minimum h (Maximum depth) is set at 0.2 m while the minimum vh (Product of maximum velocity (v) times maximum depth (h)) is set at 0 m²/s.

The creation of a flood hazard map from the model also automatically creates a flow depth map depicting the maximum amount of inundation for every grid element. The legend used by default in Flo-2D Mapper is not a good representation of the range of flood inundation values, so a different legend is used for the layout. In this particular model, the inundated parts cover a maximum land area of 77 535 744.00 m².

There is a total of 37 293 755.25 m³ of water entering the model. Of this amount, 20 278 785.44 m³ is due to rainfall while 17 014 969.81 m³ is inflow from other areas outside the model. 11 670 205.00 m³ of this water is lost to infiltration and interception, while 24 880 022.57 m³ is stored by the flood plain. The rest, amounting up to 743 534.13 m³, is outflow.

5.6 Results of HMS Calibration

After calibrating the Guinarona HEC-HMS river basin model, its accuracy was measured against the observed values (see Annex 9. Guinarona Model Basin Parameters). Figure 69 shows the comparison between the two discharge data.

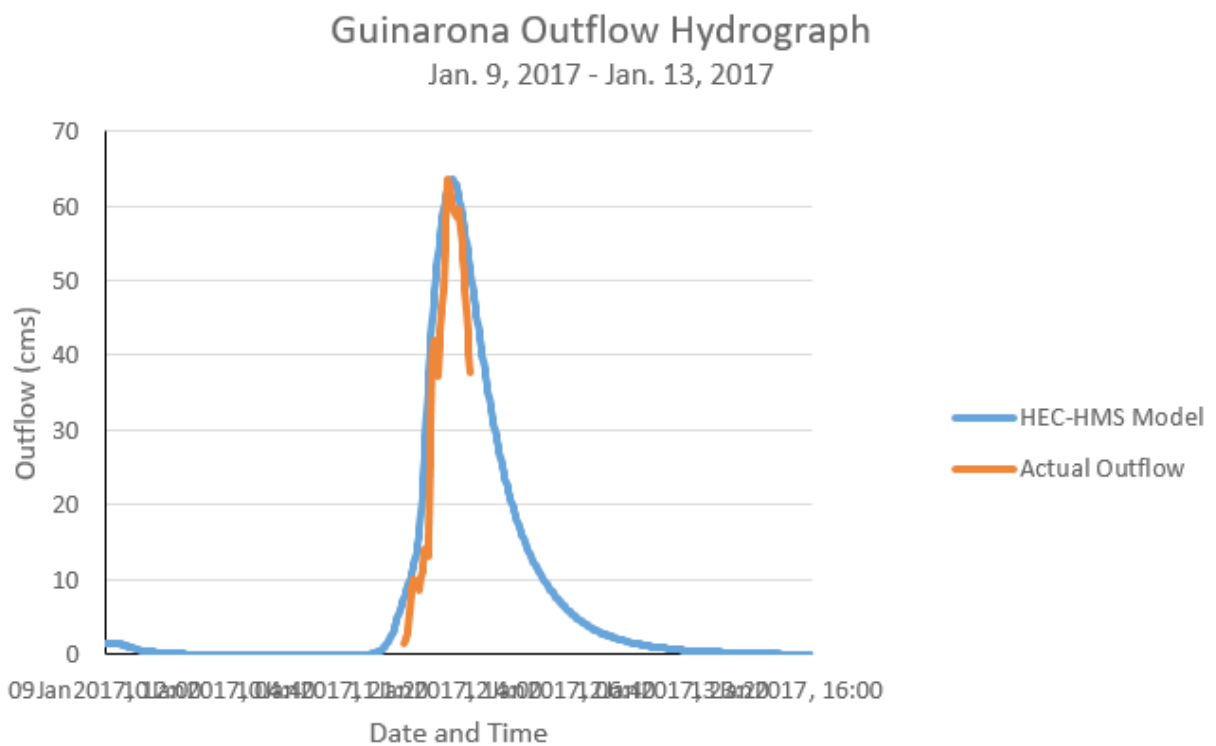


Figure 69. Outflow Hydrograph of Guinarona produced by the HEC-HMS model compared with observed outflow

Enumerated in Table 31 are the adjusted ranges of values of the parameters used in calibrating the model.

Initial abstraction defines the amount of precipitation that must fall before surface runoff. The magnitude of the outflow hydrograph increases as initial abstraction decreases. The range of values from 4mm to 11mm means that there is a minimal to average amount of infiltration or rainfall interception by vegetation.

Curve number is the estimate of the precipitation excess of soil cover, land use, and antecedent moisture. The magnitude of the outflow hydrograph increases as curve number increases. The range of 63 to 89 for curve number is advisable for Philippine watersheds depending on the soil and land cover of the area (M. Horritt, personal communication, 2012).

Table 31. Range of Calibrated Values for Guinarona

Hydrologic Element	Calculation Type	Method	Parameter	Range of Calibrated Values
Basin	Loss	SCS Curve Number	Initial Abstraction (mm) Curve Number	4 - 11 63 - 89
	Transform	Clark Unit Hydrograph	Time of Concentration (hr) Storage Coefficient (hr)	1 - 7 1 - 9
	Baseflow	Recession	Recession Constant Ratio to Peak	0.2 0.8
Reach	Routing	Muskingum-Cunge	Manning's Coefficient	0.04

Time of concentration and storage coefficient are the travel time and index of temporary storage of runoff in a watershed. The range of calibrated values from 1 to 9 hours determines the reaction time of the model with respect to the rainfall. The peak magnitude of the hydrograph also decreases when these parameters are increased.

Recession constant is the rate at which baseflow recedes between storm events and ratio to peak is the ratio of the baseflow discharge to the peak discharge. Recession constant of 0.2 indicates that the basin is likely to quickly go back to its original discharge and instead, will be higher. Ratio to peak of 0.8 indicates a milder slope of receding limb of the outflow hydrograph.

Manning's roughness coefficient of 0.04 corresponds to the common roughness in Guinarona watershed, which is determined to be cultivated with mature field crops (Brunner, 2010).

Table 32. Summary of the Efficiency Test of Guinarona HMS Model

RMSE	2.9
r ²	0.9321
NSE	0.78
PBIAS	-17.65
RSR	0.47

The Root Mean Square Error (RMSE) method aggregates the individual differences of these two measurements. It was computed as 2.9 (m³/s).

The Pearson correlation coefficient (r²) assesses the strength of the linear relationship between the observations and the model. This value being close to 1 corresponds to an almost perfect match of the observed discharge and the resulting discharge from the HEC HMS model. Here, it measured 0.9321.

The Nash-Sutcliffe (E) method was also used to assess the predictive power of the model. Here the optimal value is 1. The model attained an efficiency coefficient of 0.78.

A positive Percent Bias (PBIAS) indicates a model's propensity towards under-prediction. Negative values indicate bias towards over-prediction. Again, the optimal value is 0. In the model, the PBIAS is -17.65.

The Observation Standard Deviation Ratio, RSR, is an error index. A perfect model attains a value of 0 when the error in the units of the valuable a quantified. The model has an RSR value of 0.47.

5.7 Calculated outflow hydrographs and discharge values for different rainfall return periods

5.7.1 Hydrograph using the Rainfall Runoff Model

The summary graph (Figure 70) shows the Guinarona outflow using the Tacloban Rainfall Intensity-Duration-Frequency curves (RIDF) in 5 different return periods (5-year, 10-year, 25-year, 50-year, and 100-year rainfall time series) based on the Philippine Atmospheric Geophysical and Astronomical Services

Administration (PAG-ASA) data. The simulation results reveal significant increase in outflow magnitude as the rainfall intensity increases for a range of durations and return periods.

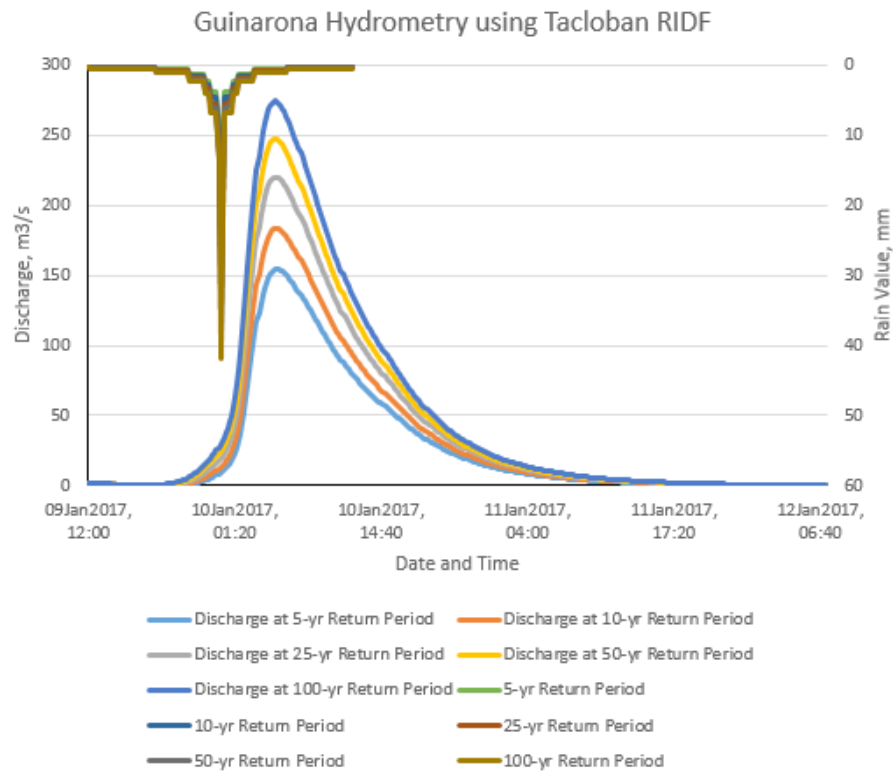


Figure 70. Outflow hydrograph at Guinarona Station generated using Tacloban RIDF simulated in HEC-HMS

A summary of the total precipitation, peak rainfall, peak outflow and time to peak of the Guinarona discharge using the Tacloban Rainfall Intensity-Duration-Frequency curves (RIDF) in five different return periods is shown in Table 33.

Table 33. Peak values of the Guinarona HEC-HMS Model outflow using the Tacloban RIDF

RIDF Period	Total Precipitation (mm)	Peak rainfall (mm)	Peak outflow (m ³ /s)	Time to Peak
5-Year	161.40	24.30	154.4	5 hours
10-Year	188.40	28.25	183.5	5 hour, 10 minutes
25-Year	222.60	33.90	220.2	5 hours
50-Year	247.90	37.90	247.2	5 hours
100-Year	273.00	41.90	274.1	5 hours

5.8 River Analysis (RAS) Model Simulation

The HEC-RAS Flood Model produced a simulated water level at every cross-section for every time step for every flood simulation created. The resulting model will be used in determining the flooded areas within the model. The simulated model will be an integral part in determining real-time flood inundation extent of the river after it has been automated and uploaded on the DREAM website. For this publication, only a sample output map river was to be shown, since only the VSU-FMC base flow was calibrated. The sample generated map of Guinarona River using the calibrated HMS base flow is shown in Figure 71.



Figure 71. Sample output of Guinarona RAS Model

5.9 Flow Depth and Flood Hazard

The resulting hazard and flow depth maps have a 10m resolution. Figure 72 to Figure 77 shows the 5-, 25-, and 100-year rain return scenarios of the Guinarona floodplain.

The floodplain, with an area of 371.87 sq. km., covers ten municipalities namely Burauen, Dagami, Dulag, Jaro, Julita, Palo, Pastrana, Tabontabon, Tanauan, and Tolosa. Table shown the percentage of area affected by flooding per municipality.

Table . Municipalities affected in Guinarona flood plain

Municipality	Total Area	Area Flooded	% Flooded
Burauen	205.31	19.65	10%
Dagami	134.08	108.06	81%
Dulag	63.65	22.78	36%
Jaro	190.65	0.44	0.2%
Julita	57.17	24.36	43%
Palo	65.34	44.12	68%
Pastrana	79.17	39.94	50%
Tabontabon	20.46	20.46	100%
Tanauan	62.78	62.68	100%
Tolosa	28.17	28.14	100%

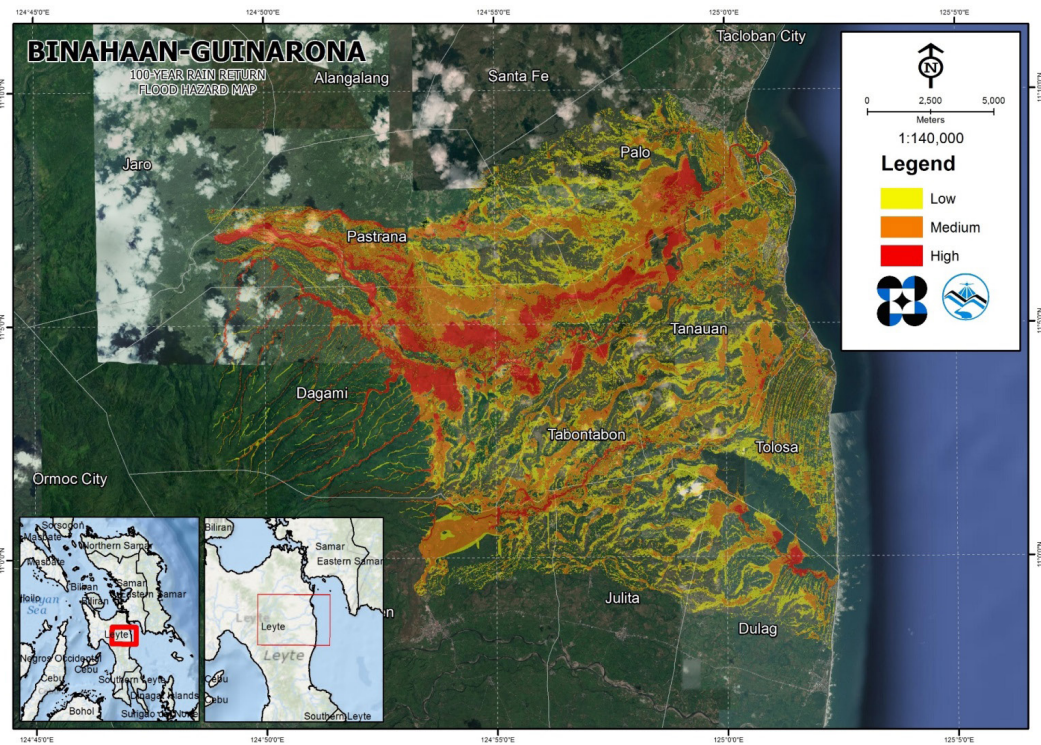


Figure 72. 100-year Rain Return Flood Hazard Map for Binahaan-Guinarona Floodplain

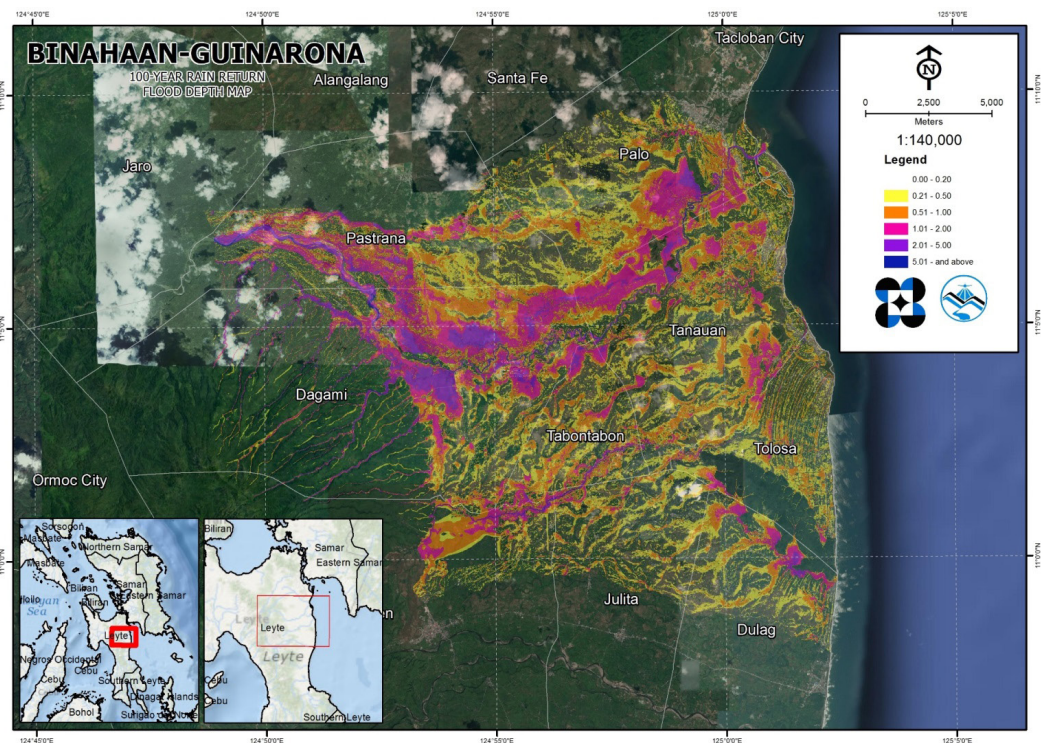


Figure 73. 100-year Rain Return Flood Depth Map for Binahaan-Guinarona Floodplain

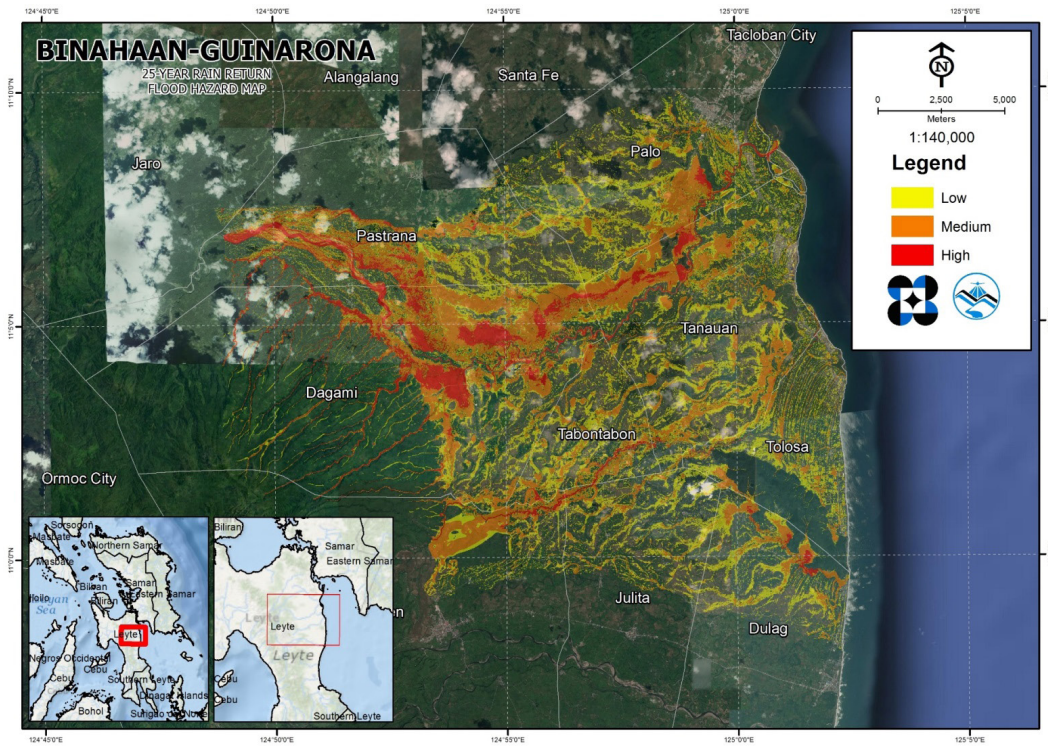


Figure 74. 25-year Rain Return Flood Hazard Map for Binahaan-Guinarona Floodplain

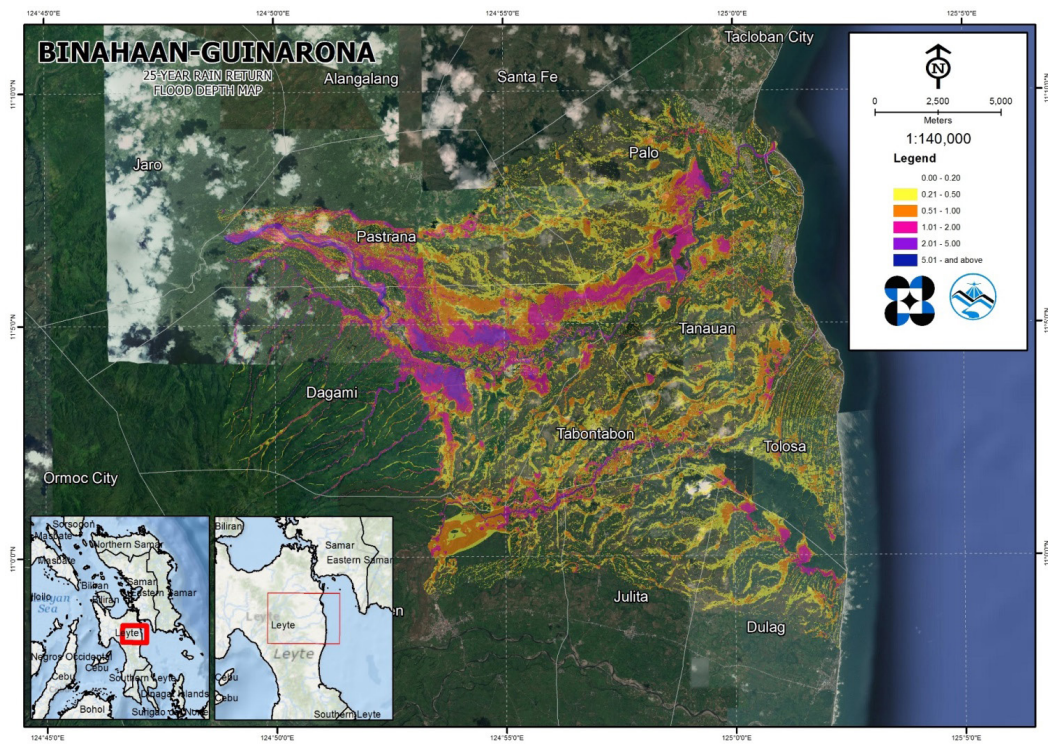


Figure 75. 25-year Rain Return Flood Depth Map for Binahaan-Guinarona Floodplain

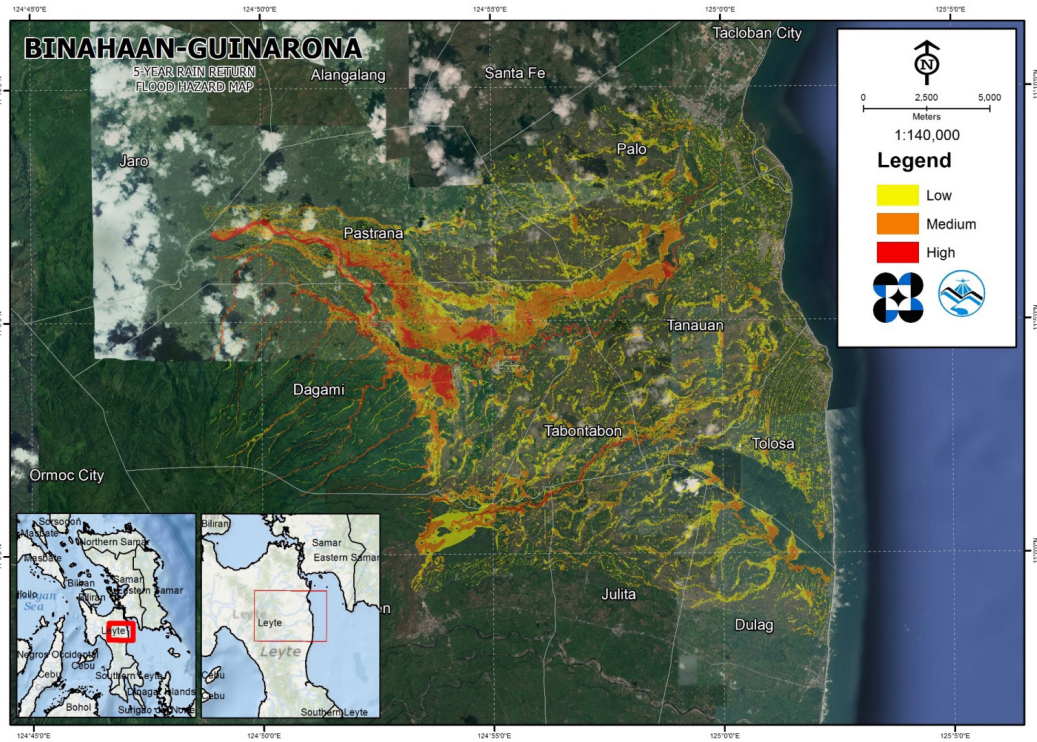


Figure 76. 5-year Rain Return Flood Hazard Map for Binahaan-Guinarona Floodplain

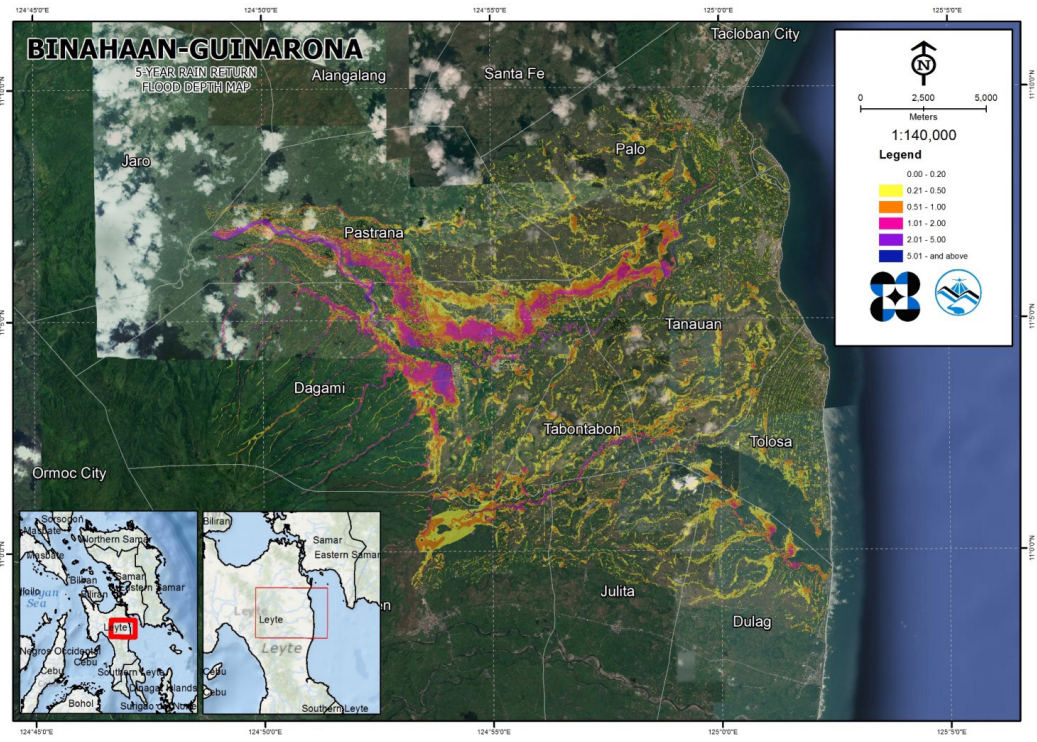


Figure 77. 5-year Rain Return Flood Depth Map for Binahaan-Guinarona Floodplain

5.10 Inventory of Areas Exposed to Flooding

Affected barangays in Binahaan river basin, grouped by municipality, are listed below. For the said basin, 7 municipality consisting of 54 barangays are expected to experience flooding when subjected to 5-yr rainfall return period. The list of all educational and health institutions affected by flooding in the Guinarona floodplain can be found in Annexes 12-13, respectively.

For the 5-year return period, 0.09% of the municipality of Burauen with an area of 205.31 sq. km. will experience flood levels of less than 0.20 meters and 0.006% of the area will experience flood levels of 0.51 to 1 meter. Listed in Table 34 are the affected areas in square kilometres by flood depth per barangay.

Table 34. Affected Areas in Burauen, Leyte during 5-Year Rainfall Return Period

Affected Area (sq. km.) by flood depth (in m.)		Total Area	Area Flooded	% Flooded
		Buri	Cadahunan	Tambis
Affected Area (sq. km)	0.03-0.20	0.054	0.11	0.029
	0.21-0.50	0	0	0
	0.51-1.00	0.013	0	0
	1.01-2.00	0	0	0
	2.01-5.00	0	0	0
	> 5.00	0	0	0

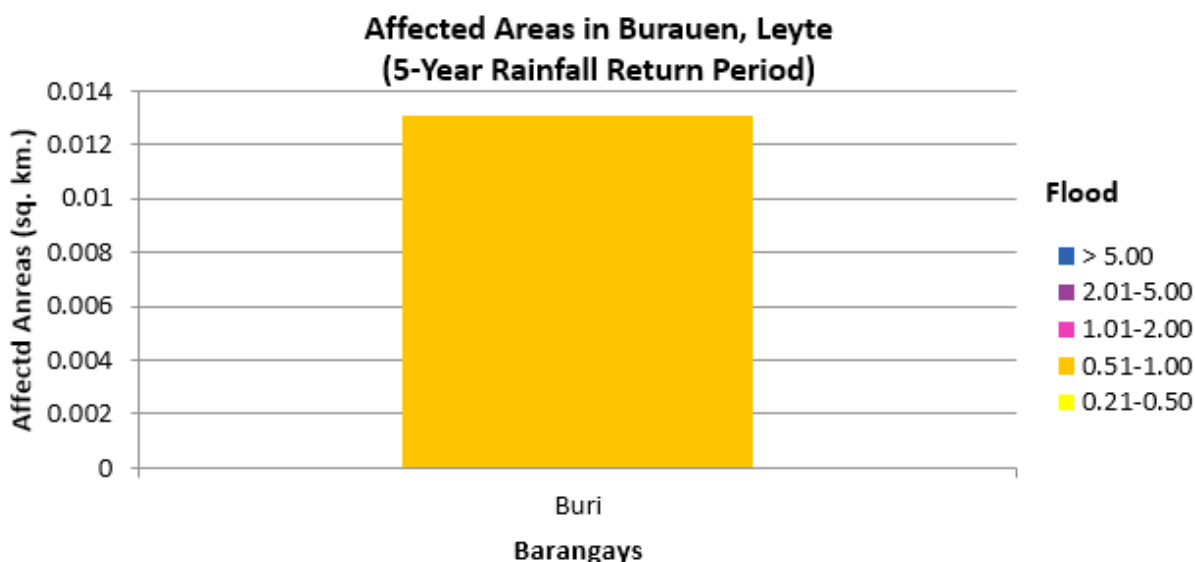


Figure 78. Affected Areas in Burauen, Leyte during 5-Year Rainfall Return Period

For the municipality of Dagami, with an area of 134.08 sq. km., 31.62% will experience flood levels of less than 0.20 meters. 7.39% of the area will experience flood levels of 0.21 to 0.50 meters while 6.59%, 5.34%, 1.26%, and 0.11% of the area will experience flood depths of 0.51 to 1 meter, 1.01 to 2 meters, 2.01 to 5 meters, and more than 5 meters, respectively. Listed in Tables 35-41 are the affected areas in square kilometres by flood depth per barangay.

Table 35. Affected Areas in Dagami, Leyte during 5-Year Rainfall Return Period

Affected Area (sq. km.) by flood depth (in m.)		Affected Barangays in Dagami (in sq. km.)										
		Abaca	Abre	Baliit	Balugo	Banayon	Bayabas	Bolirao	Buonavista	Buntay	Caanislagan	
Affected Area (sq. km)	0.03-0.20	1.07	0.047	0.2	0.1	2.77	1.12	0.79	0.28	0.74	0.49	
	0.21-0.50	0.8	0.067	0.21	0.049	0.7	0.23	0.24	0.016	0.31	0.047	
	0.51-1.00	0.61	0.2	0.32	0.31	0.2	0.033	0.032	0.018	0.4	0.0074	
	1.01-2.00	0.038	0.36	0.19	0.69	0.023	0	0	0.019	0.96	0.032	
	2.01-5.00	0.014	0.14	0.0094	0.015	0	0	0	0.012	0.076	0.024	
> 5.00	0	0	0	0	0	0	0	0	0.00026	0		

Table 36. Affected Areas in Dagami, Leyte during 5-Year Rainfall Return Period

Affected Area (sq. km.) by flood depth (in m.)		Affected Barangays in Dagami (in sq. km.)									
		Cabariwan	Cabuloran	Cabunga-An	Calipayan	Calsadahay	Caluctogan	Calutan	Camono-An	Candagara	Canlingga
Affected Area (sq. km)	0.03-0.20	0.31	0.85	1.67	1.09	0.9	0.41	0.92	0.98	0.0017	0.0047
	0.21-0.50	0.072	0.2	0.26	0.086	0.21	0.58	0.16	0.019	0	0.00061
	0.51-1.00	0.0097	0.054	0.23	0.08	0.054	0.44	0.086	0.048	0	0.021
	1.01-2.00	0	0.0077	0.12	0.18	0.001	0.23	0	0.027	0	0.093
	2.01-5.00	0	0	0.0076	0.046	0	0.0066	0	0.0021	0	0.3
> 5.00	0	0	0	0	0	0	0	0	0	0.0013	

Table 37. Affected Areas in Dagami, Leyte during 5-Year Rainfall Return Period

Affected Area (sq. km.) by flood depth (in m.)		Affected Barangays in Dagami (in sq. km.)										
		Cansamada East	Cansamada West	Capulhan	Digahongan	Guinarona	Hiabangan	Hilabago	Hinabuyan	Hinologan	Hitumnog	
Affected Area (sq. km)	0.03-0.20	1.4	0.49	0.34	0.52	0.54	0.73	0.76	1.13	0.79	0.52	
	0.21-0.50	0.23	0.15	0.061	0.093	0.16	0.12	0.14	0.9	0.26	0.13	
	0.51-1.00	0.093	0.18	0.074	0.023	0.052	0.27	0.17	0.56	0.11	0.22	
	1.01-2.00	0.056	0.12	0.063	0.017	0.0061	0.35	0.14	0.18	0.0079	0.044	
	2.01-5.00	0.12	0.021	0.046	0.042	0.0079	0.051	0.062	0.0032	0.0082	0	
> 5.00	0	0	0	0	0	0	0	0	0	0	0	

Table 38. Affected Areas in Dagami, Leyte during 5-Year Rainfall Return Period

Affected Area (sq. km.) by flood depth (in m.)		Affected Barangays in Dagami (in sq. km.)										
		Katipunan	Lapu-lapu Poblacion	Lobe-Lobe East	Los Martires	Lusad Poblacion	Macaalang	Maliwaliw	Maragondong	Ormocay	Palacio	
Affected Area (sq. km)	0.03-0.20	3.16	0.046	0.51	0.44	0.044	0.74	2.34	0.67	0.24	1.72	
	0.21-0.50	0.099	0.026	0.087	0.11	0.0075	0.036	0.35	0.15	0.04	0.39	
	0.51-1.00	0.13	0.015	0.017	0.095	0	0.032	0.13	0.18	0	0.51	
	1.01-2.00	0.11	0	0	0.049	0.019	0.022	0.024	0.19	0	0.43	
	2.01-5.00	0.022	0.011	0	0.031	0	0	0	0.12	0	0.14	
> 5.00	0	0	0	0.04	0	0	0	0	0.0022	0	0	

Table 39. Affected Areas in Dagami, Leyte during 5-Year Rainfall Return Period

Affected Area (sq. km.) by flood depth (in m.)		Affected Barangays in Dagami (in sq. km.)										
		Panda	Paraiso	Patoc	Poponton	Rizal	Salvacion	Sampaguita	Sampao East Poblacion	Sampao West Poblacion	San Antonio Poblacion	
Affected Area (sq. km)	0.03-0.20	0.17	2.06	0.42	0.063	1.2	1.6	0.78	0.08	0.071	0.058	
	0.21-0.50	0.14	0.096	0.12	0.17	0.016	0.086	0.11	0.04	0.012	0.019	
	0.51-1.00	0.22	0.045	0.082	0.64	0.025	0.043	0.016	0.0099	0.016	0	
	1.01-2.00	0.21	0.034	0.073	0.29	0.04	0.036	0.0079	0	0.025	0	
	2.01-5.00	0.023	0	0.047	0.0079	0.017	0.047	0	0	0.0000024	0.0065	
> 5.00	0	0	0.034	0	0	0	0	0	0	0	0	

Table 40. Affected Areas in Dagami, Leyte during 5-Year Rainfall Return Period

Affected Area (sq. km.) by flood depth (in m.)		Affected Barangays in Dagami (in sq. km.)										
		San Benito	San Jose Poblacion	San Roque Poblacion	Santo Domingo	Sawahon	Sirab	Sta. Mesa Poblacion	Tagkip	Talinhugon	Tin-Ao	
Affected Area (sq. km)	0.03-0.20	0.34	0.028	0.044	0.83	0.58	0.26	0.092	0.8	0.22	0.31	
	0.21-0.50	0.2	0.025	0.0013	0.1	0.078	0.086	0.021	0.14	0.066	0.26	
	0.51-1.00	0.26	0.0026	0.0042	0.03	0.21	0.12	0.014	0.28	0.05	0.37	
	1.01-2.00	0.099	0.005	0	0.043	0.22	0.071	0	0.45	0.072	0.28	
	2.01-5.00	0.0046	0	0.015	0.0032	0.0079	0.023	0	0.11	0.013	0.0079	
> 5.00	0	0.014	0	0	0	0.036	0	0.011	0.0032	0		

Table 41. Affected Areas in Dagami, Leyte during 5-Year Rainfall Return Period

Affected Area (sq. km.) by flood depth (in m.)		Affected Barangays in Dagami (in sq. km.)	
		Tunga	Tuya
Affected Area (sq. km)	0.03-0.20	0.017	0.45
	0.21-0.50	0.0018	0.15
	0.51-1.00	0.00015	0.047
	1.01-2.00	0.0075	0.000013
	2.01-5.00	0	0
	> 5.00	0.000045	0

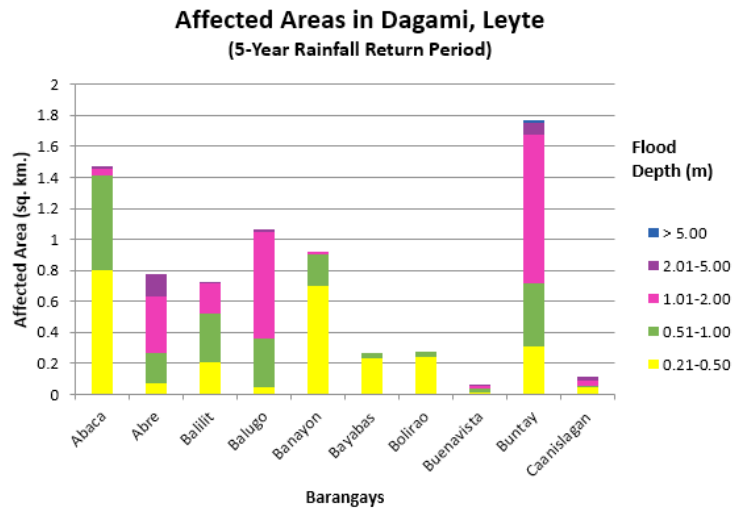


Figure 79. Affected Areas in Dagami, Leyte during 5-Year Rainfall Return Period

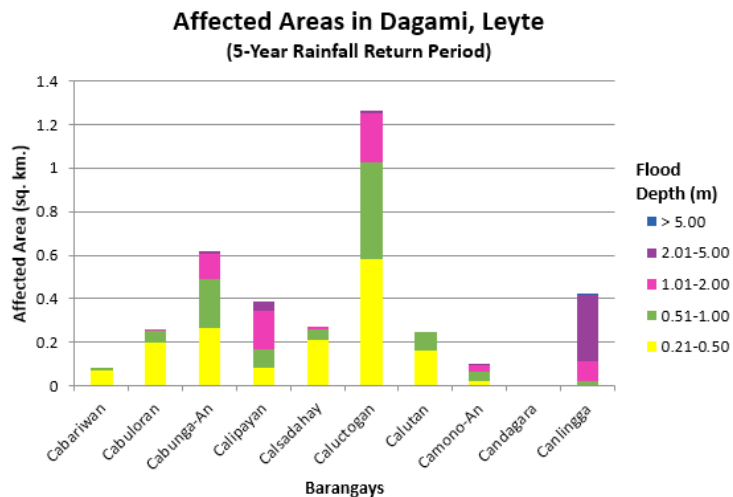


Figure 80. Affected Areas in Dagami, Leyte during 5-Year Rainfall Return Period

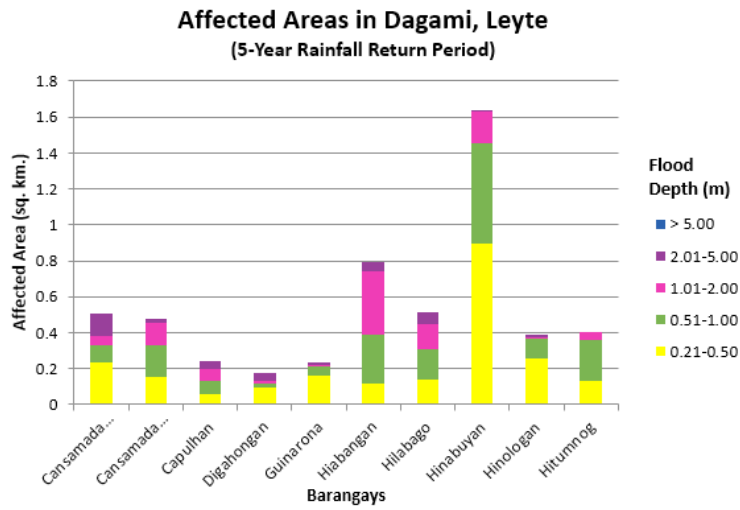


Figure 81. Affected Areas in Dagami, Leyte during 5-Year Rainfall Return Period

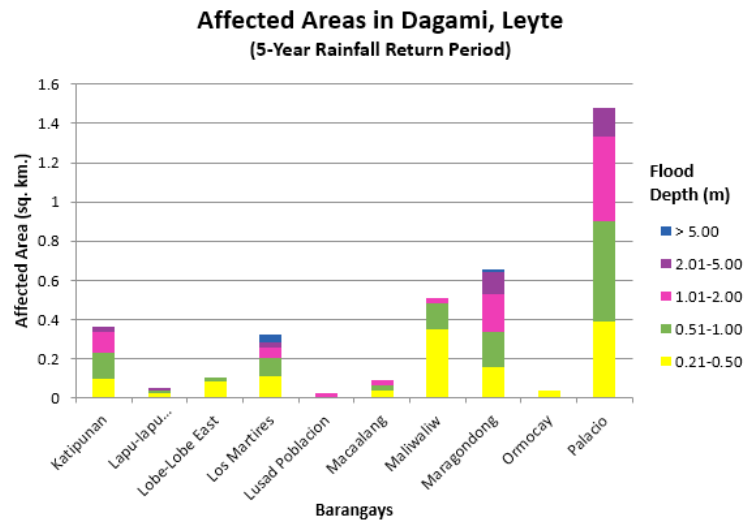


Figure 82. Affected Areas in Dagami, Leyte during 5-Year Rainfall Return Period

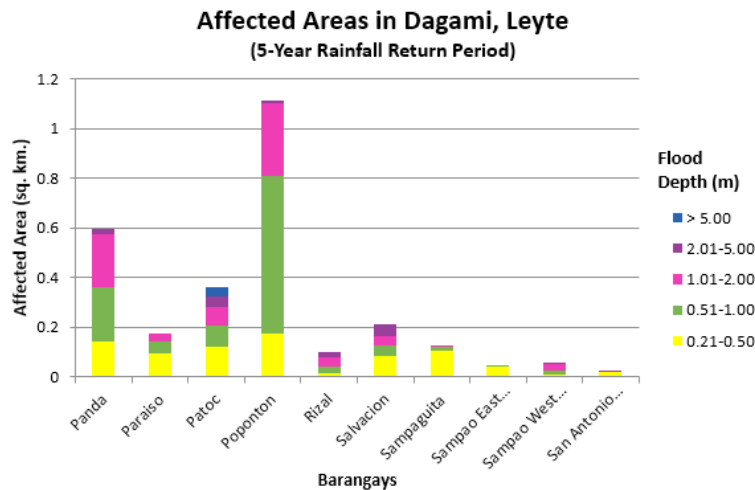


Figure 83. Affected Areas in Dagami, Leyte during 5-Year Rainfall Return Period

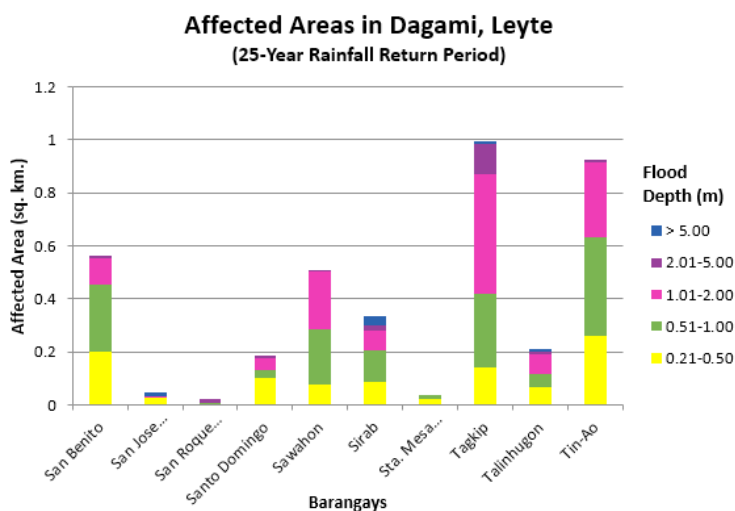


Figure 84. Affected Areas in Dagami, Leyte during 5-Year Rainfall Return Period

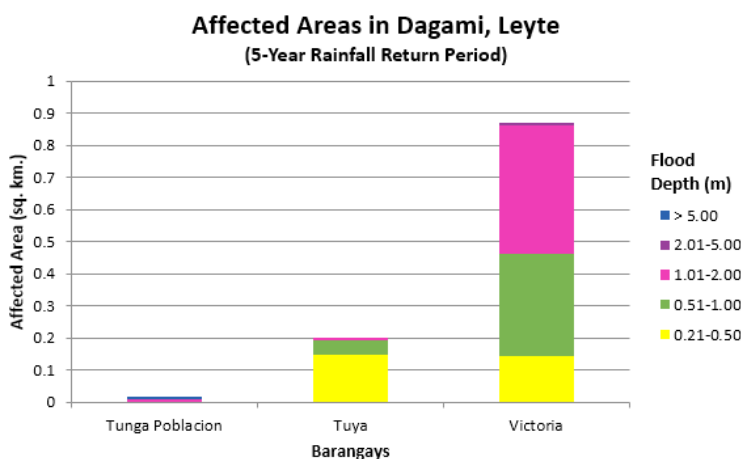


Figure 85. Affected Areas in Dagami, Leyte during 5-Year Rainfall Return Period

For the municipality of Jaro, with an area of 190.65 sq. km., 0.09% will experience flood levels of less 0.20 meters. 0.02% of the area will experience flood levels of 0.21 to 0.50 meters while 0.004%, 0.004%, 0%, and 0.004% of the area will experience flood depths of 0.51 to 1 meter, 1.01 to 2 meters, 2.01 to 5 meters, and more than 5 meters, respectively. Listed in Table 42 are the affected areas in square kilometres by flood depth per barangay.

Table 42. Affected Areas in Jaro, Leyte during 5-Year Rainfall Return Perio

Affected Area (sq. km.) by flood depth (in m.)		Affected Barangays in Dagami (in sq. km.)	
		Parasan	
Affected Area (sq. km)	0.03-0.20	0.18	
	0.21-0.50	0.038	
	0.51-1.00	0.0079	
	1.01-2.00	0.0079	
	2.01-5.00	0	
	> 5.00	0.0079	

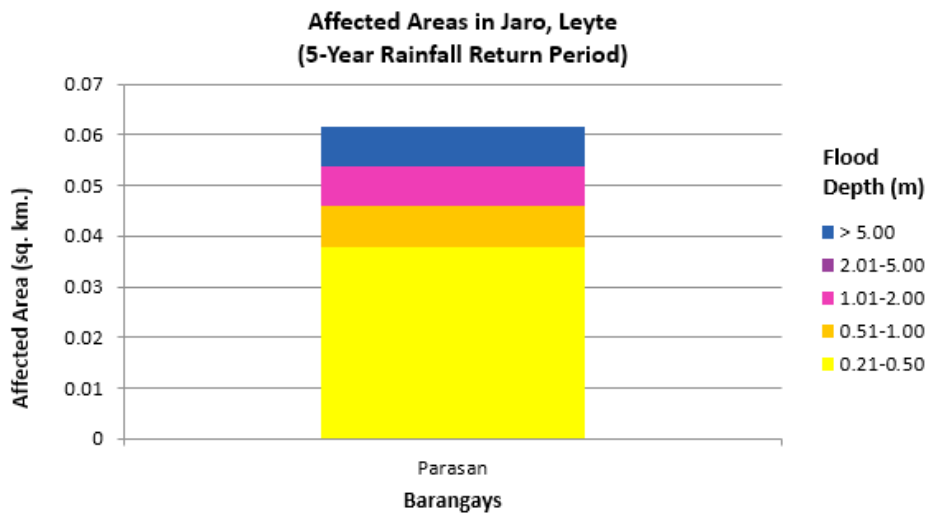


Figure 86. Affected Areas in Jaro, Leyte Samar during 5-Year Rainfall Return Period

For the municipality of Pastrana, with an area of 79.17 sq. km., 32.53% will experience flood levels of less 0.20 meters. 6.90% of the area will experience flood levels of 0.21 to 0.50 meters while 3.84%, 3.17%, 1.13%, and 0.03% of the area will experience flood depths of 0.51 to 1 meter, 1.01 to 2 meters, 2.01 to 5 meters, and more than 5 meters, respectively. Listed in Tables 46-47 are the affected areas in square kilometres by flood depth per barangay.

For the municipality of Tabontabon, with an area of 20.46 sq. km., 32.47% will experience flood levels of less 0.20 meters. 6.93% of the area will experience flood levels of 0.21 to 0.50 meters while 1.73%, 0.116%, and 0.08% of the area will experience flood depths of 0.51 to 1 meter, 1.01 to 2 meters, and more than 2 meters, respectively. Listed in Table are the affected areas in square kilometres by flood depth per barangay.

For the municipality of Tanauan, with an area of 62.78 sq. km., 41.50% will experience flood levels of less 0.20 meters. 9.69% of the area will experience flood levels of 0.21 to 0.50 meters while 4.53%, 1.97%, 0.29%, and 0.06% of the area will experience flood depths of 0.51 to 1 meter, 1.01 to 2 meters, 2.01 to 5 meters, and more than 5 meters, respectively. Listed in Tables 49-53 are the affected areas in square kilometres by flood depth per barangay.

For the 25-year return period, 0.08% of the municipality of Burauen with an area of 205.31 sq. km. will experience flood levels of less 0.20 meters. 0.003% of the area will experience flood levels of 0.21 to 0.50 meters while 0.011% of the area will experience flood depths of 0.51 to 1 meter. Listed in Table are the affected areas in square kilometres by flood depth per barangay.

For the municipality of Jaro, with an area of 190.65 sq. km., 0.086% will experience flood levels of less 0.20 meters. 0.023% of the area will experience flood levels of 0.21 to 0.50 meters while 0.009%, 0.003%, 0.002%, and 0.0003% of the area will experience flood depths of 0.51 to 1 meter, 1.01 to 2 meters, 2.01 to 5 meters, and more than 5 meters, respectively. Listed in Table 62 are the affected areas in square kilometres by flood depth per barangay.

For the municipality of Palo, with an area of 65.34 sq. km., 40.17% will experience flood levels of less 0.20 meters. 17.43% of the area will experience flood levels of 0.21 to 0.50 meters while 6.64%, 2.56%, 0.52%, and 0.12% of the area will experience flood depths of 0.51 to 1 meter, 1.01 to 2 meters, 2.01 to 5 meters, and more than 5 meters, respectively. Listed in Tables 63-65 are the affected areas in square kilometres by flood depth per barangay.

For the municipality of Pastrana, with an area of 79.17 sq. km., 23.40% will experience flood levels of less 0.20 meters. 9.37% of the area will experience flood levels of 0.21 to 0.50 meters while 6.90%, 5.90%, 2.18%, and 0.09% of the area will experience flood depths of 0.51 to 1 meter, 1.01 to 2 meters, 2.01 and 5 meters, and more than 5 meters, respectively. Listed in Tables 66-67 are the affected areas in square kilometres by flood depth per barangay.

For the municipality of Tabontabon, with an area of 20.46 sq. km., 26.87% will experience flood levels of

less 0.20 meters. 9.40% of the area will experience flood levels of 0.21 to 0.50 meters while 3.92%, 3.92%, 1.00%, and 0.035% of the area will experience flood depths of 0.51 to 1 meter, 1.01 to 2 meters, 2.01 to 5 meters, and more than 5 meters, respectively. Listed in Table 68 are the affected areas in square kilometres by flood depth per barangay.

For the municipality of Tanauan, with an area of 62.78 sq. km., 32.93% will experience flood levels of less 0.20 meters. 12.80% of the area will experience flood levels of 0.21 to 0.50 meters while 8.37%, 5.91%, 0.59%, and 0.13% of the area will experience flood depths of 0.51 to 1 meter, 1.01 to 2 meters, 2.01 to 5 meters, and more than 5 meters, respectively. Listed in Tables 69-73 are the affected areas in square kilometres by flood depth per barangay.

For the 100-year return period, 0.003% of the municipality of Burauen with an area of 205.31 sq. km. will experience flood levels of 0.21 to 0.50 meters while 0.011%, 0.0012% of the area will experience flood depths of 0.51 to 1 meter, and 1.01 to 2 meters. Listed in Table 74 are the affected areas in square kilometres by flood depth per barangay.

For the municipality of Dagami, with an area of 134.08 sq. km., 21.99% will experience flood levels of less 0.20 meters. 6.50% of the area will experience flood levels of 0.21 to 0.50 meters while 8.61%, 9.86%, 5.07%, and 0.28% of the area will experience flood depths of 0.51 to 1 meter, 1.01 to 2 meters, 2.01 to 5 meters, and more than 5 meters, respectively. Listed in Tables 75-81 are the affected areas in square kilometres by flood depth per barangay.

For the municipality of Jaro, with an area of 190.65 sq. km., 0.075% will experience flood levels of less 0.20 meters. 0.03% of the area will experience flood levels of 0.21 to 0.50 meters while 0.013%, 0.004%, 0.0026%, and 0.0004% of the area will experience flood depths of 0.51 to 1 meter, 1.01 to 2 meters, 2.01 to 5 meters, and more than 5 meters, respectively. Listed in Table 82 are the affected areas in square kilometres by flood depth per barangay.

For the municipality of Palo, with an area of 65.34 sq. km., 29.83% will experience flood levels of less 0.20 meters. 18.11% of the area will experience flood levels of 0.21 to 0.50 meters while 11.38%, 6.78%, 1.17%, and 0.156% of the area will experience flood depths of 0.51 to 1 meter, 1.01 to 2 meters, 2.01 to 5 meters, and more than 5 meters, respectively. Listed in Tables 83-85 are the affected areas in square kilometres by flood depth per barangay.

For the municipality of Pastrana, with an area of 79.17 sq. km., 19.08% will experience flood levels of less 0.20 meters. 9.93% of the area will experience flood levels of 0.21 to 0.50 meters while 8.27%, 7.53%, 2.88%, and 0.14% of the area will experience flood depths of 0.51 to 1 meter, 1.01 to 2 meters, 2.01 to 5 meters, and more than 5 meters, respectively. Listed in Table 86-87 are the affected areas in square kilometres by flood depth per barangay.

For the municipality of Tabontabon, with an area of 20.46 sq. km., 21.53% will experience flood levels of less 0.20 meters. 10.25% of the area will experience flood levels of 0.21 to 0.50 meters while 5.44%, 3.09%, 0.91% of the area will experience flood depths of 0.51 to 1 meter, 1.01 to 2 meters, and more than 2 meters, respectively. Listed in Table 88 are the affected areas in square kilometres by flood depth per barangay.

For the municipality of Tanauan, with an area of 62.78 sq. km., 25.07% will experience flood levels of less 0.20 meters. 12.76% of the area will experience flood levels of 0.21 to 0.50 meters while 11.38%, 10.10%, 1.21%, and 0.22% of the area will experience flood depths of 0.51 to 1 meter, 1.01 to 2 meters, 2.01 to 5 meters, and more than 5 meters, respectively. Listed in Tables 89-93 are the affected areas in square kilometres by flood depth per barangay.

Among the barangays in the municipality of Burauen, Cadahunan is projected to have the highest percentage of area that will experience flood levels at 0.08%. Meanwhile, Buri posted the second highest percentage of area that may be affected by flood depths at 0.05%.

Among the barangays in the municipality of Dagami, Banayon is projected to have the highest percentage of area that will experience flood levels at 2.75%. Meanwhile, Katipunana posted the second highest percentage of area that may be affected by flood depths at 2.63%.

Among the barangays in the municipality of Jaro, Parasan is projected to have the highest percentage of

area that will experience flood levels at 0.18%.

Among the barangays in the municipality of Palo, San Joaquin is projected to have the highest percentage of area that will experience flood levels at 6.12%. Meanwhile, Cangumbang posted the second highest percentage of area that may be affected by flood depths at 4.05%.

Among the barangays in the municipality of Pastrana, Yapad is projected to have the highest percentage of area that will experience flood levels 3.80%. Meanwhile, Bahay posted the second highest percentage of area that may be affected by flood depths at 3.58%.

Among the barangays in the municipality of Tabontabon, Belisong is projected to have the highest percentage of area that will experience flood levels at 1.33%. Meanwhile, Guingawan posted the second highest percentage of area that may be affected by flood depths at 1.23%.

Among the barangays in the municipality of Tanauan, Binongto-An is projected to have the highest percentage of area that will experience flood levels at 1.99%. Meanwhile, Guindag-An posted the second highest percentage of area that may be affected by flood depths at 1.63%.

Moreover, the generated flood hazard maps for the Binahaan Floodplain were used to assess the vulnerability of the educational and medical institutions in the floodplain. Using the flood depth units of PAG-ASA for hazard maps - "Low", "Medium", and "High" - the affected institutions were given their individual assessment for each Flood Hazard Scenario (5 yr, 25 yr, and 100 yr).

Of the 144 identified Educational Institutions in Binahaan Flood plain, 26 schools were assessed to be exposed to the Low level flooding during a 5 year scenario while 11 schools were assessed to be exposed to Medium level flooding. In the 25 year scenario, 32 schools were assessed to be exposed to the Low level flooding while 25 schools were assessed to be exposed to Medium level flooding and 2 schools were assessed to be exposed to High level flooding in the same scenario. For the 100 year scenario, 33 schools were assessed for Low level flooding and 29 schools for Medium level flooding. In the same scenario, 7 schools were assessed to be exposed to High level flooding. See Annex 12 for a detailed enumeration of schools inside Guinarona floodplain.

Of the 37 identified Medical Institutions in Binahaan Flood plain, 8 were assessed to be exposed to the Low level flooding during a 5 year scenario while 1 were assessed to be exposed to Medium level flooding in the same scenario. In the 25 year scenario, 9 were assessed to be exposed to the Low level flooding while 8 were assessed to be exposed to Medium level flooding. For the 100 year scenario, 9 schools were assessed for Low level flooding and 10 for Medium level flooding. In the same scenario, 2 schools were assessed to be exposed to High level flooding, which is a health center in Brgy. Los Martines and Cangumbang. See Annex 13 for a detailed enumeration of health insitutions inside Guinarona floodplain.

5.11 Flood Validation

In order to check and validate the extent of flooding in different river systems, a validation survey was performed. Field personnel gathered secondary data regarding flood occurrence in the area within the major river system in the Philippines.

From the flood depth maps produced by Phil-LiDAR 1 Program, multiple points representing the different flood depths for different scenarios were identified for validation.

The validation personnel went to the specified points identified in a river basin and gathered data regarding the actual flood level in each location. Data gathering was done through a local DRRM office to obtain maps or situation reports about the past flooding events and through interviews of some residents with knowledge of or have had experienced flooding in a particular area.

The actual data from the field were compared to the simulated data to assess the accuracy of the Flood Depth Maps produced and to improve the results of the flood map.

The flood validation consists of 219 points randomly selected all over the Guinarona flood plain. The points were grouped depending on the RIDF return period of the event.

The RMSE value for each flood depth map is listed in the table below:

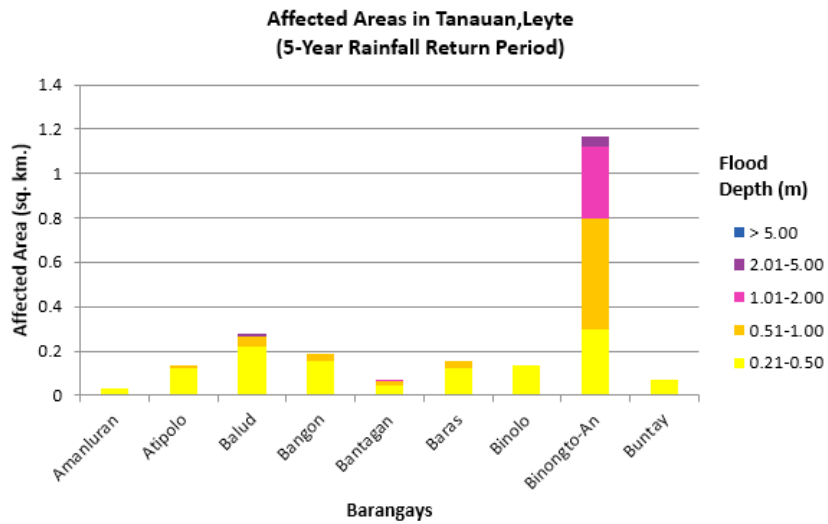


Figure 93. Affected Areas in Tanauan, Leyte during 5-Year Rainfall Return Period

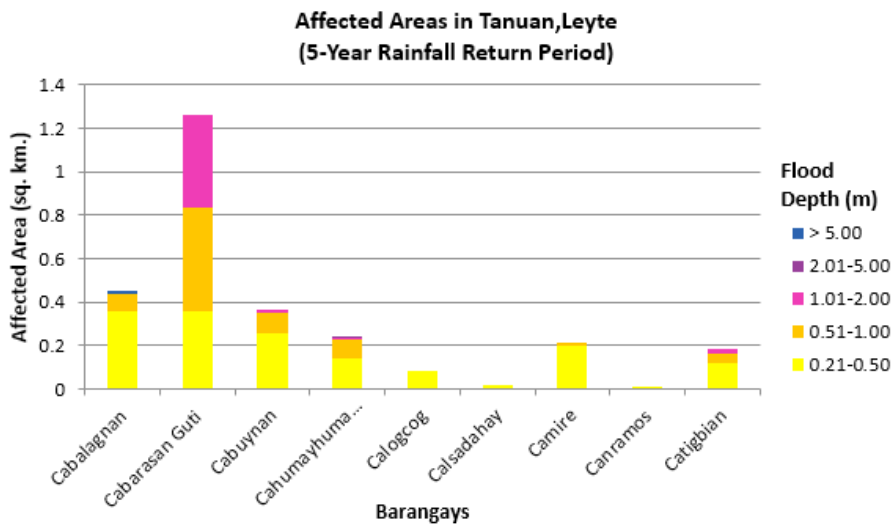


Figure 94. Affected Areas in Tanauan, Leyte during 5-Year Rainfall Return Period

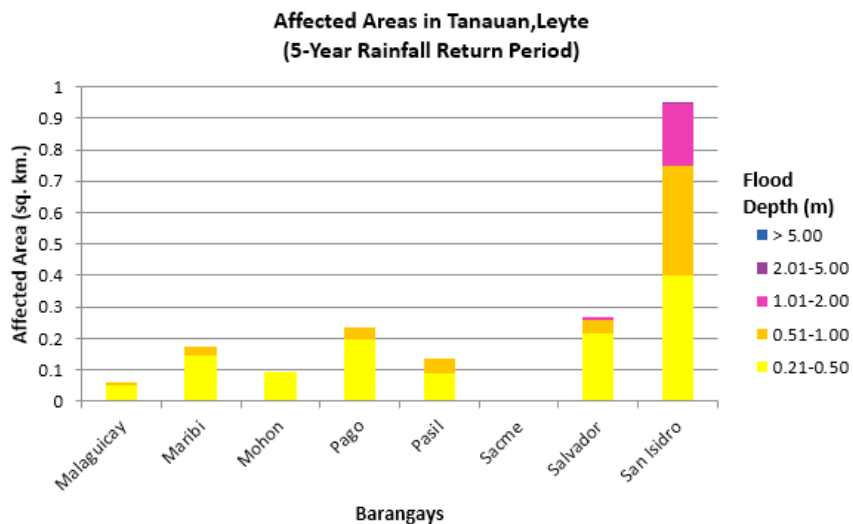


Figure 95. Affected Areas in Tanauan, Leyte during 5-Year Rainfall Return Period

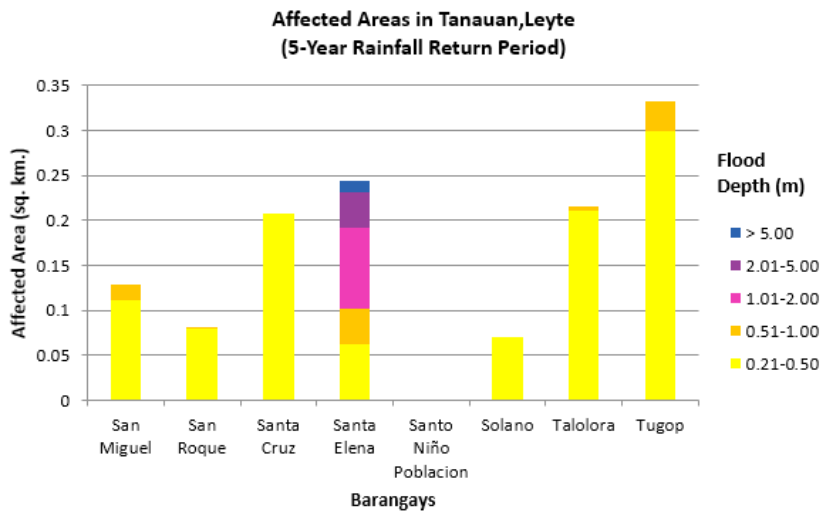


Figure 96. Affected Areas in Tanauan, Leyte during 5-Year Rainfall Return Period

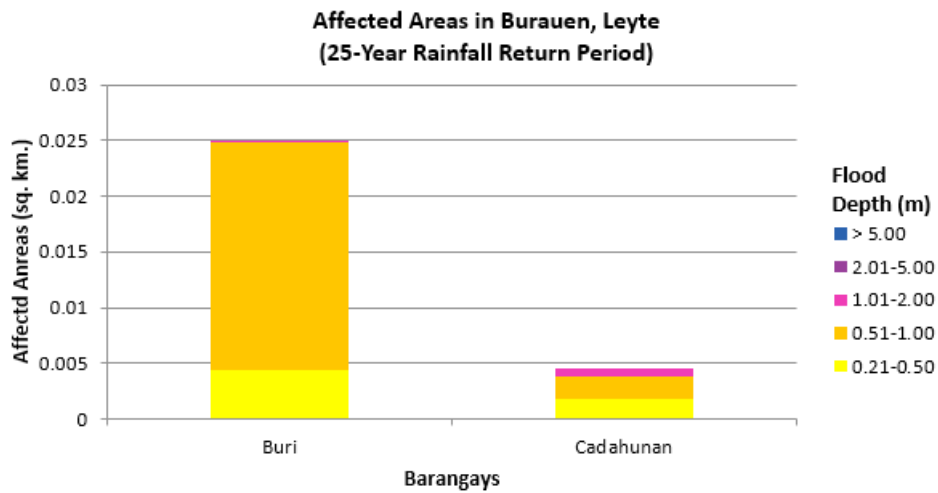


Figure 97. Affected Areas in Burauen, Leyte during 25-Year Rainfall Return Period

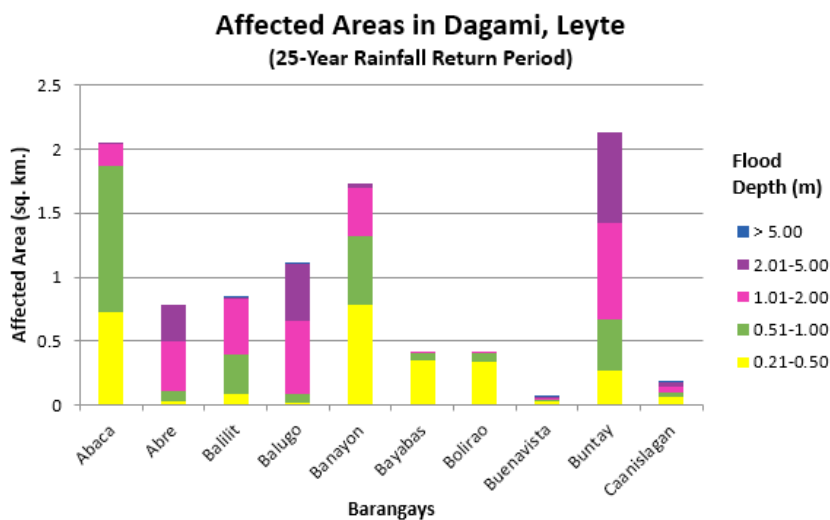


Figure 98. Affected Areas in Dagami, Leyte during 25-Year Rainfall Return Period

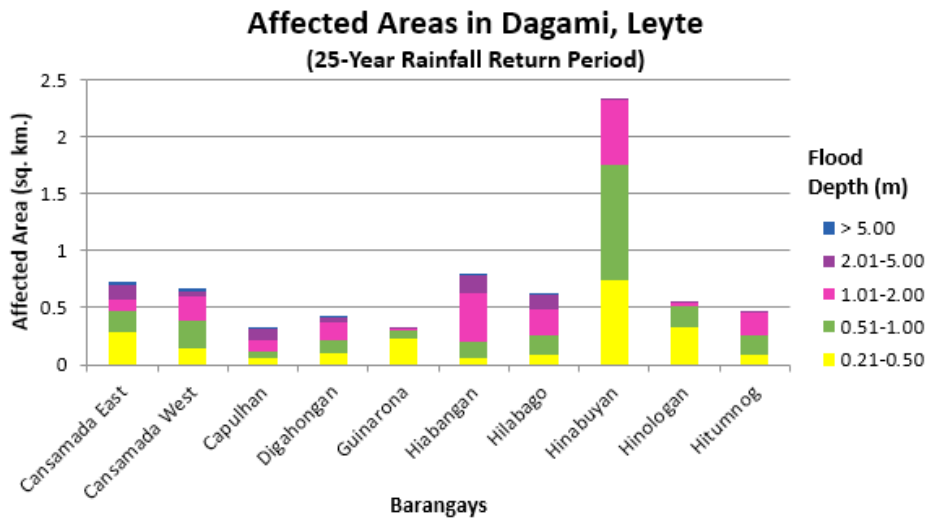


Figure 99. Affected Areas in Dagami, Leyte during 25-Year Rainfall Return Period

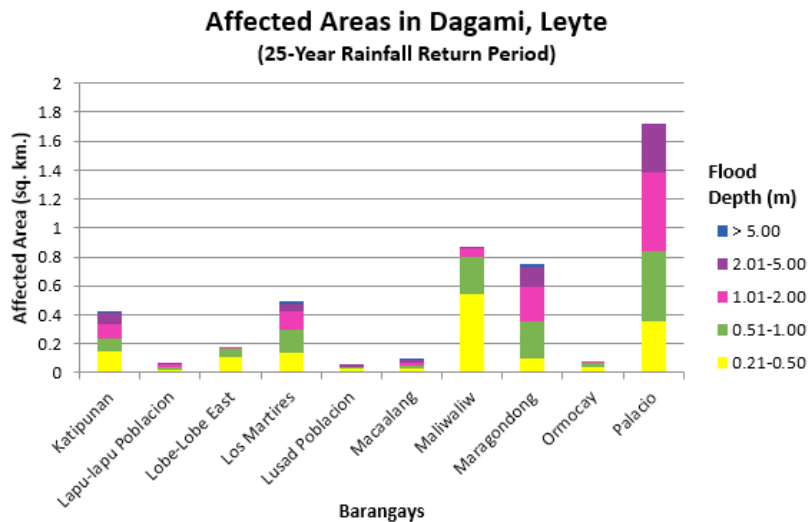


Figure 100. Affected Areas in Dagami, Leyte during 25-Year Rainfall Return Period

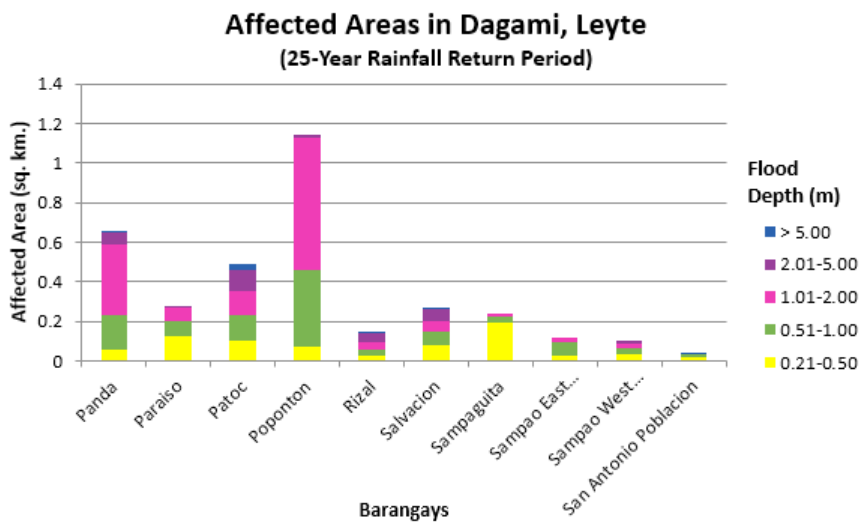


Figure 101. Affected Areas in Dagami, Leyte during 25-Year Rainfall Return Period

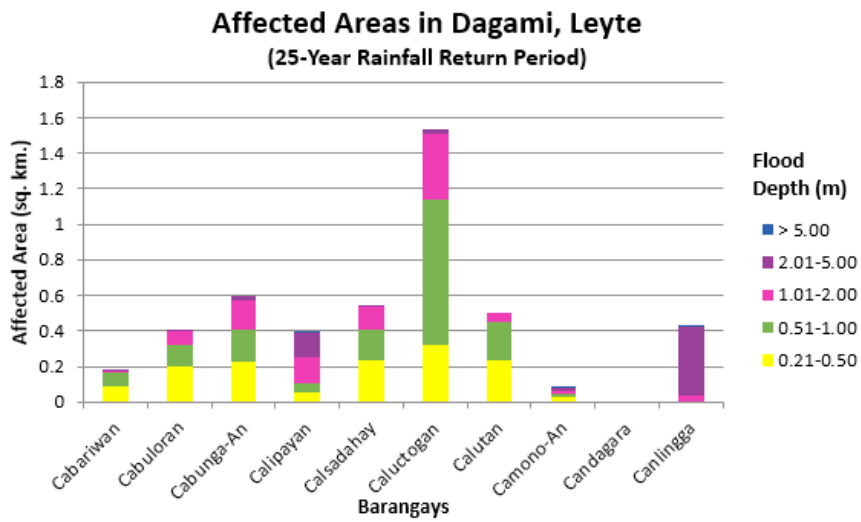


Figure 102. Affected Areas in Dagami, Leyte during 25-Year Rainfall Return Period

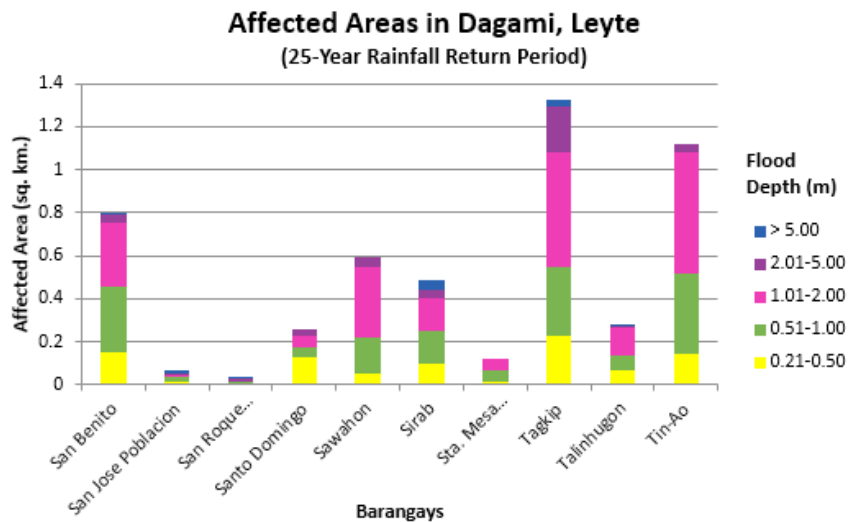


Figure 103. Affected Areas in Dagami, Leyte during 25-Year Rainfall Return Period

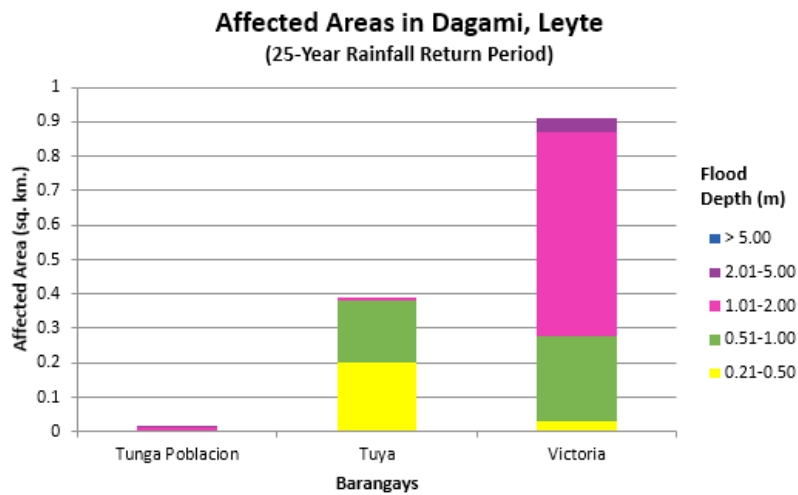


Figure 104.

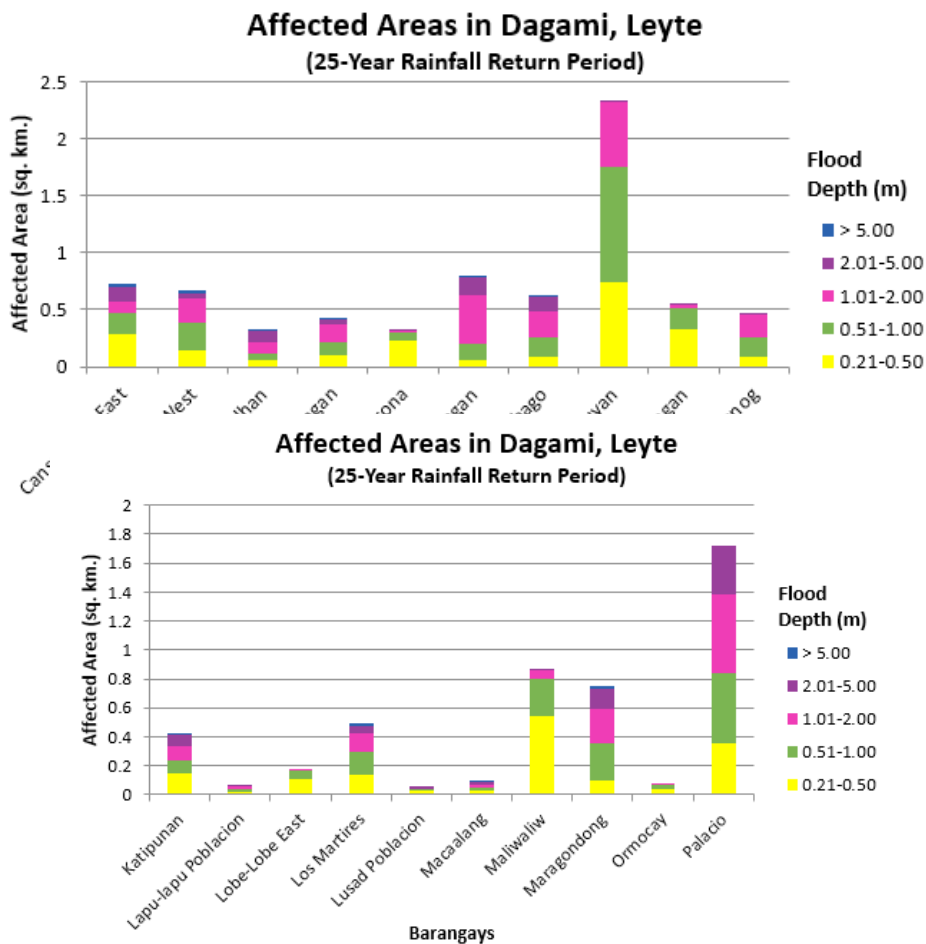


Figure 100. Affected Areas in Dagami, Leyte during 25-Year Rainfall Return Period

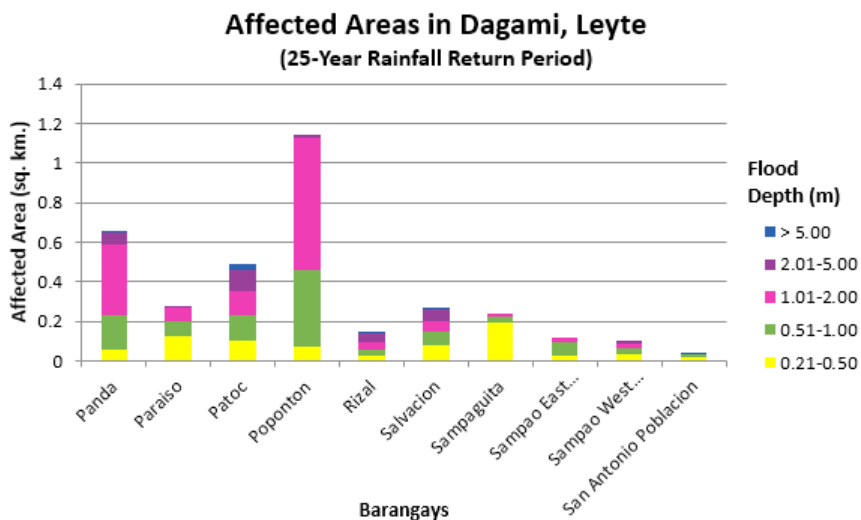


Figure 101. Affected Areas in Dagami, Leyte during 25-Year Rainfall Return Period

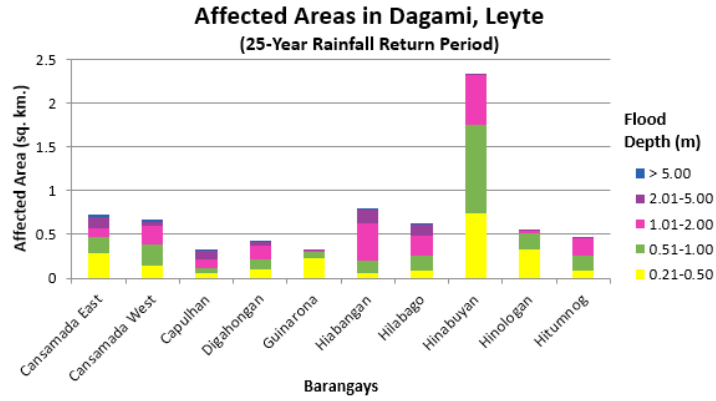


Figure 99. Affected Areas in Dagami, Leyte during 25-Year Rainfall Return Period

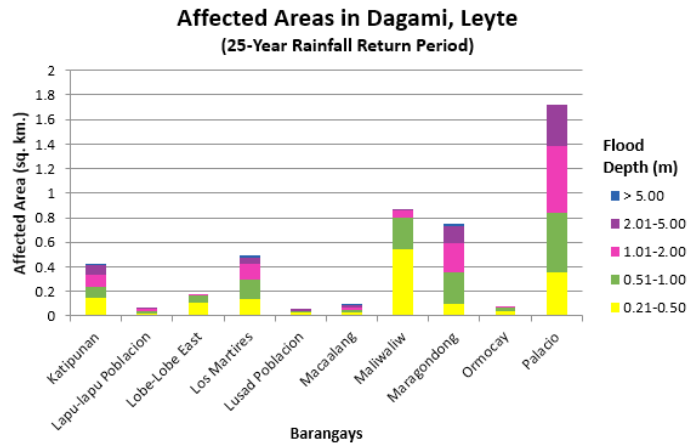


Figure 100. Affected Areas in Dagami, Leyte during 25-Year Rainfall Return Period

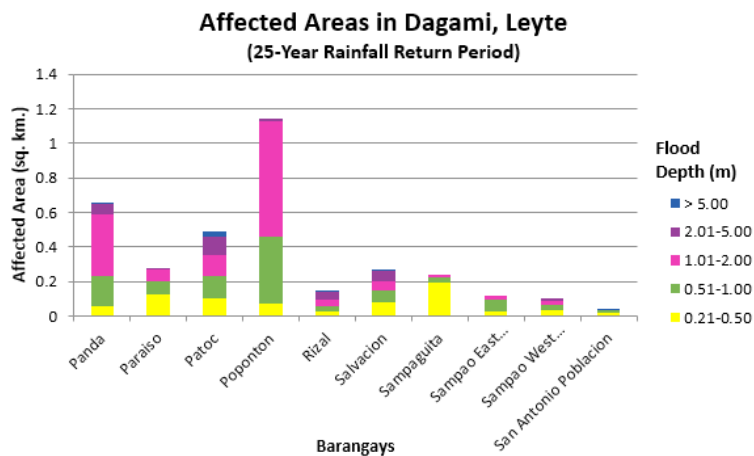


Figure 101. Affected Areas in Dagami, Leyte during 25-Year Rainfall Return Period



